



Université  
de Toulouse

# THÈSE

En vue de l'obtention du

## DOCTORAT DE L'UNIVERSITÉ DE TOULOUSE

Délivré par :

Institut National Polytechnique de Toulouse (INP Toulouse)

Discipline ou spécialité :

Réseaux, Télécommunications, Systèmes et Architecture

---

Présentée et soutenue par :

M. HAMDY AYED

le jeudi 27 novembre 2014

Titre :

ANALYSE ET OPTIMISATION DES RESEAUX AVIONIQUES  
HETEROGENES

---

Ecole doctorale :

Mathématiques, Informatique, Télécommunications de Toulouse (MITT)

Unité de recherche :

Institut de Recherche en Informatique de Toulouse (I.R.I.T.)

Directeur(s) de Thèse :

M. CHRISTIAN FRABOUL

M. AHLEM MIFDAOUI

Rapporteurs :

M. LAURENT GEORGE, UNIVERSITE DE MARNE LA VALLEE

M. YE-QIONG SONG, UNIVERSITE DE LORRAINE

Membre(s) du jury :

M. LAURENT GEORGE, UNIVERSITE DE MARNE LA VALLEE, Président

M. AHLEM MIFDAOUI, ISAE TOULOUSE, Membre

M. CHRISTIAN FRABOUL, INP TOULOUSE, Membre

M. JUAN LOPEZ, AIRBUS FRANCE, Membre

M. LUIS ALMEIDA, UNIVERSIDADE DO PORTO PORTUGAL, Membre



## Acknowledgments

I would like to express my sincere gratitude to my supervisor Christian Fraboul and Co-supervisor Ahlem Mifdaoui for their constant support, guidance and patience during my research. I thank them for their precious advice, availability and kindness they have shown during my thesis. Without their help and support in the difficult moments this thesis would not have been possible.

I am thankful for Ye-Qiong Song and Laurent George for accepting to be my thesis referees. I am also very honored to count them among the members of the jury of my thesis as well as Luis Almeida and Juan Lopez.

I would like to thank Sylvie Eichen for her precious help in administrative tasks.

I thank all the people that i worked or interacted with at the Department of Computer Science, Mathematics and Automatics (DMIA) of the ISAE (Jolimont site). In particular, I am grateful to Emmanuel Lochin, Fabrice Frances, Jerome Lacan, Patrick Senac, Tanguy Perennou and Pierre de-Saqui-Sannes for the many useful discussions and precious advice. I thank Thomas, Remi, Hugo, Anh-Dung, Nicolas, Victor, Léo, Jonathan, Tuan, Khanh, Viet, Rami, Karine, Ahmed and everyone in the DMIA department for providing me a friendly working environment.

Finally, I thank my parents and all my family for their encouragement and support.



## Abstract

The complexity of avionic communication architecture is increasing due to the growing number of interconnected end-systems and the expansion of exchanged data. To be effective in meeting the emerging requirements in terms of bandwidth, latency and modularity, the current avionic communication architecture consists of an Avionics Full Duplex Switched Ethernet (AFDX) network to interconnect the critical end-systems and some Input/ Output (I/O) data buses (e.g., Controller Area Network (CAN) bus) for sensors and actuators. Clusters are then interconnected via specific devices, called Remote Data Concentrators (RDCs), standardized as ARINC 655. RDC devices are modular gateways distributed throughout the aircraft to handle heterogeneity between the AFDX backbone and I/O data buses. Although RDC devices enhance avionics modularity and reduce maintenance efforts, they become one of the major challenges in the design process of such multi-cluster avionic architectures. The existing implementations of RDC are usually based on direct frames translation and do not consider resource savings issue. Resource utilization efficiency is important for avionic applications to guarantee easy incremental design, and enhance margins for future avionic functions additions. Therefore, the design of an optimized RDC device integrating resource saving mechanisms becomes a necessity to enhance the scalability and performances of avionic applications. In this context, the main objective of this thesis is to design and validate an enhanced RDC device offering an efficient bandwidth utilization, considered as a main resource to save, while meeting real-time constraints.

To achieve this aim, first, we design an enhanced CAN-AFDX RDC device compliant with the ARINC 655 specifications. The main elementary functions integrated into the proposed RDC are: (i) frame packing applied on upstream flows, i.e., flows generated by sensors and destined to the AFDX, to minimize communication overheads, and consequently bandwidth utilization; (ii) hierarchical traffic shaping applied on downstream flows, i.e., flows generated by AFDX sources and destined to actuators, to reduce interferences on CAN, and thus to enhance communication efficiency. Moreover, our proposed RDC may connect multiple I/O CAN buses using a partitioning process to guarantee the isolation between different criticality levels.

Second, to analyze the effects of our proposed RDC on the system's performance, we detail the modeling of the CAN-AFDX architecture, and especially the RDC device and its implemented functions. Afterwards, we conduct timing analysis to compute end-to-end delay bounds and to verify real-time constraints. Preliminary performance analysis of our proposed RDC device through simple examples shows the efficiency of frame packing and traffic shaping processes to enhance resource savings in terms of AFDX bandwidth utilization.

Many RDC configurations can meet the system requirements while enhancing resource savings. Hence, we proceed to tuning of our RDC parameters to maximize as much as possible resource savings, and consequently to minimize the AFDX bandwidth utilization while meeting the system constraints. However, this RDC tuning problem turned to be a NP-hard problem, and adequate heuristic methods are introduced to find the accurate RDC parameters. Preliminary performance evaluation of our optimized RDC device has been performed, and obtained results show significant enhancements in terms of bandwidth utilization reduction, with reference to the currently used RDC device.

Finally, the performances of the proposed RDC device are validated through a realistic CAN-AFDX avionics architecture. Different I/O CAN loads have been considered to check the scalability of the integrated RDC functions, i.e., frame packing and traffic shaping. The obtained results confirm our first conclusions and highlight the ability of our proposed RDC device to maximize resource savings, while meeting the real-time constraints. For instance, the optimized RDC device offers a bandwidth utilization reduction of more than 40% compared to current RDC device.

**Keywords:** Multi-cluster avionics networks, AFDX, CAN, RDC design, Timing analysis, performance optimization, Validation

# List of Publications

- [**RTSS2011**] Hamdi Ayed, Ahlem Mifdaoui and Christian Fraboul. *Gateway Optimization for an Heterogeneous Avionics Network AFDX-CAN*. In: WIP session of the 32nd IEEE Real-Time Systems Symposium (RTSS), 29 Nov - 02 Dec 2011, Vienna, Austria.
- [**ETFA2012**] Hamdi Ayed, Ahlem Mifdaoui and Christian Fraboul. *Frame Packing Strategy within Gateways for Multi-cluster Avionics Embedded Networks*. In: 17th Emerging Technologies & Factory Automation (ETFA), Krakow, 17-21 Sept. 2012.
- [**ECRTS2013**] Hamdi Ayed, Ahlem Mifdaoui and Christian Fraboul. *Interconnection Optimization for Multi-Cluster Avionics Networks*. In: 5th Euromicro Conference on Real-Time Systems (ECRTS), 2013, 9-12 July 2013.
- [**SIES2014**] Hamdi Ayed, Ahlem Mifdaoui and Christian Fraboul. *Hierarchical Traffic Shaping and Frame Packing to Reduce Bandwidth Utilization in the AFDX*. In: 9th IEEE International Symposium on Industrial Embedded Systems (SIES), Pisa, 18-20 June.
- [**ESL2014**] Hamdi Ayed, Ahlem Mifdaoui and Christian Fraboul. *Enhanced RDC Device to Maximize Resource Savings for Avionics Networks*. In: IEEE Embedded Systems Letters (under submission).





# Contents

List of Publications	vii
List of Figures	xiii
List of Tables	xvii

<b>Introduction</b>
---------------------

Context and Motivation . . . . .	1
Original Contributions . . . . .	3
Thesis Outline . . . . .	4

<b>1 Background and Problem Statement</b>
---

1.1 Progress of Avionic Communication Architecture and Main Challenges . .	7
1.1.1 History of Avionic Architecture . . . . .	8
1.1.2 Appearance of Multi-cluster Avionic Networks . . . . .	9
1.2 Description of Network Standards . . . . .	13
1.2.1 ARINC 664: Backbone Network . . . . .	13
1.2.2 Sensors/Actuators Networks . . . . .	17
1.3 Description of RDC Standard: ARINC 655 . . . . .	22
1.3.1 RDC Requirements . . . . .	22
1.3.2 Functional Specifications . . . . .	24
1.3.3 Architectural Specifications . . . . .	25
1.4 Design Opportunities for Multi-Cluster Avionic Networks . . . . .	26
1.5 Conclusion . . . . .	28

<b>2 Related Work: Performance Optimization for Multi-Cluster Networks</b>
--

2.1	Optimizing Traffic-Source Mapping . . . . .	29
2.1.1	Avionics End-Systems . . . . .	30
2.1.2	Automotive End-Systems . . . . .	32
2.2	Optimizing Communication Network Performance . . . . .	33
2.2.1	Work on the AFDX Network . . . . .	34
2.2.2	Work on Sensors/Actuators Networks . . . . .	38
2.3	Optimizing Interconnection Devices . . . . .	41
2.3.1	CAN-Ethernet Bridge . . . . .	41
2.3.2	CAN-FlexRay Gateway . . . . .	42
2.3.3	ARINC 429-AFDX Gateway . . . . .	45
2.4	Need for Optimized CAN-AFDX Gateway . . . . .	46
2.5	Conclusion . . . . .	48

<b>3 Design of an Enhanced CAN-AFDX RDC</b>
---

3.1	Current RDC Device . . . . .	51
3.2	Enhanced RDC Functional Overview . . . . .	54
3.3	Frame Packing Strategies . . . . .	57
3.3.1	Related Work . . . . .	57
3.3.2	Dynamic Strategy: FWT . . . . .	59
3.3.3	Static Strategy: MSP . . . . .	60
3.4	Data Mapping & Formatting . . . . .	60
3.4.1	Data Mapping . . . . .	60
3.4.2	Frame Formatting . . . . .	61
3.5	Traffic Shaping Mechanism . . . . .	64
3.5.1	Related Work . . . . .	64
3.5.2	HTS Algorithm . . . . .	66
3.6	Conclusion . . . . .	67

<b>4 Modeling and Timing Analysis of the Enhanced RDC</b>
---

4.1	CAN-AFDX RDC Modeling . . . . .	69
4.1.1	Frame Packing Strategies Modeling . . . . .	71
4.1.2	HTS Mechanism Modeling . . . . .	75
4.2	Timing Analysis . . . . .	76
4.2.1	Sufficient Schedulability Test . . . . .	76
4.2.2	Timing Analysis for Upstream Flows . . . . .	78

4.2.3	Timing Analysis for Downstream Flows . . . . .	84
4.3	Preliminary Performance Analysis . . . . .	87
4.3.1	Considered Test Cases . . . . .	87
4.3.2	Impact of Frame Packing Strategy . . . . .	89
4.3.3	Impact of HTS Mechanism . . . . .	93
4.4	Conclusion . . . . .	95

<b>5 Performance Optimization of the Enhanced RDC</b>
---

5.1	Problem Formulation . . . . .	97
5.2	Optimization Process under FWT Strategy . . . . .	99
5.3	Optimization Process under MSP Strategy . . . . .	102
5.3.1	Bandwidth Best Fit Decreasing Heuristic . . . . .	104
5.3.2	Branch & Bound Algorithm . . . . .	106
5.4	Optimization process under HTS Mechanism . . . . .	110
5.4.1	Heuristic Approach . . . . .	110
5.4.2	Example . . . . .	111
5.5	Preliminary Performances Analysis . . . . .	112
5.5.1	Results under Optimized FWT Strategy . . . . .	113
5.5.2	Results under Optimized MSP Strategy . . . . .	114
5.5.3	Results under Optimized HTS Mechanism . . . . .	116
5.6	Conclusion . . . . .	117

<b>6 Avionics Case Study</b>
------------------------------

6.1	Description . . . . .	119
6.1.1	CAN-AFDX Architecture . . . . .	119
6.1.2	Communication Traffic . . . . .	120
6.1.3	Test Scenarios . . . . .	122
6.2	Benefits of Frame Packing Strategies . . . . .	122
6.2.1	Under FWT . . . . .	123
6.2.2	Under MSP . . . . .	124
6.2.3	Comparative Analysis and Conclusion . . . . .	124
6.3	Benefits of HTS Mechanism . . . . .	125
6.3.1	Impact of I/O CAN Bus Sharing on Frame Packing . . . . .	125
6.3.2	On the Effects of HTS Mechanism . . . . .	128
6.4	Conclusion . . . . .	129

**Conclusions and Prospectives**

Conclusions . . . . . 131  
Prospectives . . . . . 134

**A Network Calculus Overview**

A.1 Network Calculus Theory . . . . . 137  
    A.1.1 Cumulative Functions . . . . . 137  
    A.1.2 Arrival Curve . . . . . 138  
    A.1.3 Service Curve . . . . . 140  
    A.1.4 Network Calculus Bounds . . . . . 141  
    A.1.5 Concatenation and Blind Multiplexing . . . . . 142  
    A.1.6 Application to AFDX . . . . . 142  
A.2 WoPANets Performance Analysis Tool . . . . . 143  
    A.2.1 WoPANets Features and Structure . . . . . 144  
    A.2.2 Propagation Analysis Algorithm . . . . . 145  
    A.2.3 Illustrative Example . . . . . 147  
    A.2.4 Obtained Results . . . . . 148

**B Generalization for TTCAN bus**

B.1 TTCAN Description . . . . . 151  
B.2 TTCAN-AFDX RDC design . . . . . 154  
    B.2.1 FWT strategy . . . . . 154  
    B.2.2 MSP strategy . . . . . 156  
B.3 Timing Analysis . . . . . 157  
    B.3.1 Timing Analysis for RDC . . . . . 158  
    B.3.2 Timing Analysis on TTCAN . . . . . 159  
    B.3.3 Illustrative Example . . . . . 159

**Bibliography** **163**

# List of Figures

1.1	<i>Avionic network architecture: dedicated I/O networks</i>	11
1.2	<i>Centralized avionic architecture</i>	11
1.3	<i>Multi-cluster avionic network architecture</i>	12
1.4	<i>Distributed avionic architecture</i>	13
1.5	<i>Example of AFDX virtual links</i>	14
1.6	<i>Virtual Link bandwidth control mechanism</i>	14
1.7	<i>Three AFDX Virtual Links carried by a 100 Mbps Ethernet link</i>	15
1.8	<i>Example of application data flow on AFDX</i>	15
1.9	<i>AFDX frame format</i>	16
1.10	<i>ARINC 653 partitioning for AFDX end systems</i>	17
1.11	<i>Communication from application to application over AFDX with ARINC 653</i>	18
1.12	<i>ARINC 429 network architectures</i>	19
1.13	<i>ARINC 429 frame format</i>	19
1.14	<i>CAN protocol: CSMA/CR access mechanism</i>	20
1.15	<i>CAN 2.0 A frame structure</i>	21
1.16	<i>Synchronous mode for CAN-AFDX RDC</i>	25
1.17	<i>Asynchronous mode for CAN-AFDX RDC</i>	26
2.1	<i>Data packing and VLS allocation</i>	31
2.2	<i>Periodic execution of Partitions</i>	31
2.3	<i>Data packing of CAN frames</i>	32
2.4	<i>Multi-cluster automotive network architecture</i>	33
2.5	<i>Example of communication network</i>	36
2.6	<i>Optimization of sensors/actuators network performance</i>	38
2.7	<i>CAN-Ethernet communication architecture</i>	41
2.8	<i>CAN-FlexRay communication architecture</i>	43
2.9	<i>CAN-FlexRay Gateway functional structure</i>	43
2.10	<i>CAN-FlexRay Gateway operation diagram</i>	44
2.11	<i>Example of AFDX frame including multiple ARINC 429 labels</i>	45

2.12	<i>CAN-AFDX avionics architecture</i>	46
3.1	<i>Current CAN-AFDX RDC functional structure</i>	52
3.2	<i>Mapping table for the current RDC device</i>	52
3.3	<i>The current CAN-AFDX RDC: (1:1) strategy</i>	53
3.4	<i>Current CAN-AFDX RDC interconnection topology</i>	53
3.5	<i>Enhanced CAN-AFDX RDC functional structure</i>	54
3.6	<i>Packing CAN messages into AFDX frames</i>	55
3.7	<i>Frame unpacking process</i>	56
3.8	<i>FWT frame packing strategy for upstream flows</i>	59
3.9	<i>MSP frame packing strategy on upstream flows</i>	60
3.10	<i>Mapping table for enhanced RDC device</i>	61
3.11	<i>Structure of AFDX payload (ARINC 664)</i>	62
3.12	<i>Chosen AFDX payload structure</i>	62
3.13	<i>Explicit AFDX frame structure</i>	63
3.14	<i>Implicit AFDX frame structure</i>	63
3.15	<i>Hierarchical Traffic Shaping structure</i>	66
4.1	<i>CAN-AFDX network architecture</i>	69
4.2	<i>Upstream flows modeling from end-to-end</i>	70
4.3	<i>Downstream flows modeling from end-to-end</i>	70
4.4	<i>Example of CAN messages mapping onto AFDX VLs</i>	71
4.5	<i>Example of AFDX VLs allocation under FWT strategy</i>	73
4.6	<i>Example of AFDX VLs allocation under MSP strategy</i>	75
4.7	<i>End-to-end delay metric definition</i>	76
4.8	<i>Worst-case waiting time under FWT strategy</i>	78
4.9	<i>Worst-case waiting time under MSP strategy</i>	79
4.10	<i>Comparison between exact WCRT and upper bound (Example 2)</i>	84
4.11	<i>Test case 1: one sensors CAN bus interconnected to the AFDX</i>	87
4.12	<i>Test case 2: one sensors/actuators CAN bus interconnected to the AFDX</i>	88
4.13	<i>CAN WCRT of upstream flows</i>	94
4.14	<i>CAN WCRT of downstream flows</i>	94
5.1	<i>Optimization for FWT strategy</i>	99
5.2	<i>Impact of the waiting timer <math>\Delta</math> on the AFDX bandwidth consumption</i>	100
5.3	<i>Optimization for MSP strategy</i>	102
5.4	<i>Bandwidth-Best-Fit Decreasing heuristic</i>	105
5.5	<i>BB based algorithm example</i>	109

---

5.6	<i>Optimization for HTS mechanism</i>	110
5.7	<i>Example with the HTS heuristic approach (scenario 1)</i>	112
5.8	<i>Example with the HTS heuristic approach (scenario 2)</i>	113
5.9	<i>CAN WCRT of downstream flows</i>	116
6.1	<i>CAN-AFDX case study</i>	120
6.2	<i>AFDX network architecture (Courtesy of: ARTIST2 - IMA A380)</i>	121
6.3	<i>Impact of FWT frame packing strategy on AFDX bandwidth consumption</i>	123
6.4	<i>Impact of MSP frame packing strategy on AFDX bandwidth consumption</i>	124
6.5	<i>Bandwidth Utilization on the AFDX with shared I/O network</i>	126
6.6	<i>WCRT on CAN of upstream flows with shared I/O network</i>	127
6.7	<i>Impact of HTS mechanism on AFDX bandwidth consumption</i>	128
A.1	<i>Examples of Input and Output cumulative functions</i>	138
A.2	<i>Arrival curve</i>	139
A.3	<i>Example of leaky bucket arrival curve</i>	139
A.4	<i>Example of rate latency service curve</i>	140
A.5	<i>Backlog and delay bounds</i>	141
A.6	<i><math>\delta_T</math> service curve</i>	143
A.7	<i>WOPANETS Structure</i>	145
A.8	<i>The Input Topology of the Case Study</i>	147
A.9	<i>Maximal Delay Bounds Histogram (1Gbps)</i>	148
A.10	<i>Tool run time as a function of the number of hops and flows</i>	149
B.1	<i>TTCAN matrix cycle</i>	152
B.2	<i>Example of TTCAN matrix obtained using TDMA scheduling</i>	153
B.3	<i>Example of TTCAN matrix obtained using PSPQ scheduling</i>	154
B.4	<i>FWT strategy for TTCAN I/O network</i>	155
B.5	<i>MSP strategy for TTCAN bus</i>	157
B.6	<i>Worst Case Response Time on TTCAN</i>	159
B.7	<i>TTCAN bus interconnected to the AFDX</i>	160
B.8	<i>TTCAN schedule example for TTCAN upstream flows</i>	161





# List of Tables

4.1	Example 1: traffic characterization . . . . .	82
4.2	Example 1: exact WCRT vs upper bound . . . . .	83
4.3	Upstream flows description . . . . .	88
4.4	Downstream flows description . . . . .	89
4.5	Upstream flows description . . . . .	89
4.6	VLs characteristics under FWT . . . . .	90
4.7	End-to-end delay bounds under (1:1) strategy . . . . .	90
4.8	End-to-end delay bounds under FWT strategy with $\Delta_1$ , $\Delta_2$ and $\Delta_3$ . . . . .	91
4.9	MSP configurations considered for upstream flows in Table 4.3 . . . . .	91
4.10	Induced VLs characteristics under MSP configurations . . . . .	92
4.11	End-to-end delay bounds under MSP strategy . . . . .	92
4.12	Example 1: AFDX bandwidth consumption . . . . .	94
5.1	Comparative analysis of Optimization approaches . . . . .	104
5.2	Comparison between the optimization approaches for MSP configuration . . . . .	114
5.3	Impact of frame packing strategies . . . . .	115
5.4	Impact of HTS mechanism . . . . .	117
6.1	AFDX flows description . . . . .	121
A.1	Periodic Traffic Description . . . . .	147
A.2	Aperiodic Traffic Description . . . . .	148
B.1	Upstream flows description . . . . .	160
B.2	VLs characteristics under FWT for TTCAN . . . . .	161
B.3	End-to-end delay bounds under FWT strategy with $\Delta = 1ms$ . . . . .	161
B.4	MSP configurations . . . . .	162
B.5	TTCAN-AFDX RDC: schedulability test and AFDX bandwidth consumption	162



# Introduction

## Context and Motivation

The complexity of avionics communication architecture has increased rapidly due to the growing number of interconnected avionic systems and the expansion of exchanged data quantity. To follow this trend, the current architecture of new generation aircraft like the A350 consists of a high rate backbone network based on the AFDX (Avionics Full Duplex Switched Ethernet) [1] to interconnect the critical systems. Then, sensors and actuators are organized into one or more sensors/actuators networks based on low rate data buses like ARINC 429 [2] and CAN [3]. The obtained clusters are then interconnected via specific devices, called Remote Data Concentrators (RDCs) and standardized as ARINC 655 [4]. RDCs are modular gateways distributed throughout the aircraft to handle heterogeneity between AFDX-based backbone and peripheral data buses. The introduction of the RDC device aims mainly to reduce necessary cabling and to enhance the system modularity, with reference to prior network architectures. However, using RDC devices within the multi-cluster avionic networks raises challenging questions related to the impact of the RDC system performance in terms of network utilization.

The related work on the design and optimization of multi-cluster networks for avionics and automotive, and especially interconnection devices highlight the limitations of existing solutions in terms of resource management. In particular, the current RDC device implements a simple frame conversion strategy which consists in forwarding one frame on the destination network for each incoming frame from a source network. Due to frame size and data rate dissimilarities between network clusters, this frame conversion strategy may induce high communication overheads on the interconnected networks. Furthermore, current RDC device connects exactly one sensors/actuators network to the avionic backbone network which may imply an important number of RDC devices, and consequently inherent development and integration cost. Hence, the current RDC device offers the advantage of being simple to design and to configure; however, it is limited in terms of network resource savings, and it may induce additional system costs.

The objective of this thesis is to design and validate an enhanced RDC device for multi-cluster avionics networks, which integrates network resource savings techniques and meets timing constraints. To achieve this goal, we consider a CAN-AFDX case study as a representative avionic multi-cluster network, and we integrate new elementary functions within the RDC device. First, our proposed RDC implements a frame packing function to minimize the consumed AFDX bandwidth by an I/O CAN network. Then, a traffic shaping function is implemented in the RDC to isolate sensors flows from actuators flows on an I/O CAN bus. Furthermore, our proposed RDC allows the interconnection of multiple CAN buses to the AFDX backbone, while enforcing the segregation between different criticality levels using a partitioning mechanism compliant with ARINC 653 specifications [5]. The performance of our proposed CAN-AFDX RDC is evaluated using an analytical framework to prove the offered real-time guarantees when considering the nominal case of communication.

The tuning of our proposed RDC device is addressed to achieve the best RDC configuration, i.e., parameters of RDC minimizing the network resources utilization and guaranteeing the schedulability of communication. The RDC tuning problem is formulated as an optimization problem where: (i) the RDC frame packing and traffic shaping parameters are the variables; (ii) minimizing the AFDX bandwidth consumption due to the RDC device is the objective; (iii) the schedulability of communication flows crossing the CAN-AFDX network corresponds to the constraints. However, this optimization problem is considered as a NP-hard problem. Hence, to solve this latter in a polynomial time, we introduce heuristic approaches to find the accurate RDC configuration which maximizes resource savings.

The validation of our proposed RDC is done through a realistic case study under different load conditions. The analysis is conducted based on our developed tool WoPANets [6] which is able to analyze AFDX and CAN networks when integrating the impact of the different additional functions, i.e., frame packing and traffic shaping, within our proposed RDC device. The end-to-end latencies and the AFDX bandwidth consumption for the considered avionics CAN-AFDX network using our proposed RDC device are computed. The obtained results showed the efficiency of the frame packing process when applied for upstream flows to minimize AFDX bandwidth consumption. Moreover, the use of the traffic shaping mechanism when applied for downstream flows, combined with the frame packing process, has shown an interesting improvement of bandwidth utilization savings (up to 40%).

## Original Contributions

Our main contributions are as following:

- **Design of an enhanced CAN-AFDX RDC device:** the proposed RDC device consists of configurable elementary functions and it is capable to connect multiple I/O CAN buses to the AFDX backbone. The frame packing function is integrated to reduce communication overheads on the AFDX, with reference to a simple (1:1) frame conversion strategy, by grouping multiple CAN frames within the same AFDX frame. Moreover, a traffic shaping mechanism, called "Hierarchical Traffic Shaping" (HTS), is implemented in our proposed RDC device to isolate upstream and downstream flows on CAN bus, and consequently to favor frame packing process. Furthermore, our proposed RDC device is capable of interconnecting multiple I/O CAN buses to the AFDX backbone, while isolating data flows from different CAN buses by using partitioning technique compliant with ARINC 653 specifications [5]. This partitioning mechanism offers segregation between flows from different criticality levels and simplifies the data mapping process in the RDC device.
- **Performance analysis of the enhanced CAN-AFDX RDC device:** to prove the offered real-time guarantees and the capacity of our proposed RDC to save network resources, we introduce an analytical approach to evaluate the worst-case performance of a CAN-AFDX network interconnected using our enhanced RDC device. First, the modeling phase of the CAN-AFDX network including our proposed RDC device is described. Then, a timing analysis is introduced to evaluate the impact of the introduced functions within the RDC device on the communication performance.
- **Optimization of CAN-AFDX RDC parameters:** heuristic methods and algorithms for RDC device tuning are provided to increase as much as possible network efficiency in terms of AFDX network bandwidth consumption, which is considered as a relevant metric to assess network resource savings. First, we consider the case of specific CAN buses for either sensors or actuators to evaluate the impact of frame packing strategies on AFDX bandwidth consumption. Then, we consider the general case where an RDC device can support many I/O CAN buses interconnecting both sensors and actuators. The impact of the contention between upstream and downstream flows on AFDX bandwidth consumption is integrated.

- **Validation of the enhanced RDC device:** The validation of RDC capacity to save network resources and to meet avionics requirements is done through a realistic case study under different load conditions. The considered CAN-AFDX network includes several I/O CAN buses and an AFDX backbone with hundreds of AFDX flows. The interconnection of CAN buses to the AFDX is done using our enhanced RDC device. A performance evaluation is conducted under different test cases to highlight the ability of our proposed RDC device to save resources and to guarantee real-time constraints.

## Thesis Outline

This thesis consists of six chapters. **Chapter 1** gives an overview of the avionic context and the main requirements. First, a brief history of avionic architectures and the appearance of multi-cluster communication networks are described. Then, the main avionic network technologies are presented, and particularly the main features of ARINC 655 standard [4] for RDC devices. Finally, the design opportunities of multi-cluster avionic networks are discussed, and especially the impact of RDC devices on real-time performances of avionic networks.

**Chapter 2** presents the most relevant work related to the design and the optimization of multi-cluster avionics network. This state of the art covers different aspects varying from optimizing the performance analysis of the AFDX backbone and sensors/actuators networks, to tuning the traffic source mapping and interconnection devices configuration. Then, the main motivations and challenges to design and optimize the RDC device for CAN-AFDX network are detailed.

In **Chapter 3**, we introduce an enhanced CAN-AFDX RDC device. The proposed RDC consists of a set of elementary functions which aims to improve the RDC performance, with reference to the currently used RDC device. First, an overview of the functional structure of the enhanced RDC device is provided. Then, the integrated elementary functions within the RDC device are detailed, such as frame packing and traffic shaping functions.

In **Chapter 4**, to evaluate the timing performance of our proposed RDC device and to verify communication schedulability, we model the CAN-AFDX network architecture

including the enhanced RDC device. Then, a timing analysis process taking into account the impact of the new functions integrated into the RDC device on the communication performance is provided. Then, preliminary performance analysis is conducted through small scale test cases to estimate the offered network resource savings and to prove the real-time guarantees of our proposed RDC device.

Since many RDC configurations may be schedulable while offering different levels of resource savings on CAN-AFDX networks, we address in **Chapter 5** the tuning of the RDC device to achieve the best configuration, i.e., the parameters of the RDC functions minimizing the network utilization while meeting the time constraints. The tuning process of our proposed RDC device is first formulated as an optimization problem. Then, adapted heuristic approaches to find optimal RDC configuration are detailed. Afterwards, preliminary results obtained using the optimized CAN-AFDX RDC device with small scale test cases are provided.

In **Chapter 6**, to validate our proposed CAN-AFDX RDC device, we consider a realistic avionics case study with various load conditions. The end-to-end latencies and the AFDX bandwidth consumption induced by our proposed RDC device are computed. Then, a comparative study between different RDC configurations and under various traffic load conditions is conducted to highlight the capacity of our proposed RDC device to save network resources, while meeting the hard real-time constraints of the avionics applications.

Finally, we conclude with a discussion about the performance of our enhanced RDC device. Then, we present some directions that can be explored in the future.





# Chapter 1

## Background and Problem Statement

In this chapter, an overview of the evolution of avionic architectures and the appearance of multi-cluster avionic networks are first presented. Afterward, the main network technologies used in these architectures are described. Then, the ARINC 653 standard [4] for interconnection devices is presented from functional and architectural perspectives to highlight its role in multi-cluster avionic networks. Finally, the main design opportunities for multi-cluster avionic networks are discussed.

### 1.1 Progress of Avionic Communication Architecture and Main Challenges

To handle the increasing needs of avionic systems in terms of computing and Input/Output resources, the avionic architecture has evolved from federated architecture [7], i.e., functions are hosted by dedicated hardware, to Integrated Modular Architecture (IMA) [7], i.e., functions share common hardware modules (e.g. CPU module, I/O module). As a part of the avionic architecture, the communication networks have also evolved from low rate dedicated data buses (e.g. ARINC 429 [2]) to multiplexed field-buses (e.g. MIL-STD-1553B [8], ARINC 629 [9], CAN [3]), and more recently switched networks, e.g. ARINC 664 [1]. Although this progress offers a more scalable architecture to support distributed avionic functions, it has raised at the same time several challenges related mainly to the system's performance and resources utilization. In this section, we first present an overview of avionic architecture evolution. Afterwards, we focus on multi-cluster networks, used in modern aircraft to support communication between avionic end-systems, and we identify their main challenges.

### 1.1.1 History of Avionic Architecture

At the beginning of aircraft's industry, avionics functions were hosted by dedicated hardware with their proper processing units, which are directly attached to their Input/Output interfaces to get required data and perform some computations. Then, processed data are exchanged with other avionic functions. This avionic architecture, called federated architecture, has been used for decades for avionics systems to support safety-critical functions and to guarantee system's requirements. This avionic architecture offers a high isolation level due to the dedicated hardware, i.e., dedicated processing resources and I/O interfaces. However, with the increasing number of avionic functions, the federated architecture reached its limits due to the important number of required hardware, and consequently inherent system weight and costs.

In the last two decades, Integrated Modular Architecture (IMA) has been introduced as an alternative to federated architecture. The IMA concept consists in using a set of common hardware modules (e.g. CPU module, I/O module) to support several applications with different safety levels. Hence, the system's resources have become shared between several avionic functions, while isolation is still guaranteed at the software level using partitioning techniques. For instance, the ARINC 653 [5] standard specifies a partitioning mechanism, which provides isolation between avionics functions hosted within the same avionics system. This isolation is achieved by restricting the address space of each partition and limiting the amount of CPU time reserved for each partition. The objective is to ensure that an errant avionics function running in one partition will not affect functions running in other partitions

As the avionic architecture evolved, the avionic communication system has also evolved to follow the increasing demand on communication resources and the emerging requirements of IMA architecture. Using federated avionic architecture implied a low exchanged data between subsystems, and consequently using point-to-point connections, such as ARINC 429 [2] bus standard, was efficient. However, with the IMA approach, an increasing number of avionic functions and exchanged data quantity have to be supported. Hence, the ARINC 429 bus became no longer effective due to its low data transmission rate and high required cabling. Therefore, new communication standards have been introduced to meet these emerging requirements with IMA architectures. For instance, AFDX [1] standard, based on Switched Ethernet at 100 Mbps was introduced by Airbus in the A380 as a high speed backbone network.

## 1.1.2 Appearance of Multi-cluster Avionic Networks

In this section, we first present the main avionics requirements. Then, we review the recent progress of the avionic communication networks, used with IMA architecture.

### 1.1.2.1 Avionics Requirements

The avionic network as a part of the avionics system has to fulfill a set of requirements [10]. The main ones are as follows:

- **Predictability:** The avionic network must behave in a predictable way and appropriate proofs to guarantee its determinism have to be provided by the network designer. For example, the communication latencies, the backlog in a network node or the packet loss rate have to be bounded. The required proof depends on the avionics application. For instance, consider an air pressure sensor that produces a measurement each 10 ms and sends it through the avionic network to one or many calculators to perform some computations. To meet predictability requirement, a network designer can check that each pressure measurement is delivered to its destinations within 10 ms from its production instant to its end of reception at the calculator. Moreover, the average loss rate of pressure measurements may also be assessed to estimate the calculation quality.
- **Reliability:** The avionic network must be fault-tolerant and fulfill minimum safety levels. One aspect related to the avionics system reliability consists in preventing failed nodes in the network from affecting the normal operations. Several mechanisms can be used to improve the reliability and the robustness of the communication network in avionics context. It is common to use multiple redundant data paths to enhance the network fault tolerance, such a mechanism is supported by the AFDX protocol [1]. Moreover, retransmission mechanisms can be implemented inside network nodes to recover packet losses. Furthermore, redundant nodes can be used to recover and replace a faulty node during operation time.
- **Modularity:** This requirement is related to the flexibility and exchangeability of components between avionic systems. An important step towards enhancing the avionics system modularity has been taken by adopting IMA approach for avionic architecture design. Avionic systems consist of common elementary components, which can be configured to fit different avionic applications. The integration of such components requires well-defined hardware and software interfaces. The hardware

configuration of avionic systems must allow easy maintenance. The modularity of avionic systems allows to exchange components and even systems with minimum configuration and readjustment effort. This fact facilitates system's maintenance and future evolution, such as adding new avionics functions or replacing existing ones.

- **Cost and life cycle:** These requirements are related to the maintainability, manageability and direct costs associated with the avionics system development and maintenance. One important step towards reducing avionics system costs was done with the modular design introduced by the IMA approach. The flexibility and configurability of avionic systems reduce development cycle duration, and ease incremental design process and maintenance operations. Furthermore, the use of commercial off-the shelf (COTS) technologies and components, which are cheap and largely available, aims to reduce development and deployment costs of the avionics system. Although the use of COTS technologies in the avionics context required additional development effort due to the strict avionics requirements, this choice offers significant system's cost reduction and it is currently an attractive alternative for aircraft manufacturers. The introduction of the AFDX [1] network protocol, based on Switched Ethernet, is a typical example on how COTS technologies may be adopted for avionics use with additional development effort to fulfill avionics requirements and to reduce costs.

### 1.1.2.2 Description and Main Challenges

The complexity of avionic communication architecture is increasing rapidly due to the growing number of interconnected subsystems and the expansion of exchanged data quantity. To follow this trend, the architecture of new generation aircraft, such as the A380, consists of a high rate backbone network based on the AFDX [1] to interconnect the critical subsystems, as shown in Figure 1.1. Then, each specific avionic subsystem is directly connected to its associated Input/Output (I/O) network based on low rate data buses, such as ARINC 429 [2] and CAN [3].

Although this architecture simplifies the design process and reduces the time to market, it leads at the same time to inherent weight and integration costs due the important number of sensors/actuators networks. In addition, this architecture makes the avionics subsystems closely dependent on their Inputs/Outputs and no longer interchangeable. However, for avionic applications, it is essential that the communication architecture ful-

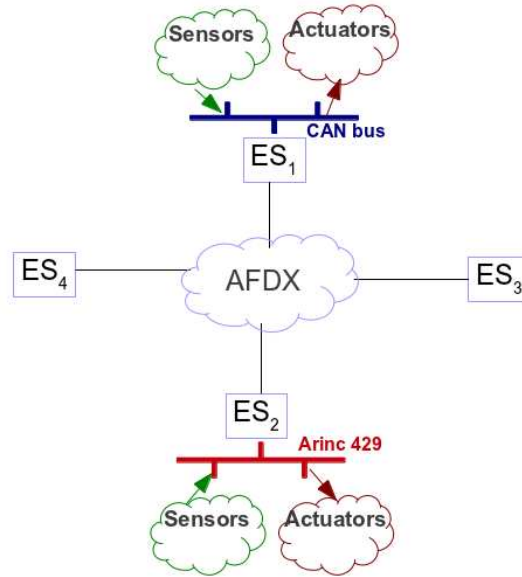


Figure 1.1: Avionic network architecture: dedicated I/O networks

fills the emerging requirements in terms of modularity and performance to guarantee an easy incremental design process and the possibility of adding new functions during the aircraft lifetime.

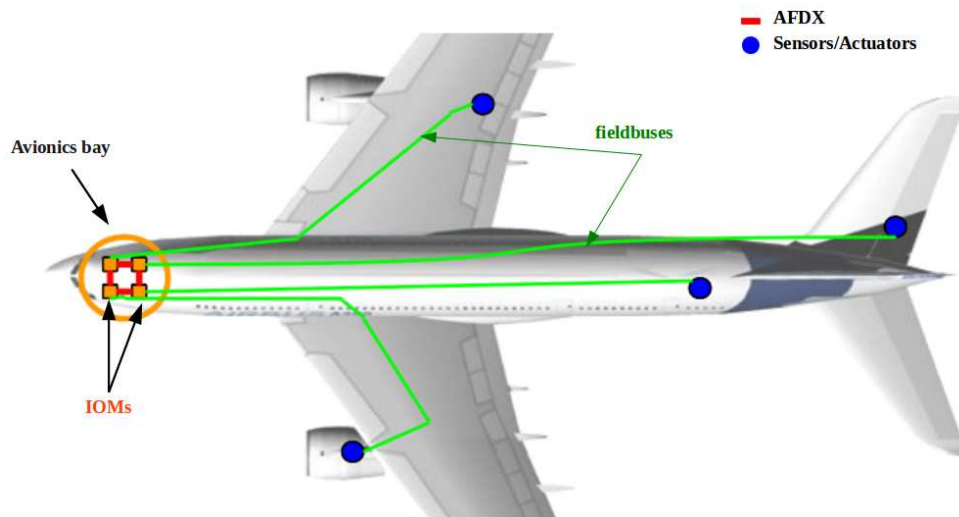


Figure 1.2: Centralized avionic architecture

On the other hand, as shown in Figure 1.2, systems connected using AFDX were centralized in the avionic bay. This fact implies high cabling quantities, since each I/O

network requires dedicated cabling to communicate with its corresponding AFDX end-system. This cabling is done through long distances going generally from the aircraft wings and tail, where most of sensors and actuators are located, to the main avionic bay at the front of the aircraft.

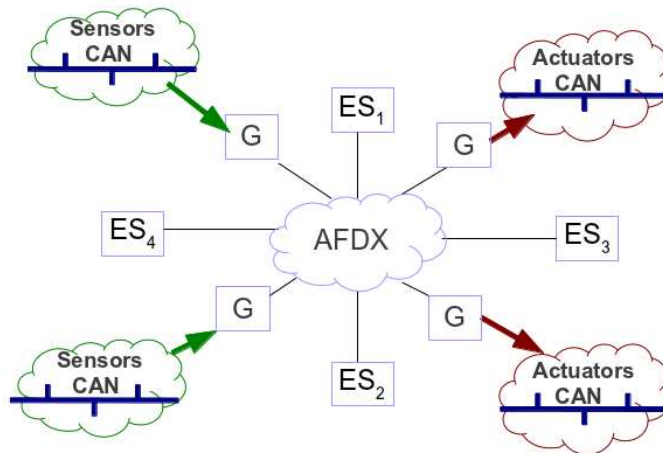
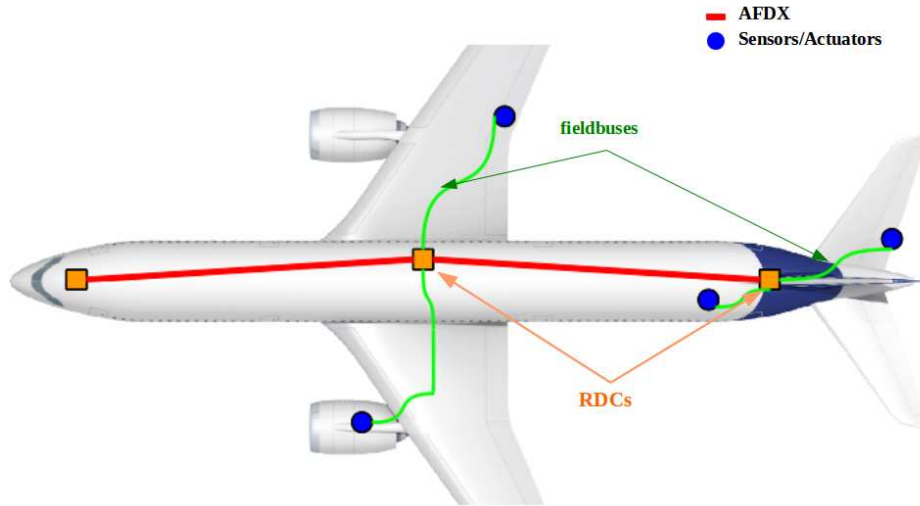


Figure 1.3: *Multi-cluster avionic network architecture*

To handle these limitations, the solution, implemented in recent aircraft, such as A350 and A400M, consists in keeping the AFDX as a backbone network to interconnect the critical avionic systems, and dissociating the sensors and actuators from their corresponding end-systems. As shown in Figure 1.3, the obtained clusters are interconnected via specific devices, called Remote Data Concentrators (RDCs), and standardized as ARINC 653 [4]. RDCs are modular gateways distributed throughout the aircraft, as shown in Figure 1.4, to handle heterogeneity between the AFDX backbone network and peripheral data buses.

This alternative architecture enhances the avionic subsystems modularity and simplifies the reconfiguration process. The RDC actually becomes the main node that needs to be reconfigured in case of sensor or actuator modification. Furthermore, distributing RDC devices in the aircraft reduces considerably the required network cabling. However, at the same time it represents one of the major challenges in the design process of such multi-cluster avionic networks.

Figure 1.4: *Distributed avionics architecture*

## 1.2 Description of Network Standards

In this section, we present the main features of the AFDX network used in current avionics architectures as a high speed backbone network. Then, we describe the main network technologies used for I/O networks: ARINC 429 and CAN.

### 1.2.1 ARINC 664: Backbone Network

The AFDX [1] network is based on Full Duplex Switched Ethernet at 100 Mbps, successfully integrated into new generation civil aircraft, such as the A380 and the A400M. This technology succeeds to support the important amount of exchanged data and to guarantee timing requirements, due to its high data rate, its policing mechanism in switches and the Virtual Link (VL) concept.

#### 1.2.1.1 Virtual Link

AFDX virtual link gives a way to reserve a guaranteed bandwidth to each traffic flow. The VL represents a multicast virtual channel which originates at a single end-system and delivers its packets to a fixed set of end-systems, as shown in Figure 1.5. Each VL is characterized by: (i) BAG (Bandwidth Allocation Gap), ranging in powers of 2 from 1 to 128 milliseconds, which represents the minimal inter-arrival time between two consecutive

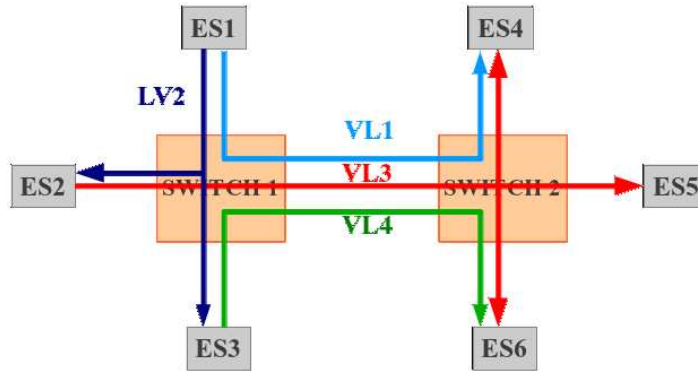


Figure 1.5: Example of AFDX virtual links

frames; (ii) MFS (Maximal frame size), ranging from 64 to 1518 bytes, which represents the size of the largest frame that can be sent during each BAG. The VL control mechanism is illustrated in Figure 1.6.

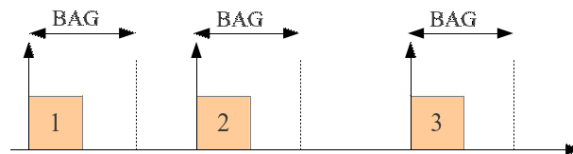


Figure 1.6: Virtual Link bandwidth control mechanism

Using the VL control mechanism, a 100 Mbps Ethernet link can support multiple Virtual Links. For instance, in Figure 1.7 three Virtual Links are carried by a single Ethernet physical link. The figure also shows that the messages sent on AFDX Ports 1, 2, and 3 are carried as sub-VLs by VL 1. Similarly, messages sent on AFDX Ports 6 and 7 are carried by VL 2, and messages sent on AFDX Ports 4 and 5 are carried by VL 3.

### 1.2.1.2 Message flows & Frame Structure

The end-to-end communication of a message using AFDX requires the configuration of the source end-system, the AFDX network and the destination end-systems to deliver correctly the message to the corresponding receive ports. Figure 1.8 shows a message M being sent to Port 1 by the avionics subsystem. End system 1 encapsulates the message in an AFDX frame and sends it to the AFDX into the VL 100 (the destination addresses are specified by VLID 100). The forwarding tables in the network switches are configured



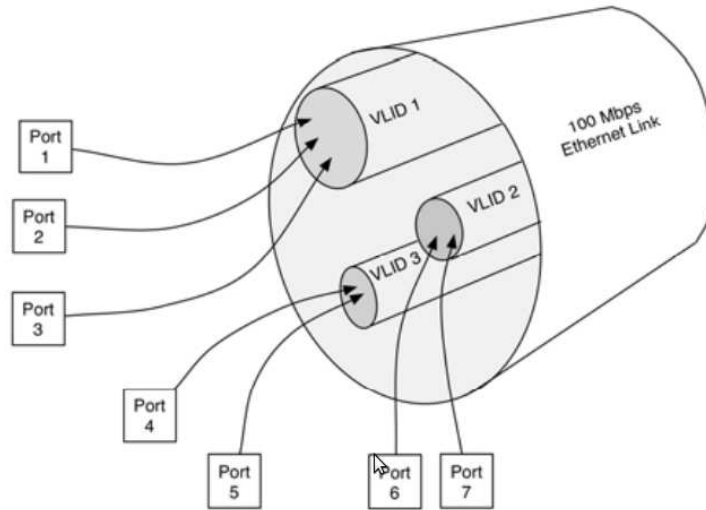


Figure 1.7: Three AFDX Virtual Links carried by a 100 Mbps Ethernet link

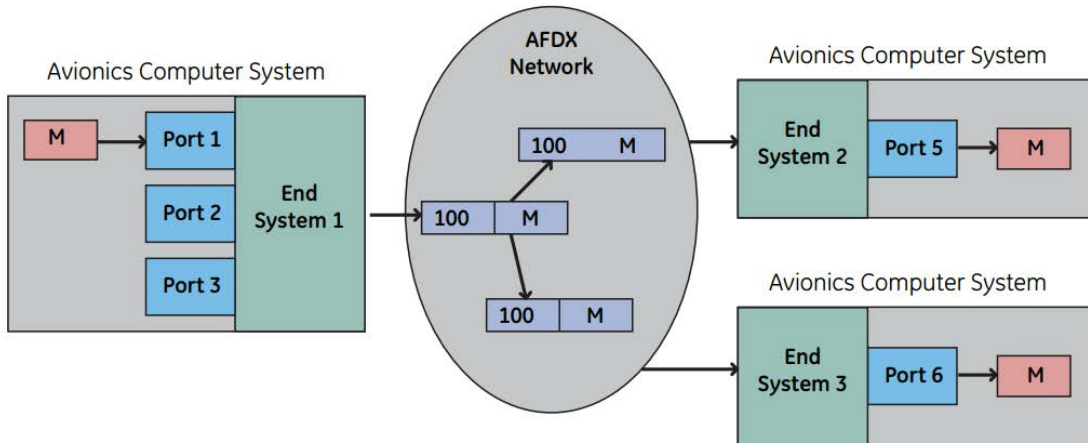


Figure 1.8: Example of application data flow on AFDX

to deliver the frame to both end-systems 2 and 3. The end-systems are configured to be able to determine the destination ports for the message contained in the frame. In this case, the message is delivered by end-systems 2 and 3 to ports 5 and 6, respectively.

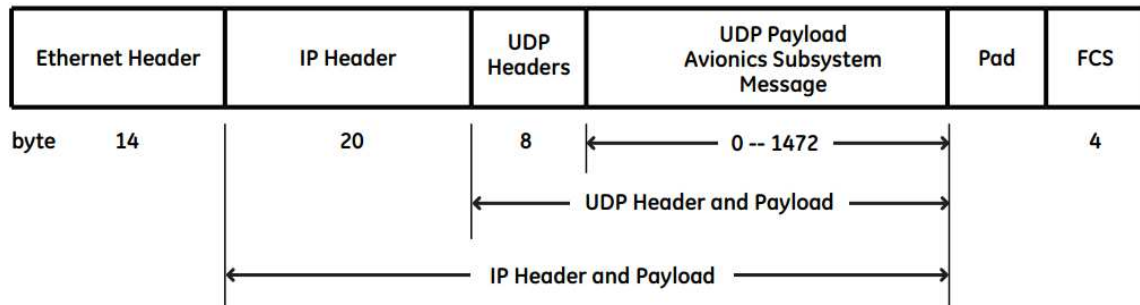


Figure 1.9: AFDX frame format

An AFDX frame is based on the Ethernet frame, as shown in Figure 1.9. The Ethernet header allows the identification of the source and destinations end-systems. The IP and UDP headers allow each destination end-system to find the corresponding destination port for the received message within the Ethernet payload. The Ethernet payload consists of the IP packet (header and payload). Then, the IP packet payload contains the UDP packet (header and payload), which contains the message sent by the avionics applications. Padding is used only when UDP payload is smaller than 18 bytes, to ensure a minimum AFDX frame size of 64 bytes. The maximum frame size is 1518 bytes without counting the IFG (Inter-Frame Gap) of 12 bytes and the preamble of 8 bytes. This IFG and preamble have to be considered when performing timing analysis to take into account the overhead of data transmission over the AFDX network.

### 1.2.1.3 Application Layer: ARINC 653 Specifications

As shown in Figure 1.10, an avionics system is connected to the AFDX network through an end-system. In general, an avionics system is capable of supporting multiple avionics subsystems. A partitioning mechanism, compliant with ARINC 653 [5] specifications, provides isolation between avionics subsystems within the same avionics system. This isolation is achieved by restricting the address space of each partition and by placing limits on the amount of CPU time reserved for each partition. The objective is to ensure that an errant avionics subsystem running in one partition will not affect subsystems running on other partitions.

Hence, avionics applications are assigned to ARINC 653 partitions and communication between them is ensured using communication ports. In the example of Figure 1.11, three AFDX end-systems communicate through an AFDX network. Each end-system runs two

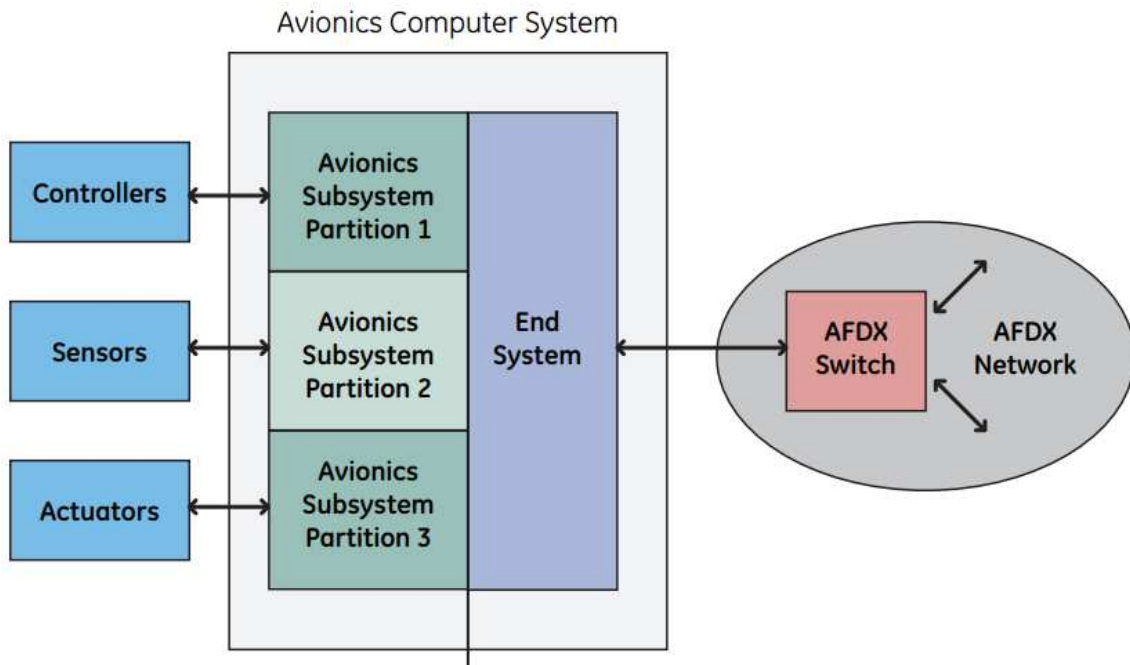


Figure 1.10: *ARINC 653 partitioning for AFDX end systems*

partitions which host avionics applications. Partition 1 of end-system 1 communicates with partition 1 of end-system 2 using partitions ports (source port 1 of partition 1 of end-system 1 and destination port 2 of partition 1 of end-system 2). As we can see from this example, data flows originated from the same ARINC 653 partition in an AFDX end-system can share the same VL at the MAC layer. However, data flows from different partitions are not allowed to share VLs to guarantee segregation between partitions on AFDX network.

## 1.2.2 Sensors/Actuators Networks

### 1.2.2.1 ARINC 429

The ARINC 429 standard [2] is a widely used avionic data bus that has been deployed in various avionic applications for decades. This standard relies on unidirectional communications with a single transmitter and up to twenty receivers. Connected devices, Line Replaceable Units (LRUs), can be organized in a star or bus topologies as shown in Figure 1.12. Each LRU may host multiple transmitters or receivers communicating on different ARINC 429 buses. This simple architecture of ARINC 429 bus offers a highly reliable

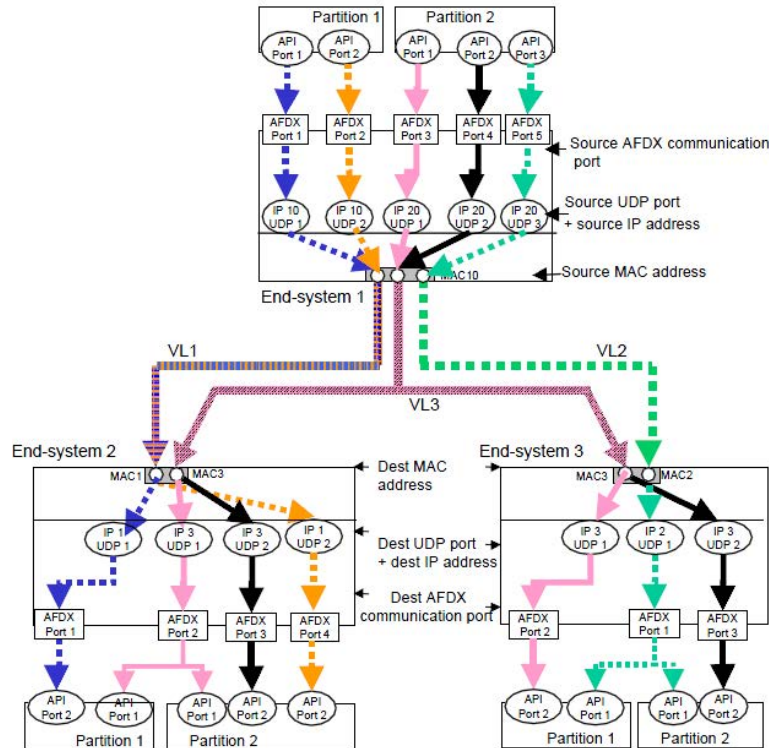


Figure 1.11: *Communication from application to application over AFDX with ARINC 653*

communication with short transmission latencies.

ARINC 429 data transfer is based on 32 bit data word, as described in Figure 1.13. ARINC 429 data words are made up of five primary fields:

- Parity (1 bit): allowing error check to guarantee accurate data reception;
- Sign/Status Matrix (SSM) (2 bits): can be used to indicate the sign or direction of the words data, or to report source equipment operating status. This field is dependant on the data type;
- Data/Payload (19 bits): containing the word’s data information;
- Source/Destination Identifier (SDI) (2 bits): indicating which source is transmitting the data or for which receivers the data is destined;
- Label (8 bits): is used to identify the word’s data type and can contain instructions

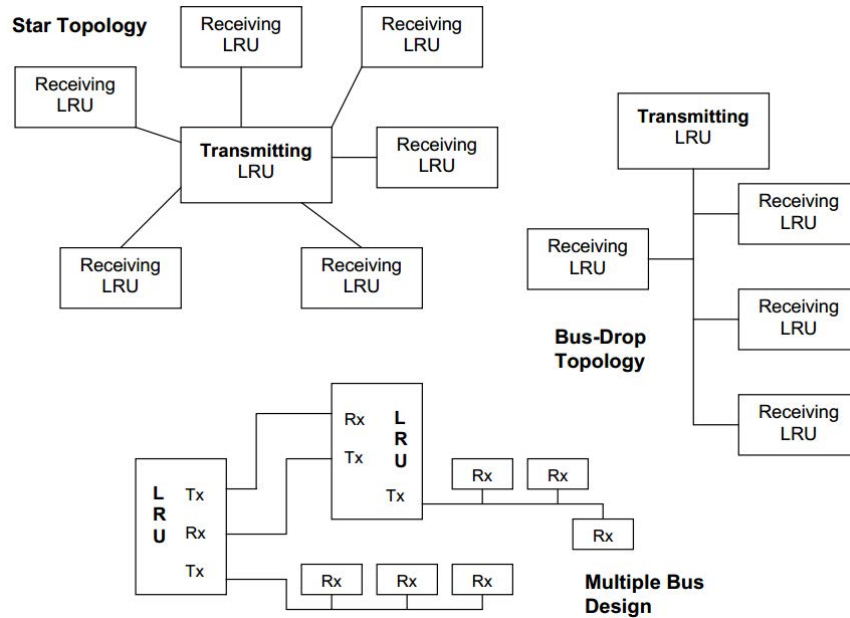


Figure 1.12: ARINC 429 network architectures

or data reporting information. Labels may be further refined using the first 3 bits of the data field as an Equipment Identifier to identify the source.

ARINC 429 specifies two speeds for data transmission: high speed operates at 100 Kbit/s and low speed operates at 12.5 Kbit/s. ARINC 429 operates in such a way that each single transmitter communicates in a point-to-point connection with its receivers. This fact requires an important amount of cables which significantly increases the overall aircraft weight. This traditional data bus is no longer effective in meeting the emerging requirements of avionic applications in terms of throughput demand and modularity.

<b>MSB</b>																<b>LSB</b>															
32	31	30	29	28	27	26	25	24	23	22	21	20	19	18	17	16	15	14	13	12	11	10	9	8	7	6	5	4	3	2	1
<b>P</b>	<b>SSM</b>	<b>Data</b>														<b>LSB</b>	<b>SDI</b>	<b>Label</b>													

Figure 1.13: ARINC 429 frame format

### 1.2.2.2 CAN

The Controller Area Network (CAN) data bus was designed in the 80s by Robert Bosch GmbH [3] for automotive applications. Its success due to its reliability and its versatility attracted the attention of manufacturers in other industries, including process control, medical equipment, and recently avionics.

The CAN bus operates at data rates up to 1Mbps for cable lengths less than 40m, and 125Kbps when the length is around 500m. Two versions of the CAN protocol are specified: CAN 2.0 A and CAN 2.0 B. The first uses the standard frame format, that supports a 11-bit identifier, while the second uses an extended frame format in which the identifier consists of 18 additional bits (for a total of 29 bits). Controllers connected to the CAN bus must transmit and receive data while avoiding collisions using the Carrier Sense Multiple Access with Collision Resolution (CSMA/CR) mechanism.

- **Message arbitration:** a bus terminal can start a new transmission only when the bus is idle. However, if two terminals try to transmit at the same time, then an arbitration protocol is implemented to allow the transmission of the message with the highest priority (Arbitration based on Message Priority or AMP).

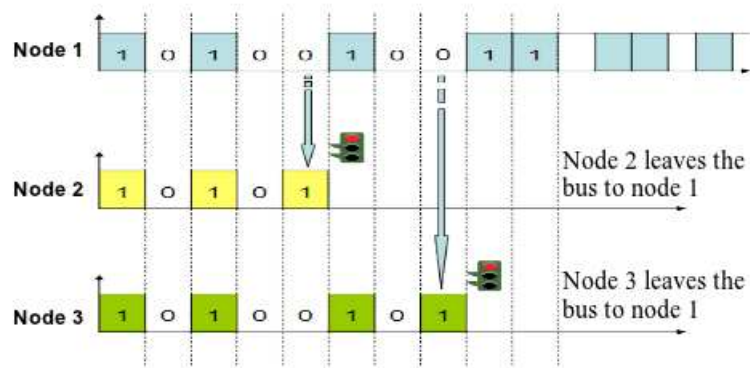


Figure 1.14: CAN protocol: CSMA/CR access mechanism

The bus signal can have two logic values, dominant and recessive: whenever two terminals attempt a simultaneous transmission of a dominant bit and a recessive bit, a dominant logic value will result on the bus. In a typical implementation of a wired connection 0 is the dominant value, and consequently this is often called an AND implementation. As shown in Figure 1.14, the first controller that loses the contention, i.e., sending a recessive bit and reading a dominant value resulting on

the bus, must immediately stop its transmission. This fact results in an arbitration technique based on the message header, which determines the communication priority. CAN is based on broadcast communications where each transmitted frame is received by all the connected terminals. Each node will determine if the received frame is relevant to that particular system or not, and drop packets that were not addressed to it.

- **Frame structure** as shown in Figure 1.15, CAN data frames consist of a payload up to 8 bytes and an overhead of 6 bytes due to the different headers and bit stuffing mechanism.

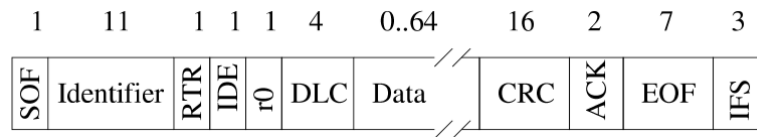


Figure 1.15: CAN 2.0 A frame structure

Each CAN frame consists of the following bit fields:

- Start Of Frame (SOF) (1 bit): is always a dominant bit marking the beginning of a transmission;
- Arbitration (13 bits): consists of the Identifier, the Remote Transmission Request (RTR) for a standard frame (or the Substitute Remote Request (SRR) for an extended frame), and finally the Extension bit IDE to determine if the frame is standard or extended. It identifies the type of CAN message and defines its transmission priority on CAN bus;
- Control (5 bits): is composed of  $r_0$  and  $r_1$ , reserved bits that are always dominant; and the Data Length Code (DLC) of 4 bits, which specifies the number of bytes present in the Data field;
- Data (1-64 bits): contains the actual information;
- CRC (16 bits): is used to guarantee data integrity;
- ACK (2 bits): allows receivers to acknowledge correct received messages;

- End Of Frame (EOF) ( 7 bits): indicates the end of the CAN frame;
- Intermission Frame Space (IFS) (3 bits): is the minimum number of bits separating consecutive messages. During this intermission period no other communication can start on the CAN bus.

To ensure a strong synchronisation, the protocol avoids the presence of more than 5 consecutive bits of the same value in the transmitted frame by adding a stuffing bit with the opposite value. Stuff bits increase the maximum transmission time of CAN messages. Including stuff bits and the inter-frame space, the maximum transmission time  $C_m$  of a CAN message  $m$  including  $b_m$  data bytes were proven in [11] and are given by the following expressions:

- for 11-bit identifiers,

$$C_m = (55 + 10 * b_m) * \tau_{bit} \quad (1.1)$$

- and for 29-bit identifiers,

$$C_m = (80 + 10 * b_m) * \tau_{bit} \quad (1.2)$$

where  $\tau_{bit}$  is the transmission time for a single bit.

## 1.3 Description of RDC Standard: ARINC 655

The Remote Data Concentrator (RDC) [4] is a gateway that performs protocol conversion to guarantee interoperability between avionic systems with different communication interfaces and specific communication protocols. Typically, it translates data from various sources, e.g. sensors and actuators, into a format usable by avionic computing resources. It also converts data from computing resources into appropriate formats usable by various sensors and actuators equipments. ARINC 655 standard [4] was introduced as a high-level design guide for RDCs. It mainly reviews the requirements to fulfill by RDC devices for avionic networks. Moreover, it provides guidelines concerning the design of RDC devices.

### 1.3.1 RDC Requirements

The RDC device inherits from avionics requirements described in Section 1.1.2.1 and particularly:



- **Predictability:** the process of reception and transmission of data by the RDC device introduces additional network latency. For critical avionics applications, the system designer must ensure that the end-to-end data latency is less than the required deadline. Therefore, it is important to determine the permissible latency for each system that uses this information at the beginning of the design process.
- **Reliability:** the designer of RDC device should consider a fault tolerant design. The level of fault tolerance is determined by the analysis of the system integrity goals, the required availability of the function and the overall maintenance procedure.
- **Modularity:** RDC device should be modular, i.e., composed of standard modules that can be easily replaced. RDC devices should be exchangeable and reconfigurable, such that the replacement of a RDC device does not require long and complex adjustments.
- **Cost and life cycle:** network designer should consider minimizing the different types and number of required RDCs for an avionic network. This fact aims at reducing manufacturing costs, by reducing the system weight and simplifying its development.

Furthermore, an RDC device has to meet some additional requirements related to its role as an interconnection device:

- **Interoperability:** the primary purpose of an RDC device is to ensure interoperability of avionic systems of different manufacturers. Appropriate network interfaces should be integrated into the RDC and data formats conversion functions should be implemented to guarantee communication transparency between avionic systems. The mapping of packets format has to be ensured between a source and a destination network interconnected by the RDC device.
- **Adaptability:** the RDC should be able to interface with a variety of data buses and other network technologies used in aircraft. The RDC should be configurable to be customized for different interconnection applications with different performance requirements.

- **Resources utilization efficiency:** the RDC should keep communication overheads as low as possible when forwarding data flows from a source to a destination network. This fact saves network resources and keeps margins for the future evolution of the avionic architecture.

To meet the main RDC requirements, the ARINC 655 specifications provide some recommendations and guidelines which can be grouped into two categories: functional and architectural. These specifications will be detailed in the next sections.

### 1.3.2 Functional Specifications

The RDC device should include appropriate functions to receive, process and forward data from typical avionic I/O networks to the processing computers and vice versa. The main functions that should be integrated into the RDC device are:

- **Data Mapping:** the RDC should perform the conversion of the received data format to fit the target network format. A configurable mapping table should be used to map data type and address to fit the requirements of the destination networks. The mapping table should be static and well configured to guarantee the required safety and timing performance levels. Furthermore, as several RDCs devices may be used within the same network, a consistent mapping process should consider all the mapping tables in RDC devices;
- **Data Forwarding:** the RDC should forward data received from an input network interface to one or several output interfaces. The RDC may be used to connect two or more network clusters. Therefore, a forwarding function is required to define for each received data the output interfaces. A simple solution consists in using a static forwarding table that is configured offline in the RDC device by the network designer;
- **Data processing:** the RDC may include software functions, such as data sampling, filtering and monitoring. These software functions may also perform range checking, data validity and fault detection. These functions may increase end-to-end communication latencies, and should be taken into account during the timing analysis and the validation of the RDC behavior.

### 1.3.3 Architectural Specifications

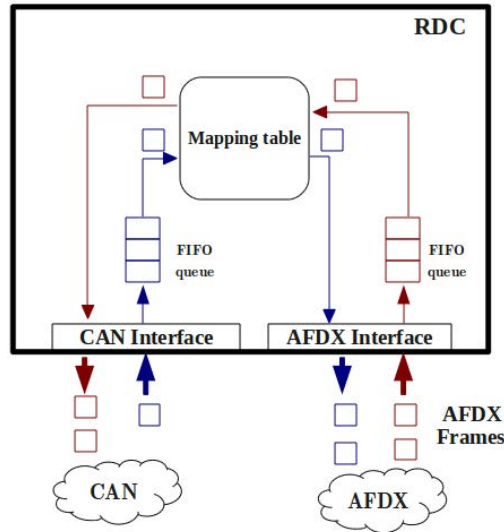


Figure 1.16: *Synchronous mode for CAN-AFDX RDC*

The main RDC's architectural recommendations are:

- **Communication scheme:** two communication schemes are described in ARINC 653 specifications:
  - *Synchronous RDC:* in this case, the processing and forwarding of a received data by the RDC is triggered by the event of data reception. An example of a synchronous CAN-AFDX RDC is shown in Figure 1.16.
  - *Asynchronous RDC:* in this case, the rates and instants of data exchanges between the RDC and connected networks are determined by the RDC. The RDC implements a write/read table where data from different equipments communicating with the RDC are gathered. An example of an asynchronous CAN-AFDX RDC device is shown in Figure 1.17. For each type of messages, a received message in the RDC overwrites the old one and a binary freshness indicator is used. The transmission of data flows is done periodically with transmission rates defined in the RDC. One significant advantage of this asynchronous mode consists in adapting data rates between the source producing and the destinations receiving data. For example, consider a sensor producing the air pressure measurement each 2 ms. Consider computing systems consuming this data to perform a computation

once each 10 ms. Since sensor data is produced at a higher rate than the required one, then the RDC may adapt production rates by reading the pressure data from its write/read memory once each 10 ms.

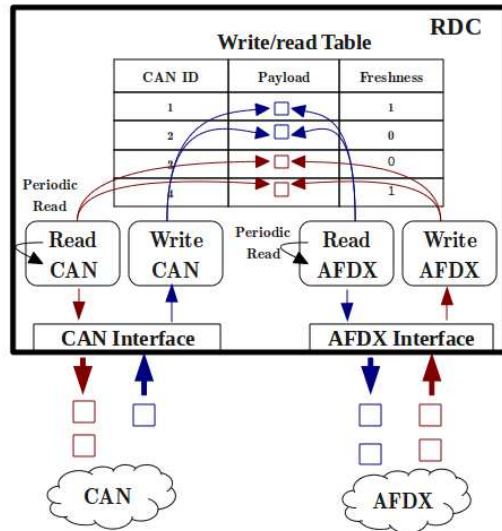


Figure 1.17: Asynchronous mode for CAN-AFDX RDC

- **Partitioning:** the RDC should interconnect multiple sub-networks which may have different levels of criticality. Therefore, a partitioning process should be used in the RDC to keep isolation between communication flows having different criticality levels.

## 1.4 Design Opportunities for Multi-Cluster Avionic Networks

As described in Section 1.1.2.2, the main benefits of multi-cluster avionic networks are the use of old equipments with new ones, and the reduction of weight and I/O resources. For instance, the use of RDC devices allows cabling reduction, and enhances the modularity and exchangeability of the avionic end-systems.

However, the use of multi-cluster networks in the avionics context arises mainly the following challenges:

- **Software/Hardware (SW/HW) Mapping:** the avionics system consists of a set of applications which need to exchange data; and a set of communicating nodes via data buses or other network technologies. Each node can host one or multiple applications. The mapping of applications onto network nodes is an important task when designing the avionics networks. This mapping will clearly impact the resource utilization and real-time performance of the avionics system, and it has to be considered during network integration phase. Hence, the designer should select the SW/HW mapping maximizing the resource savings while meeting real-time requirements.
- **End-to-end communication performance:** avionics networks have to fulfill real-time constraints requirements. Bounding the total delay of each data from a source to one or many destination nodes is an important issue to fulfill the predictability requirement, and particularly the stability for closed loop control in avionics. In multi-cluster networks, the latency between data input and its corresponding output are due to: (a) communication latency through network clusters (e.g. data buses and backbone networks); (b) interconnection latency due to the traversal of gateways. These delays depend on the scheduling policies used in the network nodes (e.g. source and destination end-systems, switches and gateways), and the observed contentions on shared networks. Hence, appropriate modeling and analysis techniques should be used to prove that the avionics network meets the real-time requirements.
- **Design of interconnection device and interoperability issues:** the interconnection devices have a major importance in multi-cluster avionics networks, since they allow heterogeneous network technologies to exchange data and to keep end-to-end connectivity between avionics systems. The RDC [4] is an avionics interconnection device used typically to connect sensors/actuators networks with the backbone network connecting computing units. Therefore, the RDC device has: (i) to ensure frame formats conversion and consistent addressing of data packets between source and destination networks; (ii) to offer bounded latency and a predictable behaviour; (iii) to ensure the isolation of data flows with different criticality levels. Furthermore, the inter-cluster communication through the RDC device may induce high communication overheads due to the dissimilarities between interconnected network clusters in terms of rates and frame formats. Hence, the impact of RDC device on resource utilization has to be considered, and design choices reducing the communication overheads between interconnected networks should be integrated.

## **1.5 Conclusion**

Current civil avionic communication architecture consists of several network clusters, interconnected using RDC devices standardized under the ARINC 655. These multi-cluster networks present the advantage of allowing the use of old data buses in conjunction with new network technologies, such as the AFDX protocol. This fact reduces development costs of new equipments and guarantees the incremental design of avionics systems. However, the performance optimization of multi-cluster avionic networks arise several challenges, which are mainly due to: (i) the difficulty of performing software/hardware mapping; (ii) the complexity of performance analysis and meeting the real-time constraints; (iii) the design of interconnection devices and interoperability issues.

In the next chapter, we present the main related work on performance optimization for multi-cluster embedded networks, and especially the main existing work dealing with the interconnection devices.

# Chapter 2

## Related Work: Performance Optimization for Multi-Cluster Networks

In the area of performance optimization for embedded networks in avionics and automotive, various approaches have been integrated into different parts of the end-to-end communication path, including traffic sources, communication networks and interconnection devices. We review in this chapter the most relevant work in this area for avionics and automotive applications. First, we present optimization approaches for traffic-source mapping, where the main concern is the mapping of the application data onto frames. Then, main existing approaches for performance optimization for communication networks are detailed, including, timing analysis and data routing for both AFDX and sensors/actuators networks. Finally, the optimization of interconnection devices is reviewed and existing protocol conversion approaches to guarantee real-time performance and resource utilization efficiency are detailed.

### 2.1 Optimizing Traffic-Source Mapping

Traffic-source mapping consists in affecting data produced by a source application to the frames supported by the communication network. A simple mapping consists in including each generated data into a dedicated frame. However, this choice may induce a high communication overhead. A more advanced mapping approach consists in grouping multiple data produced by one or many applications in the same network frame. The traffic-source mapping has a direct impact on the network utilization. The grouping pro-

cess of elementary data allows reducing the protocol overheads, and consequently saving network capacity and improving communication efficiency. Different strategies have been introduced for avionics end-systems and automotive ECUs (Electronic Control Units) and have shown significant enhancements in terms of network capacity utilization.

### 2.1.1 Avionics End-Systems

The AFDX network is considered as a promising communication technology for modern avionics architectures. The AFDX is based on routing frames through isolated data channels, called Virtual Links (VLs).

In [12], the authors introduced a method to define VLs characteristics to minimize the AFDX network utilization rate. The method presented in [12] is illustrated in Figure 2.1 and it consists in packing data from different AFDX applications hosted by the same AFDX end-system within the same AFDX frame. The transmission of each resulting AFDX frame is supported by an AFDX VL respecting the frame characteristics. The authors in [12] proposed an approach to find VLs configuration minimizing the bandwidth consumption on AFDX network to improve network resources utilization and to ease the addition of new VLs. First, an algorithm to find the optimal VLs allocation for periodic or sporadic data generated by the same AFDX application was proposed. This algorithm is based on data segmentation and has as objective minimizing the consumed bandwidth on the AFDX network. Afterwards, this algorithm was extended to find the optimal allocation for a set of data generated by the same end-system. The applicability of this approach was illustrated on a representative avionics benchmark, and the results showed its efficiency to save network bandwidth utilization. However, this approach did not integrate the verification of the time constraints.

Another interesting work in this area was presented in [13]. This work concerns the adequate mapping of avionics functions onto processing modules while meeting real-time and resource constraints. Avionics applications are hosted by partitions compliant with ARINC 653 [5]. Each partition has its own memory space and it is executed periodically during a reserved time slot. As illustrated in Figure 2.2, two partitions  $P_1$  and  $P_2$  are executed on the same processing unit with respect to their associated periods. The period of the obtained schedule is called the Major Frame (MAF).

In [13], the authors formulated an optimization problem for mapping avionics partitions onto processing resources of an IMA architecture. The formulation takes into



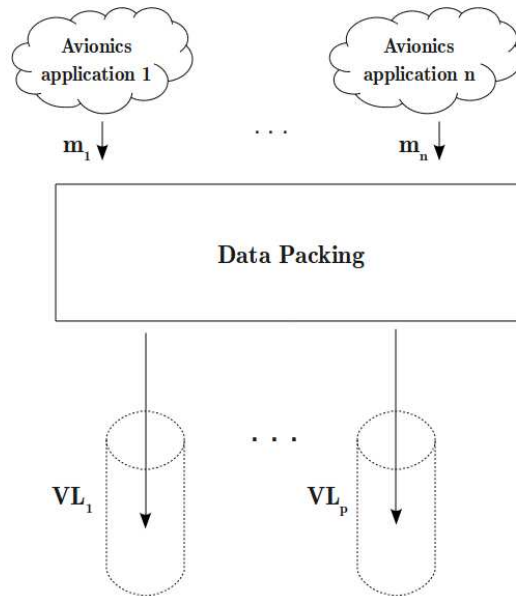


Figure 2.1: Data packing and VLs allocation

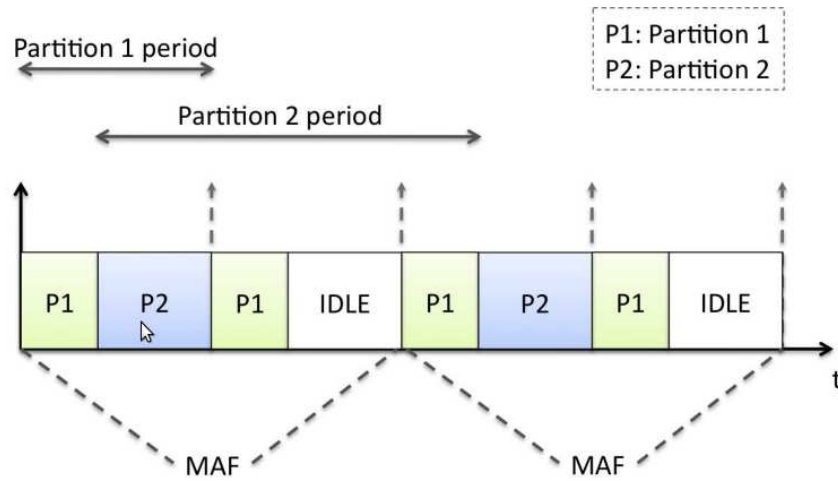


Figure 2.2: Periodic execution of Partitions

account resources as well as timing constraints of mapped avionics functions. The main objective was to maximize the evolution margins and to ease future avionics functions addition to the system. A method to solve this optimization problem was provided. However, this mapping problem considered only AFDX communication network, and the impact of an interconnected communication network, as currently used in avionics, on the software/hardware mapping was not considered.

### 2.1.2 Automotive End-Systems

For automotive applications, mapping periodic or sporadic data flows produced by applications sharing the same ECU onto frames has been widely studied to minimize bus utilization rate. Frame packing is a classic technique used in automotive context to achieve this aim. In [14] and [15], authors proposed the use of frame packing to allocate signals produced by source applications to CAN frames. This approach is illustrated in Figure 2.3. The proposed frame packing strategy consists in fixing the groups of data to pack based on an arbitrary criterion. Then, a periodic CAN frame is defined per group of data respecting the maximal CAN payload size. In [14] and [15], the authors proved that the data packing problem is NP-hard and proposed several algorithms to select adequate frame packing strategies processed in a polynomial time. A comparative study of the different algorithms has been conducted to select the most resource efficient configuration. However, these methods assume a synchronous behaviour of the different applications hosted by the same ECU. This assumption is not always verified in the general case and the proposed method could be complex to generalize.

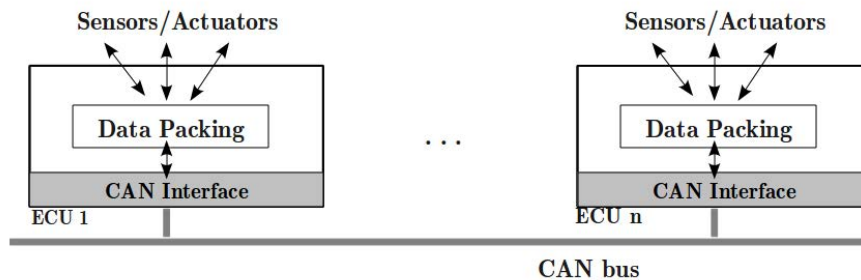


Figure 2.3: *Data packing of CAN frames*

In [16], the authors considered a multi-cluster communication architecture, as described in Figure 2.4. This architecture consists of two heterogeneous communication buses: Event-Triggered and Time-Triggered. For instance, authors considered CAN bus as a representative technology of event-triggered data buses, and TTP/C as a representative technology of time-triggered data buses. A gateway is used to support communication between both data buses. In [16], the authors proposed a frame packing strategy inside source nodes of both network clusters, to achieve higher bus utilization rate and to improve flows schedulability. In this approach, the timing constraints of messages were integrated, and a schedulability analysis which takes into account the queuing delays in the gateways was provided. However, The frame packing was implemented only in source nodes, while the gateway was considered as a simple conversion node, e.g., each received

frame in the gateway from a source cluster implies exactly one forwarded frame to the other cluster. Although this approach showed interesting bandwidth consumption savings, further enhancements may be achieved by considering the role of the gateway in reducing communication overheads.

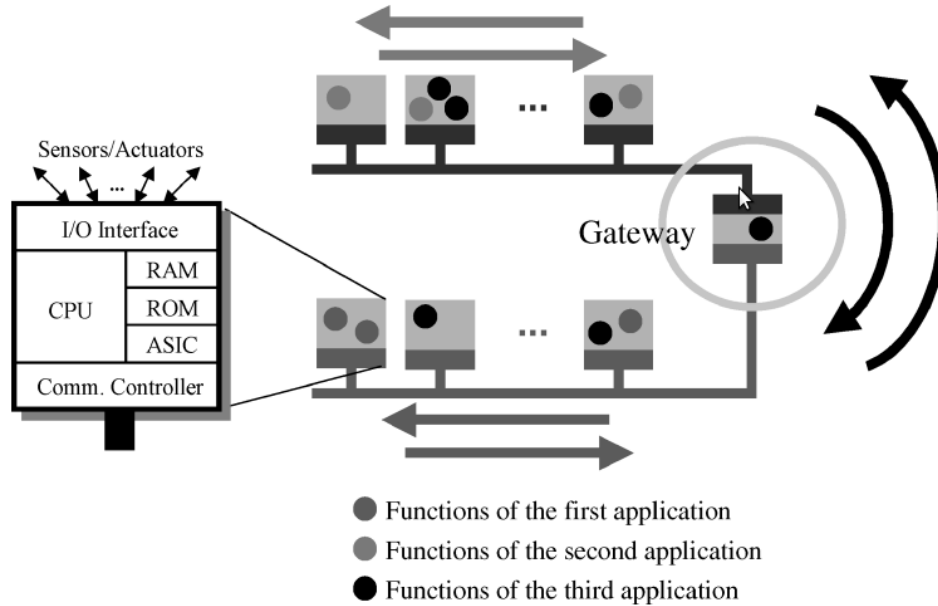


Figure 2.4: *Multi-cluster automotive network architecture*

## 2.2 Optimizing Communication Network Performance

Various analytical methods have been introduced to compute end-to-end communication latencies. These methods were used in the literature to analyze and optimize the performances of critical embedded networks. Furthermore, routing algorithms have been studied for embedded networks to improve network timing performances and to guarantee a better load balance in the network. First, we present the main related work to AFDX performance analysis and optimization. Then, we give an overview of the main work concerning sensors/actuators networks.

## 2.2.1 Work on the AFDX Network

### 2.2.1.1 Timing Analysis techniques

In avionics networks, for certification reasons, it is necessary to prove that the communication latency for each message does not exceed its deadline. To achieve this aim, several techniques have been introduced in the literature to analyze the timing performance of avionics networks. In particular, the AFDX network has been largely studied and several methods to prove the predictability of communication over AFDX has been proposed such as Network Calculus [17], Trajectory approach [18] and Model checking [19]. These methods can be organized into two categories:

- Methods computing an upper bound on end-to-end communication delays: Network Calculus and Trajectory approach
- Methods computing the exact end-to-end communication delays: Model checking

The **Network Calculus (NC)** formalism is based on the mathematical theory of Min-Plus algebra [20]. This theory has been widely used for analyzing performance guarantees in computer networks, and it was one of the first methods used for AFDX certification [17] [21].

To provide timing guarantees for data flows, Network Calculus formalism is based on bounding network resources. This means that traffic sources have to guarantee a maximum traffic emission, and network elements have to offer guarantees on minimum service capacity. To model the data flows generated by sources in the network, the concept of *arrival curve* is used. Then, to model the amount of service guaranteed by a network node applying some scheduling policy, the concept of *service curve* is used. Given the model of an input data flow and the model of the traversed network node, Network Calculus provides a bound on the maximal traversal delay of the network node using the horizontal deviation between the arrival curve and the service curve. Furthermore, a characterization of the output traffic from the network node using arrival curves is provided. More details about Network Calculus theory can be found in Appendix A.

In [17], the authors introduced a methodology for modeling the AFDX network using Network Calculus formalism. The AFDX data flows were modeled using arrival curves, deducted directly from the VLS characteristics, i.e., maximum frame size and minimum inter-arrival time. Moreover, each network node was modeled using service curve which

takes into account the respective scheduling policy. Then, a method for computing the end-to-end delay bound for a given AFDX flow has been introduced. This timing analysis method consists in propagating the arrival curve of a given data flow from the source end-system to the destination end-system throughout its path.

This timing analysis method based on propagating arrival curves offers upper bounds for end-to-end delays in AFDX networks. However, this approach [17] leads to pessimistic bounds, as the serialization of frames is not taken into account between two successive nodes. Consider two AFDX flows traversing a tandem of network nodes, the application of the propagation analysis approach integrates twice the impact of a flow on the other (at the first node and at the second node). To achieve tighter bounds on AFDX end-to-end delays, the authors used a "grouping" technique [21]. This technique takes into account the serialization of frames from different VLs transmitted on the same AFDX link. The "group" is defined as the set of VLs which exit from the same switch output port and enter the same switch input port, i.e. Virtual Links that share at least two segments of path. The key issue is that the frames of those VLs are serialized once when exiting the first output port. This optimized technique has been shown to offer tighter bounds compared to the propagation algorithm. However, since the first applications of Network Calculus to AFDX network, a multitude of Network Calculus algorithms have been proposed in the literature. Achieving tighter bounds with Network Calculus requires an increasing computational complexity. Therefore, there is a trade-off between the quality of the obtained upper bounds on network traversal delays and the computational complexity of the Network Calculus algorithms.

The **Trajectory approach** is a timing analysis technique introduced to get upper bounds on communication response times in distributed systems [22] [23]. For each packet from a given flow, the trajectory approach builds the packets sequence corresponding to the worst-case in each traversed node. The end-to-end delay is then deducted from delays experienced in crossed nodes throughout the packet path.

To explain the trajectory approach, we consider the example of the communication network in Figure 2.5. The communication network is composed of seven connected nodes. Each data flow follows a path in the network corresponding to the crossed nodes from end-to-end. This path is assumed to be static in the Trajectory approach and the set of crossed nodes by the data flow can be seen as an ordered sequence of nodes. In the example of Figure 2.5, two flows are considered,  $\tau_1$  and  $\tau_2$ .  $\tau_1$  follows the path  $P_1 = \{4, 5, 6, 7\}$ . The Trajectory approach assumes, with reference to a flow  $\tau_i$  with path  $P_i$ , a flow  $\tau_j$  with path  $P_j$ , such that  $P_i \neq P_j$  and  $P_i \cap P_j \neq \emptyset$ . In the example of Figure 2.5, flows  $\tau_1$  and

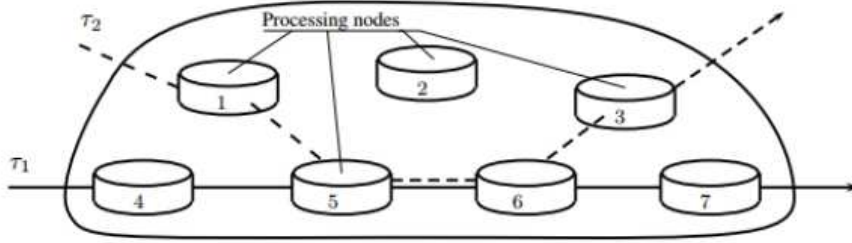


Figure 2.5: Example of communication network

$\tau_2$  verify the assumption of trajectory approach since  $P_2 = \{1, 5, 6, 3\}$  and  $P_1 \cap P_2 = \{5, 6\}$ .

Flows are scheduled in each crossed node. Each flow  $\tau_i$  has a minimum inter-arrival time between two consecutive packets at the first node of its path in the network. The end-to-end delay of a packet computed using the Trajectory approach is the sum of the times spent in each visited network node and the transmission delays on links. Considering a FIFO (First In First Out) scheduling algorithm, the time spent by a packet  $m$  in node  $h$  depends on the pending packets in  $h$  at the arrival time of  $m$  to  $h$ . In the worst-case, all these pending packets are more prior than  $m$  and will be processed before  $m$ .

In [18], the trajectory approach has been applied to AFDX network by considering that:

- An end-system is represented by a node in the trajectory approach;
- Each output port of an AFDX switch is represented by a node in the trajectory approach;
- The switches latency is represented by links in the trajectory approach;
- An AFDX VL becomes a flow in the trajectory approach.

The authors conducted a comparison between results obtained using the propagation algorithm with Network Calculus and those obtained using Trajectory approach. Obtained results showed that the upper bounds on the end-to-end delays on AFDX obtained using the Trajectory approach are tighter compared to Network Calculus bounds.

The **Model checking** [19] is another approach to guarantee the maximum transmission delay in the AFDX network, which computes the exact worst-case end-to-end communication delays. The basic idea of this approach consists in checking all the possible scenarios that the network can experience to find the exact worst-case communication delays. These scenarios form an exploration space which is often called "state-space". An attempt for applying the Model Checking approach to analyze the performance of AFDX network was done in [24]. A major difficulty is that, theoretically, the state-space of AFDX communication network is infinite (because of continuous real-time nature of the network). Therefore, using model checking for such applications requires some kind of state-space reduction. Unfortunately, the use of Model Checking is yet limited compared to Network Calculus and Trajectory approach, as it cannot cope with realistic AFDX networks, due to the combinatorial explosion problem for large configurations.

In our case, we conduct timing analysis of the AFDX network using Network Calculus approach due to its low computational complexity. Furthermore, we developed a performance analysis tool for avionics networks based on Network Calculus formalism, called WoPANets [6] (see Appendix A for more details).

### 2.2.1.2 Optimal Routing for AFDX

The AFDX network is a switched network with multiple possible paths from a given source to a destination end-system. As we explained in Section 1.2.1, in AFDX networks, VLS are routed statically. One major task when integrating the avionics architecture consists in defining VLS paths throughout the AFDX network. In [12], the authors addressed the optimization of VLS routing for the AFDX network to minimize communication latencies and to limit the maximum utilization rate of the AFDX links. Indeed, a poor VL routing may induce a high contention level between AFDX flows at the output ports of the AFDX switches, and consequently inducing high communication latencies. To overcome this problem, the authors in [12] proposed a routing algorithm that can be used to route thousands of VLS, to maximize the minimal residual capacity of the AFDX links. The main idea of this algorithm is to balance the communication load between network switches and to keep a low contention level. This fact leads to low traversal delays of the switches, and consequently low end-to-end latencies on the AFDX network. This technique optimizes the network resources utilization and lets margins for network evolution.

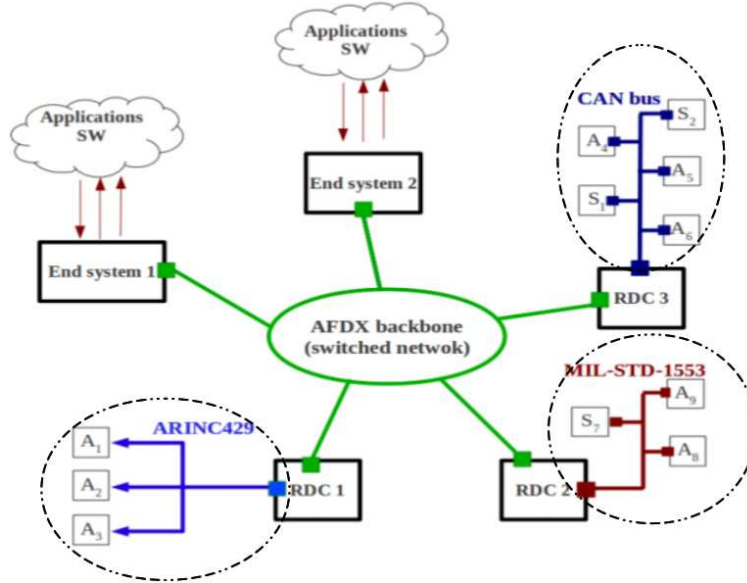


Figure 2.6: Optimization of sensors/actuators network performance

## 2.2.2 Work on Sensors/Actuators Networks

Different I/O buses may be used in multi-cluster avionics networks as shown in Figure 2.6. The timing analysis of these data buses is necessary to prove the predictability of the avionics system. This problem has been addressed for CAN bus [25] to prove its timing guarantees and thus the predictability of communications. The objective is to prove that the response time of a message, which needs to be delivered from a source to one or many destination nodes on the bus, does not exceed its Deadline.

The CAN bus has been largely used as the main communication network for automotive applications. Many approaches have been proposed in the literature for timing analysis of CAN bus to prove its capacity to meet strict real-time constraints of automotive applications. In [25], Tindell et al. were the first to introduce a method to compute exact Worst Case response Time (WCRT) on CAN bus. This result was proven to be optimistic under certain conditions by Davis et al. in [11] and a revision of the method introduced in [25] was provided. In [11], the Worst Case Response Time (WCRT) on CAN for a message  $m$  is given by:

$$R_m = \max_{q=0..Q_m-1} R_m(q) \quad (2.1)$$

$$(2.2)$$



where  $Q_m$  is the number of instances of message  $m$  that become ready to transmission before the end of the busy period relative to  $m$ , and  $R_m(q)$  is the WCRT of instance  $q$  of message  $m$ .  $R_m(q)$  is given by:

$$R_m(q) = C_m + J_m + w_m(q) - qT_m \quad (2.3)$$

$$(2.4)$$

where,

- The transmission time  $C_m$ , corresponding to the longest time that the message can take to be transmitted;
- The queuing jitter  $J_m$ , corresponding to the longest time between the initiating event and the message being queued, ready to be transmitted on the bus;
- The queuing delay  $w_m(q)$ , corresponding to the longest time that the instance  $q$  of message  $m$  can remain in the CAN controller queue, before commencing transmission on the bus;
- $T_m$  is the period of message  $m$ .

$w_m(q)$  is computed using the following iterative expression:

$$w_m^{n+1}(q) = B_m + qC_m + \sum_{k \in hp(m)} \left\lceil \frac{w_m^n + J_k + \tau_{bit}}{T_k} \right\rceil * C_k \quad (2.5)$$

where  $hp(m)$  corresponds to the set of messages with priority higher than  $m$ ,  $\tau_{bit}$  the transmission time of one bit and  $B_m$  the maximum blocking time due to the set of messages with lower priority than  $m$ , denoted by  $lp(m)$ :

$$B_m = \max_{k \in lp(m)} C_k \quad (2.6)$$

The number of instances that need to be examined  $Q_m$  is given by:

$$Q_m = \left\lceil \frac{t_m + J_m}{T_m} \right\rceil \quad (2.7)$$

where  $t_m$  corresponds to the length of the priority level- $m$  busy period, which is given by the following recurrence relation, starting with an initial value of  $t_m = C_m$ , and finishing

when  $t_m^{n+1} = t_m^n$ :

$$t_m^{n+1} = B_m + \sum_{k \in \text{hep}(m)} \left\lceil \frac{t_m^n + J_k}{T_k} \right\rceil * C_k \quad (2.8)$$

$\text{hep}(m)$  is the set of messages with priority higher or equal to  $m$ .

These expressions were introduced for native CAN protocol, which assumes a Static Priority (SP) queues in all CAN nodes to schedule messages sharing the same CAN source node. However, different CAN bus configurations have been investigated and the timing analysis in [11] has been adapted to fit the following CAN configurations:

- **CAN bus with SP and FIFO queues:** in [26], the WCRT analysis for CAN bus has been extended to cover the case where CAN nodes may implement SP or FIFO queues. This work was motivated by the fact that some CAN devices implement queueing policies that are not strictly SP-based, thus invalidating the assumption of SP queues for CAN nodes with the native CAN bus. The authors in [26] showed that using FIFO queues instead of SP queues in CAN nodes significantly degrade the overall real-time performance of the network. Therefore, they recommended the use of priority queues whenever possible. However, system integrators do not always have control over the queueing policies implemented in the communications stacks or devices of all the ECUs of the system. In this case, the analysis in [26] may be useful.
- **CAN bus with offsets:** in [27], the WCRT analysis for CAN bus has been extended to cover the case where the production of messages in CAN nodes is desynchronised using offsets. Transmitting frames with offsets means that the first instance of a stream of periodic frames is released with a delay, called the offset, with regard to a reference point. This latter is the first instant at which the station becomes ready to transmit. The frames are then sent periodically, with the first transmission as the time origin. It is worth noticing that since there is no global synchronization among the CAN stations, each station possesses its own local clock and the de-synchronization between the streams of frames remain local to each station. Unlike the native CAN analysis which is based on a synchronous transmission of frames by a CAN source, using offsets allows to avoid this worst-case scenario, and thus reduce WCRT on CAN bus. The authors in [27] proved that using offsets in CAN sources is beneficial in terms of reducing response times, especially at high CAN loads.

## 2.3 Optimizing Interconnection Devices

The use of interconnection devices for multi-cluster networks has become very common in automotive and recently in avionics context. These devices allow different communication standards and equipments to coexist with each other. As automotive and avionics networks are subject to strict real-time constraints, proofs of determinism and reliability have to be provided. As a main part of such networks, interconnection devices should be designed to guarantee correct protocol conversion between network clusters and real-time requirements, and to enhance network efficiency. In automotive and avionics context, several approaches concerning the interconnection device design and performance optimization have been proposed.

### 2.3.1 CAN-Ethernet Bridge

In [28], authors proposed a mixed CAN-Ethernet network architecture as an alternative to interconnected CAN buses. As the CAN [3] bus has limited number of supported nodes, i.e., 30 nodes at 1 Mbps, and a relatively low transmission rate compared to Ethernet, the authors proposed an extended CAN architecture where multiple CAN buses communicate with each other through Ethernet bridges, as shown in Figure 2.7.

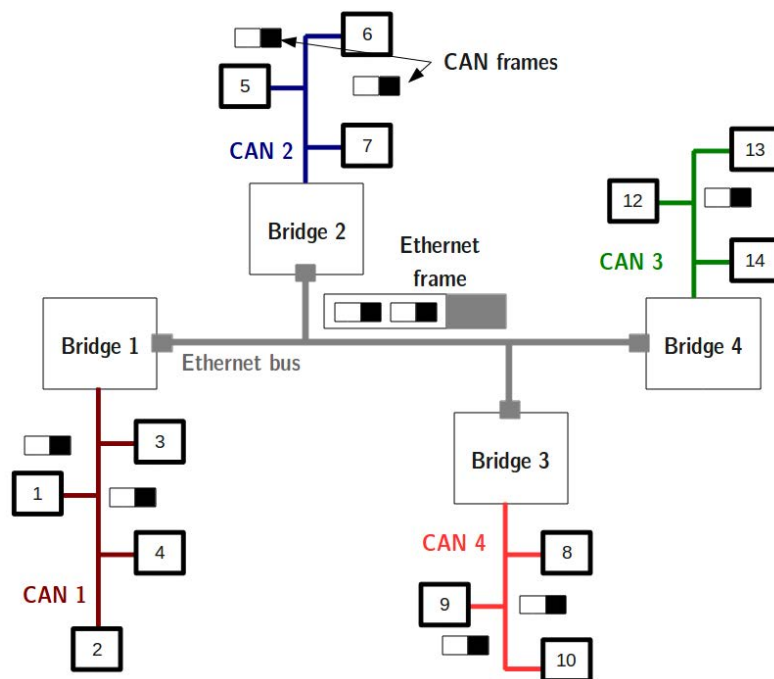


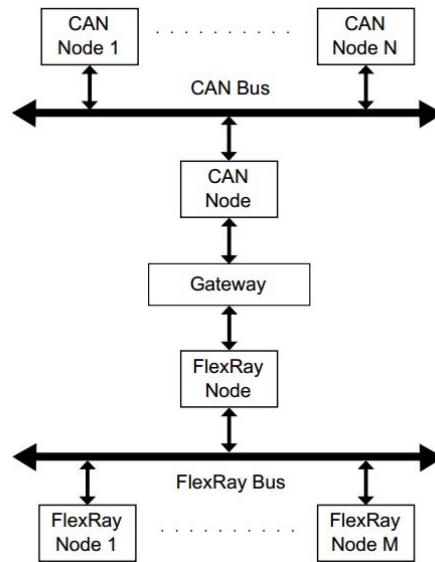
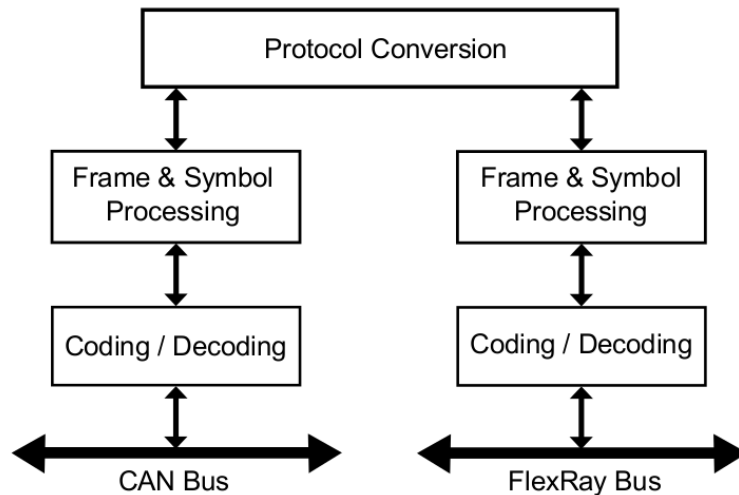
Figure 2.7: *CAN-Ethernet communication architecture*

This mixed CAN/Ethernet network allows connecting a high number of CAN terminals and consequently balancing CAN utilization and improving its scalability. Furthermore, a frame packing technique was implemented in the CAN-Ethernet bridges to reduce the induced overhead by CAN traffic on the Ethernet. This frame packing technique consists in encapsulating several CAN frames into the same Ethernet frame while respecting the maximum frame size of 1518 bytes. Furthermore, the bridge decapsulates the CAN frames received within an Ethernet frame and transmits these CAN frames to their final destinations. To analyze the network performances, the average communication latencies were analyzed using simulation. This approach is not sufficient to prove the communication determinism and the worst-case behavior required by critical embedded networks.

### 2.3.2 CAN-FlexRay Gateway

In modern cars, CAN [3] is the dominant network protocol for in-vehicle communication. However, as discussed in [29], CAN reached its limits in terms of data rate (a maximum rate of 1 Mbit/s) and maximal number of supported ECUs with the emergence of x-by-wire applications, i.e., the replacement of mechanical and hydraulic systems by electronic ones. This fact increases the number of in-vehicle functions and exchanged data volume. CAN is based on an Event-Triggered arbitration mechanism, which may induce high jitter under high utilization rates. The emerging FlexRay protocol, which has a higher transmission capacity of 10 Mbit/s and supports both time-triggered and event-triggered traffic, is expected to meet the emerging requirements of automotive applications. However, as the technology transition from CAN to FlexRay could not happen at once, both network protocols are expected to be used together in automotive in the near future. Consequently, the applications requiring low speed will still be carried out by CAN bus, while new high-speed functionality will be implemented on FlexRay network.

This situation imposes the existence of a gateway unit, which facilitates the intercommunication between CAN and FlexRay networks. In [29], a gateway for CAN and FlexRay interconnection for in-vehicle networks was proposed. The considered communication architecture is described in Figure 2.8. Authors addressed the design of high-performance gateway, offering efficient resource utilization.

Figure 2.8: *CAN-FlexRay communication architecture*Figure 2.9: *CAN-FlexRay Gateway functional structure*

The proposed gateway in [29] to interconnect CAN and FlexRay networks, is shown in Figure 2.9. Each frame received in the gateway from a source bus is first decoded. The frame is then processed to get the data included in the frame. The protocol conversion is then undertaken, i.e., the conversion of data from one protocol format to another. The data is inserted into an appropriate frame and then coded for transmission on the destination bus. For example, the protocol conversion operation from FlexRay to CAN is shown in Figure 2.10. To transmit a FlexRay message on CAN bus, the CAN-FlexRay

gateway will check if the message is compatible for transmission on the network, i.e., less than or equal to 8 bytes. If the message meets the criteria, then it will be inserted into the transmission buffer. If the message is too large, then the gateway will send the message to the transmit buffer sequentially in blocks of 8 bytes until no remaining data has to be transmitted.

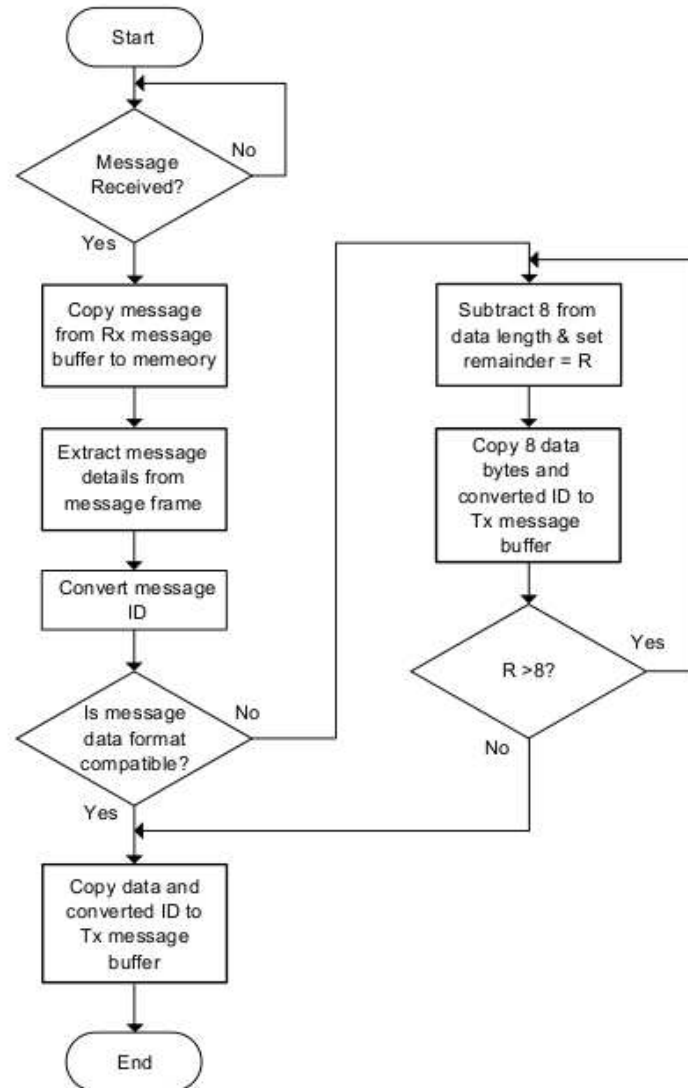


Figure 2.10: CAN-FlexRay Gateway operation diagram

The performance analysis of the CAN-FlexRay gateway, based on an experimentation platform, has shown bounded processing delays with low jitter. In our work, we address a similar problem for avionics networks which consists in interconnecting CAN and AFDX

networks. Our objective is designing an efficient gateway in terms of resources utilization, while meeting the timing constraints. However, the protocol characteristics of FlexRay are different from those of AFDX networks, especially in terms of communication schemes and frame formats. This fact makes the interconnection approach of [29] inapplicable in our case. Furthermore, this approach was limited to the functional aspects of the gateway design, whereas architectural aspects were not addressed. In our case, both functional and architectural perspectives are detailed to cover the different aspects which impact the CAN-AFDX RDC performance and resource utilization efficiency.

### 2.3.3 ARINC 429-AFDX Gateway

The transition of ARINC 429 systems to AFDX-compliant systems cannot be done in a short time. Hence, both networks need to coexist for a while and aircraft manufacturers opted for a gatewayed architecture. As described in Appendix B of ARINC 664 [1], a gateway device may be used to convert ARINC 429 messages to AFDX frames and vice versa. The gateway proceeds as follows: it encapsulates multiple ARINC 429 messages into the same AFDX frame to be then transmitted on the AFDX; and it decapsulates several ARINC 429 messages received within the same AFDX frame to be then transmitted on the ARINC 429.

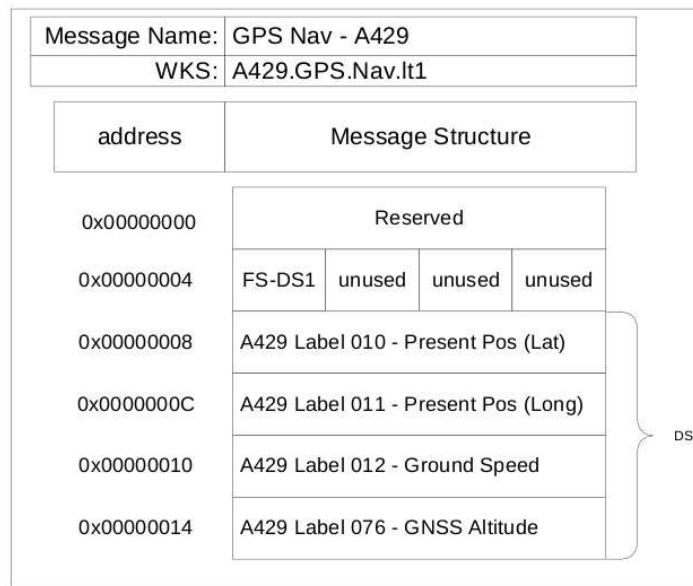


Figure 2.11: Example of AFDX frame including multiple ARINC 429 labels

An AFDX frame formatting mechanism, which allows a network designer to better

map non-AFDX data onto AFDX messages is provided in [1]. An illustrative example of the formatting of packed AFDX frames is given in Figure 2.11. In this example, 4 ARINC 429 frames are included into the same AFDX frame. However, no details are given on how to select groups of data to include within the same AFDX frame. Furthermore, performance analysis and optimization are left to the attention of network designers.

## 2.4 Need for Optimized CAN-AFDX Gateway

CAN bus has been successfully used for decades in automotive due to its high reliability, real-time properties and low cost. It became recently an attractive communication technology for aircraft manufacturers. Recent standards for avionics have been introduced, such as CANAerospace [30] and ARINC 825 [31]. A typical avionics network architecture is shown in Figure 2.12 where CAN buses are used as sensors/actuators networks. The communication with processing units connected to the high speed backbone AFDX network is ensured using RDC devices [4]. The main role of these devices is to handle protocol dissimilarities between AFDX and CAN and to guarantee interoperability between them.

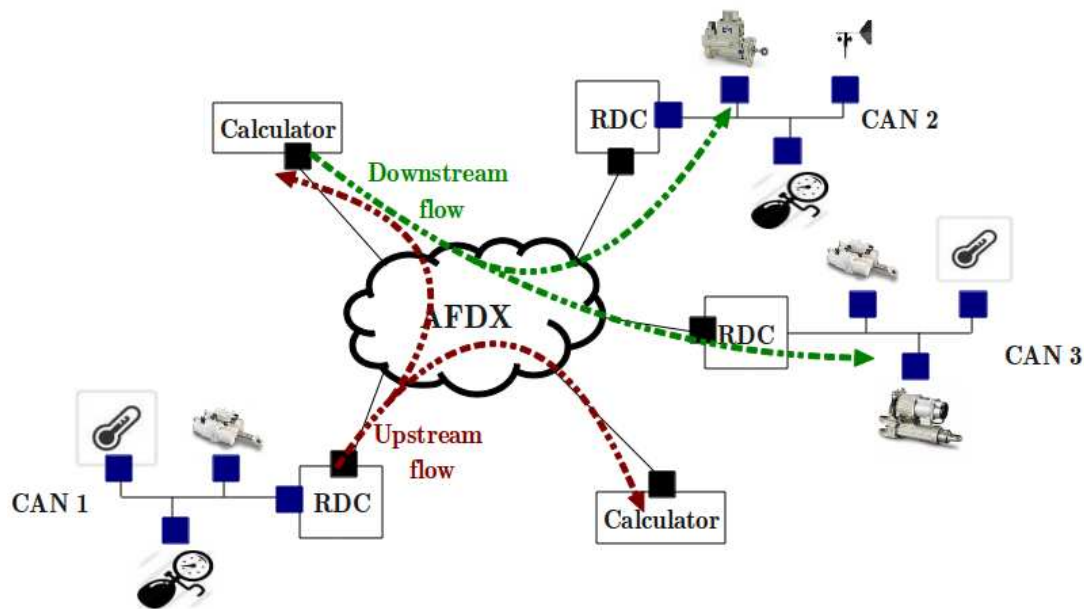


Figure 2.12: CAN-AFDX avionics architecture

Although the RDC was introduced to interconnect communication networks in avionics context, few works have addressed the design of RDC devices to interconnect CAN and



AFDX networks. The objective of our current work is to design an enhanced CAN-AFDX RDC, which offers a high network efficiency and guarantees system's requirements. The CAN-AFDX RDC should:

- correctly convert CAN frames to AFDX frames, and vice versa;
- ensure a consistent addressing between CAN and AFDX networks;
- guarantee temporal constraints of data flows from end-to-end;
- be optimized to achieve a high network efficiency in terms of resource savings.

To achieve this goal, our proposal is based on extending the RDC device standard [4] by adding new functions, to improve system's performance and enhance network efficiency. The main heterogeneity parameters between CAN and AFDX networks concern the communication paradigms, data rate and frame characteristics dissimilarities. The CAN is a multiplexed bus with a CSMA/CR access mechanism based on static priorities, whereas the AFDX is a switched network based on virtual link concept. CAN frames can support a maximal payload of 8 bytes which is very small compared to an AFDX frame, which can support up to 1472 bytes of payload. The main arising issues to design and validate a CAN-AFDX RDC device are as follows:

- **RDC design:** the key function of this specific equipment is to keep the communication transparency between an AFDX calculator and a CAN sensor or actuator to avoid the alteration of existent hardware in these equipments. Hence, for an AFDX calculator the source or the destination of the transmitted Virtual Link is the RDC device, while for a CAN sensor or actuator the transmitted data is consumed or generated by the interconnection equipment. The main characteristics of the CAN-AFDX RDC to define are:
  - *gateway strategy and addressing scheme:* we need to define an accurate method to map CAN frames onto AFDX VLs. A first basic strategy consists in associating for each CAN frame one AFDX VL using a static mapping table. This latter method will be shown to be non optimal in terms of reserved bandwidth on AFDX;
  - *data formatting:* the gateway strategy implementation requires an appropriate data formatting to send one or many CAN frames on the same AFDX VL. The

choice of this structure should take into account the AFDX standard, and reduce as much as possible the induced overhead to guarantee the bandwidth consumption efficiency on the AFDX;

- *data routing*: the RDC device should be capable to interconnect several I/O CAN buses to the AFDX backbone. The RDC should implement a routing mechanism which forwards each input data to its corresponding output RDC interface(s);
- *flows segregation*: when connecting multiple I/O CAN buses with different criticality levels to the AFDX using the same RDC device, an adapted segregation mechanism should be implemented in the RDC to guarantee the isolation between the different criticality levels.
- **Performance analysis and optimization of RDC**: the RDC device should be designed to fulfill avionics requirements in terms of predictability and resource efficiency. Hence, the main challenges are:
  - *Timing analysis*: for avionic embedded applications, it is essential that the communication network fulfills certification requirements, e.g. predictable behavior under hard real-time constraints and temporal deadlines guarantees. The use of gateways may increase the communication latencies and real-time constraints have to be met. To deal with the worst-case performance analysis of such network, an appropriate timing analysis has to be considered;
  - *Optimization process*: to increase the network efficiency, especially in terms of bandwidth consumption on the AFDX, and to enhance margins for future avionic functions addition, an optimization process of the RDC parameters is required. This process will define the most accurate RDC configuration, which respects the system's constraints and minimizes the induced network overhead, and consequently consumed network resources.

## 2.5 Conclusion

In this chapter, we reviewed the main related work in the area of performance optimization for multi-cluster embedded networks, especially those addressing the design of interconnection devices in avionics and automotive. In automotive context, several

techniques to enhance the gateway design, and consequently network performance have been proposed. However, there are less approaches addressing efficient gateways design in avionics context. Hence, there is a clear need for an optimized avionics gateway, and particularly one to interconnect CAN and AFDX networks. The main arising issues to design this latter were detailed to enhance the system's performance and resource savings.

In the next chapter, we will detail the design of our proposed RDC device to handle the identified issues.



# Chapter 3

## Design of an Enhanced CAN-AFDX RDC

In this chapter, we introduce an enhanced RDC device for CAN-AFDX networks to improve the system's performances. Compared to the current RDC device, new functions are integrated to maximize the network resource savings and to guarantee real-time performances. First, the current RDC device is described and will be considered as a reference to highlight the introduced enhancements within the proposed RDC device. Then, the functional structure overview of our proposed RDC device is presented. Finally, we detail the implemented functions within this latter, such as frame packing and traffic shaping mechanism.

### 3.1 Current RDC Device

In Figure 3.1, the currently used CAN-AFDX RDC device is presented to show the main characteristics of the current implementation. This RDC performs the frame conversion from CAN to AFDX, and vice versa using a mapping table. Data mapping is a necessary function of the RDC device connecting two network protocols with dissimilar addressing schemes. The mapping is defined within a static table which is configured offline and does not change during execution time. Within the current RDC device, the data mapping function is based on a static table associating for each CAN ID an AFDX VL ID, since no packing process is performed. This mapping is illustrated in Table 3.2, where three CAN messages required three dedicated VLs.

The main characteristics of the current RDC are:

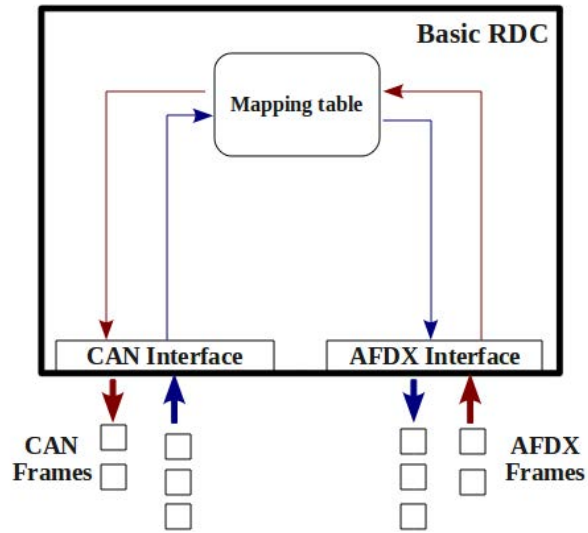


Figure 3.1: Current CAN-AFDX RDC functional structure

CAN ID	VL ID
$m_1$	$VL_1$
$m_2$	$VL_2$
$m_3$	$VL_3$

Figure 3.2: Mapping table for the current RDC device

- **(1:1) conversion strategy**: as shown in Figure 3.3, it proceeds as follows: first, each frame received at the input interface is decapsulated to extract the payload. Then, based on the static mapping table, the required header is identified and added to the extracted payload to build the corresponding frame at the output. This latter is then sent through the target network interface.

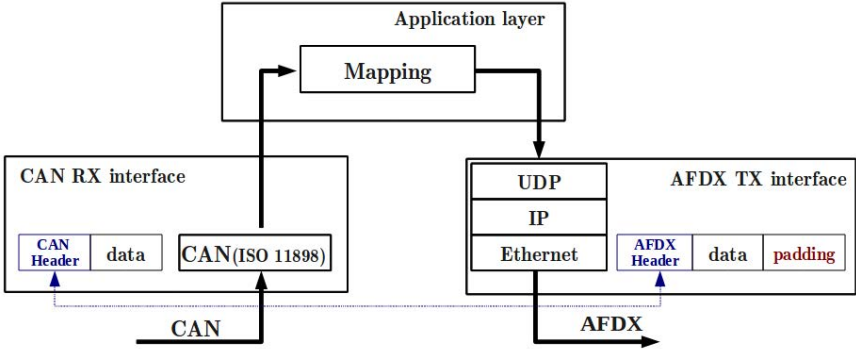


Figure 3.3: The current CAN-AFDX RDC: (1:1) strategy

- **One-to-one interconnection:** as illustrated in Figure 3.4, the current RDC can connect only one I/O bus to the AFDX. Thus, one RDC device is required per I/O network interconnected to the AFDX.

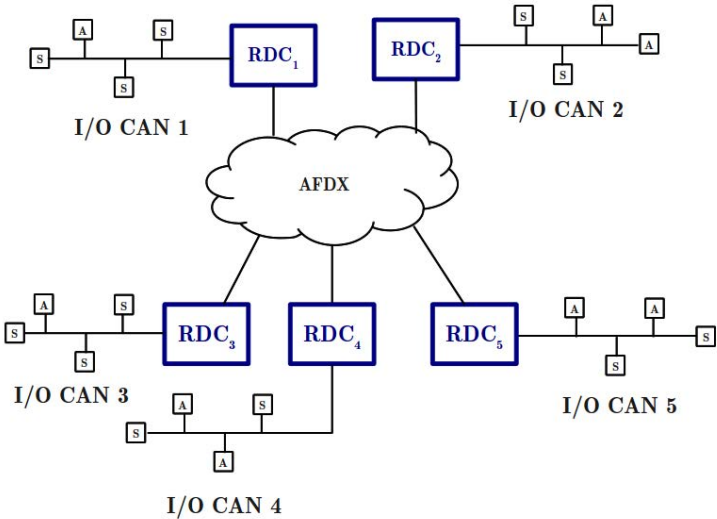


Figure 3.4: Current CAN-AFDX RDC interconnection topology

As it can be noticed, the (1:1) strategy of the current RDC device is simple to implement. However, it can induce high bandwidth consumption on the AFDX network. For the CAN-AFDX case study, implementing the (1:1) strategy in the RDC device consists in forwarding one AFDX frame with a minimum size of 84 bytes AFDX frame (IFG (Inter Frame Gap) included) for each received CAN message with a maximum payload size of 8 bytes. This clearly induces a high overhead on the AFDX network, and consequently

a poor network utilization efficiency. Furthermore, the use of one RDC device per inter-connected I/O network can lead to high hardware costs and important system's weight.

## 3.2 Enhanced RDC Functional Overview

To overcome the limitations of the current RDC, we propose an enhanced CAN-AFDX RDC with: (i) additional functions to reduce communication overheads and to maximize resource savings; (ii) the possibility to connect multiple I/O networks using one RDC device based on a software partitioning mechanism.

A modular structure of our proposed RDC is shown in Figure 3.5. It has one AFDX interface to communicate with AFDX end-systems and several CAN bus interfaces to communicate with several I/O CAN buses. Each network interface in the RDC consists of a reception interface denoted by  $Rx$  and a transmission interface denoted by  $Tx$ . For each CAN bus, a compliant-ARINC 653 [5] partition is implemented to ensure communication isolation between the different CAN buses. This choice is mainly motivated by the safety requirements, especially the need to limit errors propagation. Furthermore, we consider the synchronous communication scheme described in Section 1.3.3.

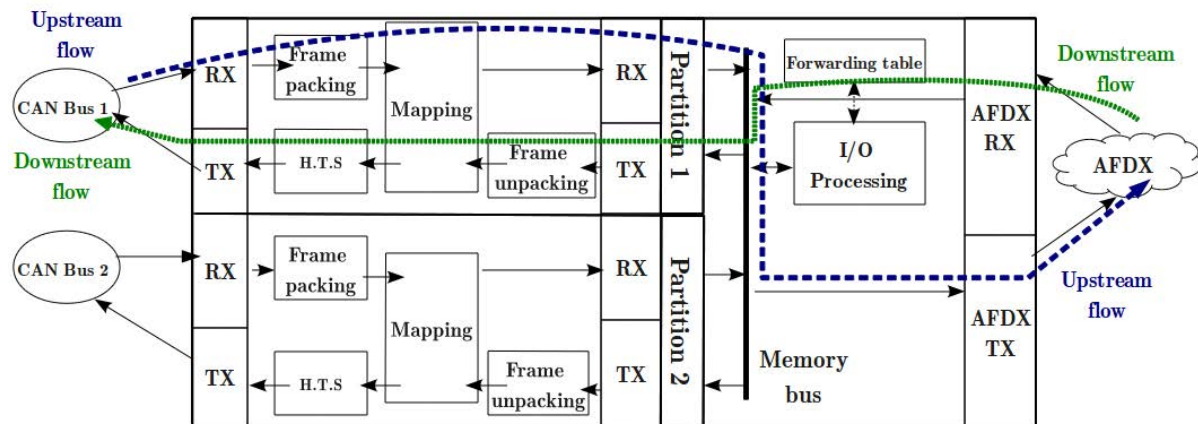


Figure 3.5: *Enhanced CAN-AFDX RDC functional structure*

Each partition handles upstream and downstream flows originating or destined to its associated CAN bus to or from the AFDX. Furthermore, an I/O processing unit is



required to forward a data received on the input AFDX interface to the appropriate partition, based on a pre-configured forwarding table.

The main new functions added to the basic RDC are:

- **Frame packing function:** is applied to upstream flows to reduce communication overhead. Frame packing of upstream flows consists in grouping several CAN data into a single AFDX frame, as shown in Figure 3.6. This fact allows to reduce required AFDX overhead, and thus AFDX bandwidth consumption to forward upstream flows from a CAN bus to the AFDX network;

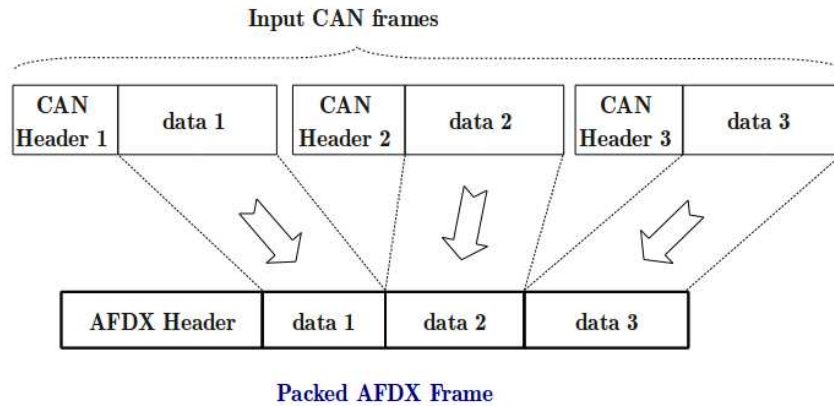


Figure 3.6: *Packing CAN messages into AFDX frames*

- **Frame unpacking function:** is applied to downstream flows. It consists in extracting multiple CAN data from a single AFDX frame when the frame packing process is activated at the AFDX source. In [12], authors introduced a frame packing algorithm in AFDX end-systems to optimize the data mapping into AFDX VLs. To handle such VLs, our proposed RDC device includes an unpacking module which reverses the packing process. As shown in Figure 3.7, the unpacking unit in the RDC will first extract the elementary data from the same AFDX frame. The knowledge of the used formatting scheme of the AFDX frames is necessary to identify the number, order and type of packed data messages, and consequently to extract correctly elementary data. Afterwards, a mapping table is used to define the CAN IDs for the extracted elementary data to obtain CAN frames;

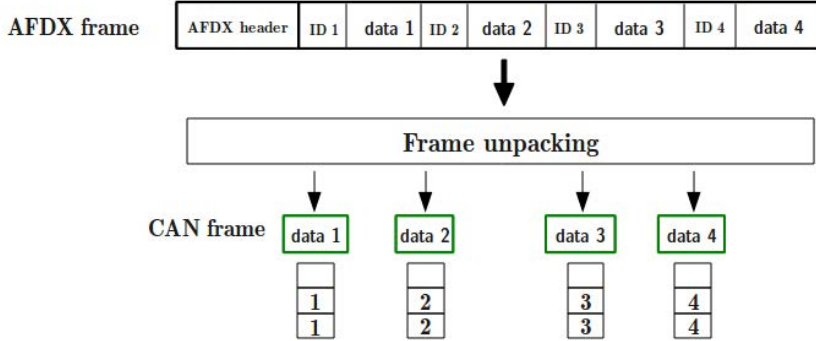


Figure 3.7: *Frame unpacking process*

- **Hierarchical traffic shaping function:** To minimize the interference on CAN bus between downstream and upstream flows, we propose the usage of Hierarchical Traffic Shaping (HTS) algorithm [32] within the RDC device. This algorithm is used to control downstream flows transmission on CAN, and consequently guarantee bandwidth isolation between upstream and downstream flows. HTS algorithm consists of a set of traffic shapers, based on the leaky bucket method [33], and connected in a hierarchical way according to a tree structure. HTS algorithm is a special case of hierarchical server-based scheduling which has been successfully implemented in various network applications [32] [34] [35] [36]. We extend the use of this algorithm within avionic RDC devices to control downstream flows and consequently to reduce bandwidth utilization on the AFDX induced by upstream flows. The proposed HTS algorithm uses two levels of traffic shaping. The first level is implemented based on greedy method [37] which comes for free to control individual downstream flows, and consequently to reduce the jitter due to the AFDX network [38]. The second level is used to shape aggregate downstream flows, scheduled according to fixed priority non-preemptive policy, to substantially reduce the number of flows introducing interference on upstream flows on CAN.

As shown in Figure 3.5, for each I/O CAN bus, our proposed CAN-AFDX RDC processes upstream and downstream flows as follows:

- **Upstream flows:** the Rx queue of a CAN interface associated to an I/O CAN bus stores the incoming CAN frames in FIFO (First In First Out) order. Afterwards, these frames are processed by the Frame Packing unit which forms groups of CAN data that may be sent in the same AFDX frame. Then, based on a predefined mapping table, a Virtual Link is affected to each group of data formed by the frame

packing unit to ensure its delivery to the AFDX end-systems. As we can see in Figure 3.5, flows from different I/O CAN buses can not be packed together. Indeed, as partitioning mechanism is implemented to isolate upstream flows coming from different CAN buses, the interaction between different upstream flows is limited to the AFDX interface which handles contention between VLs from different partitions.

- **Downstream flows:** For downstream flows, the I/O processing unit moves frames from the AFDX Rx interface to the corresponding partition, based on the forwarding table. Then, these received frames are processed within the unpacking frame unit. This latter extracts one or many elementary data from the same AFDX frame depending on the data packing performed within the initial AFDX source. Afterwards, based on a mapping table, CAN identifiers are defined and CAN data are encapsulated with the appropriate CAN headers to form CAN frames. HTS mechanism is implemented in the RDC device to eliminate the jitter due to the AFDX network, and minimize interference on CAN buses between upstream and downstream flows.

### 3.3 Frame Packing Strategies

In this section, we first review main related work to frame packing technique. Then, we introduce two frame packing strategies for the CAN-AFDX RDC device.

#### 3.3.1 Related Work

In the literature, several frame packing strategies were introduced for different applications, and can be organized into two classes:

- **Dynamic frame packing:** the groups of data messages to pack within the same AFDX frame are not fixed a priori. A specific criterion for grouping data on the fly during execution time is defined, such as the number of messages to pack;
- **Static frame packing:** the groups of data messages are fixed offline and do not change during system execution.

In [28], a dynamic frame packing approach has been proposed within CAN-Ethernet bridges. It consists in fixing the number of elementary CAN packets in each transmitted

Ethernet frame to reduce the induced Ethernet overhead by CAN flows. Using simulation, obtained communication latencies showed significant overhead savings on the Ethernet network, compared to using basic bridges with a naive (1:1) strategy for frames conversion between CAN and Ethernet networks. However, no analytical proof was provided concerning the verification of schedulability constraints as required for hard real-time applications. Another interesting dynamic packing strategy was proposed in [39] to construct network frames from applications data for non real-time networks. This latter strategy is based on a predefined frame's filling level. Hence, messages are packed in the same frame until reaching the filling level. This approach could be efficient to reduce the overhead and to minimize the bandwidth consumption for non real-time applications. However, for real-time communication with hard constraints, this approach can lead to a poor temporal behavior since the schedulability issue was not integrated in the frame packing design phase.

Static packing approaches have been introduced and studied for different applications, especially for automotive communications in [14] [15] [16] and for avionics communications in [12]. In automotive networks [14] [15], authors considered a communication network based on CAN protocol and addressed the problem of building CAN frames to support a set of data from applications hosted by an Electronic Controller Unit (ECU), i.e., an automotive terminal. Various algorithms were proposed to select the best static frame packing which minimizes the load on CAN bus while meeting the timing constraints. Obtained results have shown the efficiency of static frame packing in saving network resources, especially in terms of bandwidth utilization. However, the introduced packing approaches in [14] and [15] assumed a high synchronization level between their applications within the same ECU. This fact makes the application of these approaches complex in our case where data incoming to the RDC device are serialized after their transmission on the source network, i.e., a CAN bus for our CAN-AFDX case study.

In [16], authors introduced a static frame packing algorithm for automotive ECUs in a multi-cluster automotive architecture based on two different buses: a time-triggered and an event-triggered. Moreover, a gateway is used to support inter-buses communication. Authors used a static frame packing strategy to affect signals, i.e., elementary applications messages, to periodic frames that need to be transmitted on the communication network. Obtained results showed the enhancements of system's schedulability due to frame packing strategy within the ECUs. However, The considered gateway performs a simple (1:1) conversion strategy, and tuning the frame packing strategy parameters is a complex task. In avionics context, a static frame packing scheme was introduced in [12] to be applied

inside AFDX end-systems to map applications data into AFDX VLs. An algorithm to select the best frame packing in terms of bandwidth utilization was introduced. However, this algorithm did not integrate schedulability constraints to discard non-feasible configurations. Moreover, the proposed frame packing needs a high synchronization level between applications hosted by the same AFDX end-system. This assumption is not verified in our case since data are serialized on the source network before achieving the RDC device. This fact makes the applicability of this strategy complex in our case.

Hence, some static frame packing approaches were proposed in the literature for both automotive and avionics applications. However, these researches addressed mainly the problem of affecting elementary applications data to network frames within source nodes, and not within interconnection devices.

In the rest of this section, we present two frame packing strategies integrated in our enhanced RDC device. The first one is dynamic, called Fixed Waiting Time (FWT), while the second one is static, called Messages Set Partitioning (MSP).

### 3.3.2 Dynamic Strategy: FWT

This strategy is based on a waiting timer, as illustrated in Figure 3.8. This timer is started at the end of reception of the first CAN message at the packing queue, and it allows the accumulation of many CAN messages at the RDC CAN interface. Then, when the timer expires, the gathered data messages will be sent within the same AFDX frame. Afterwards, each AFDX frame is transmitted into one of the virtual links defined in the RDC to support the upstream flows, i.e. sensors flows.

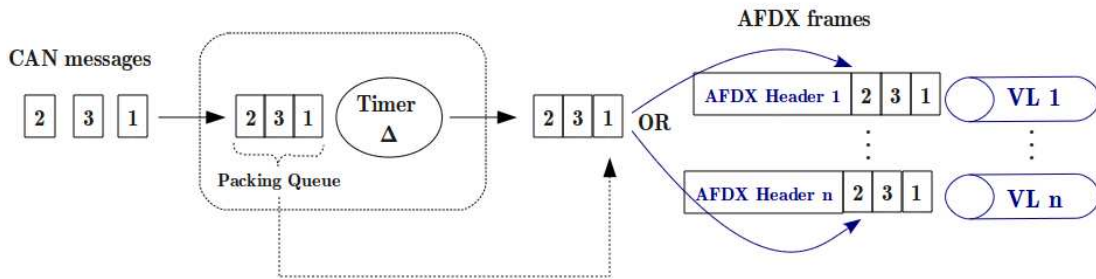


Figure 3.8: *FWT frame packing strategy for upstream flows*

### 3.3.3 Static Strategy: MSP

The MSP strategy consists in defining off-line a partition of CAN messages set, where each obtained subset represents the composition of an AFDX frame, as illustrated in Figure 3.9. An RDC device implementing MSP packing strategy proceeds as following. First, the received CAN messages are queued in the input port of the RDC device. Then, based on a static mapping table, each CAN frame is relayed to its associated output queue. The frame packing is synchronized with the reception of the most urgent CAN frame among each defined sub-partition. A timeout could be implemented to avoid losing all the accumulated messages in case of non-reception of the most urgent one. Finally, the output AFDX VLs will be multiplexed in the output port of the RDC device according to FIFO policy and then transmitted on the AFDX network.

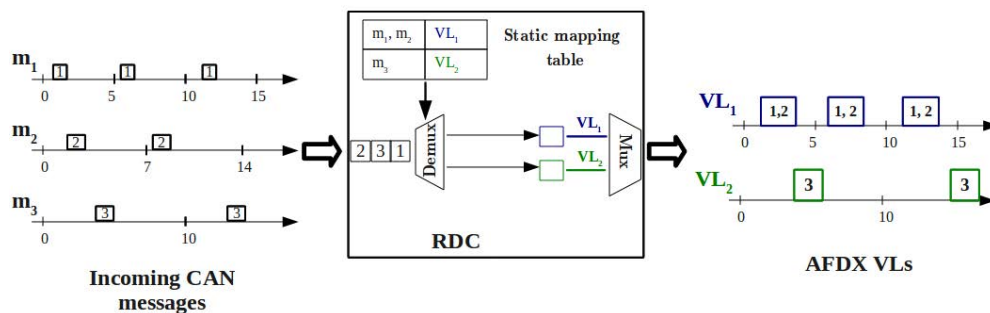


Figure 3.9: MSP frame packing strategy on upstream flows

## 3.4 Data Mapping & Formatting

To set up a frame packing and unpacking units in the RDC device, two important issues have to be considered: data mapping and frame formatting.

### 3.4.1 Data Mapping

To integrate the frame packing process with enhanced RDC device, the static mapping is no longer based on associating one VL ID for each CAN ID, but one VL to multiple CAN IDs unlike the current RDC device. This mapping is illustrated in Table 3.10, where seven CAN messages are affected to three VLs. For each frame packing strategy, the adequate mapping table should be defined and configured to respect the different addressing schemes.

CAN ID	VL ID
$m_1 m_2 m_3$	$VL_1$
$m_4 m_5$	$VL_2$
$m_6 m_7$	$VL_3$

Figure 3.10: Mapping table for enhanced RDC device

### 3.4.2 Frame Formatting

The frame packing process in the CAN-AFDX RDC device consists in including several data in the payload of one AFDX frame. This fact requires the definition of adequate AFDX frame structures, which may depend on the implemented frame packing strategy.

To define the most accurate AFDX frame structure for each considered frame packing strategy, we follow the guidelines provided by the ARINC 664 standard [1] for formatting AFDX frame payload. A payload corresponds to one or several elementary data and it is created and received at the application layer. We consider the concept of Functional Data set (FDS), introduced in the standard ARINC 664 [1]. As shown in Figure 3.11, an FDS allows grouping multiple data in the same AFDX frame and consists of two fields: (i) Data Sets (DS) that can contain several data primitives (e.g., Float, Integer, Boolean); (ii) Functional Status Set (FSS) which is a 4 Bytes field to encode the correctness and the status of at maximum 4 Data Sets. Several FDS data sets may be used to organise data included in the AFDX payload.

In order to keep communication overhead as low as possible in the AFDX payload structure, we chose the structure of Figure 3.12. One FSD is defined which is composed of one DS containing all the data messages to send within the AFDX frame and one FSS encoding the status of the supported data set.

Furthermore, the standard ARINC 664 defines two types of frame structures:

- **Explicit structure:** The frame format includes information allowing the destination of the frame to decode its payload. The structure includes identifiers to explicitly identify each elementary data encoded in the frame, and length parameter to define how long the structure is. An explicit formatting structure is shown in Figure 3.13: one identifier of 1 byte per data type is used for data identification, and the number and order of elementary data can vary according to the maximum frame size.

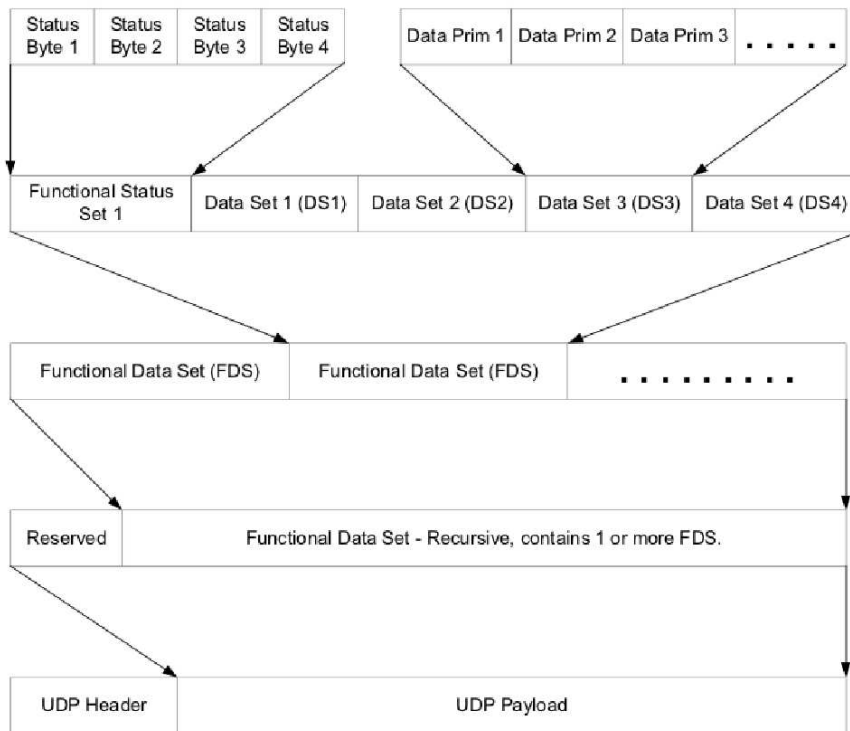


Figure 3.11: Structure of AFDX payload (ARINC 664)

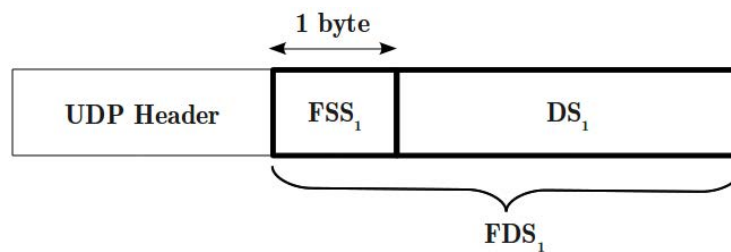


Figure 3.12: Chosen AFDX payload structure

- **Implicit structure:** Unlike the explicit structure, the frame in this case contains only elementary data without explicit identifiers. Then, the destination application will interpret correctly the frame format according to the identifier of the reception AFDX port. This concept is common in the Internet world with the Well Known Service (WKS) concept. For example, the File Transfer Protocol (FTP) service is available on port 21. In a similar way, we can affect to the AFDX port 6 a structure containing pressure measurement encoded on 8 bytes, followed by temperature measurement encoded on 4 bytes.



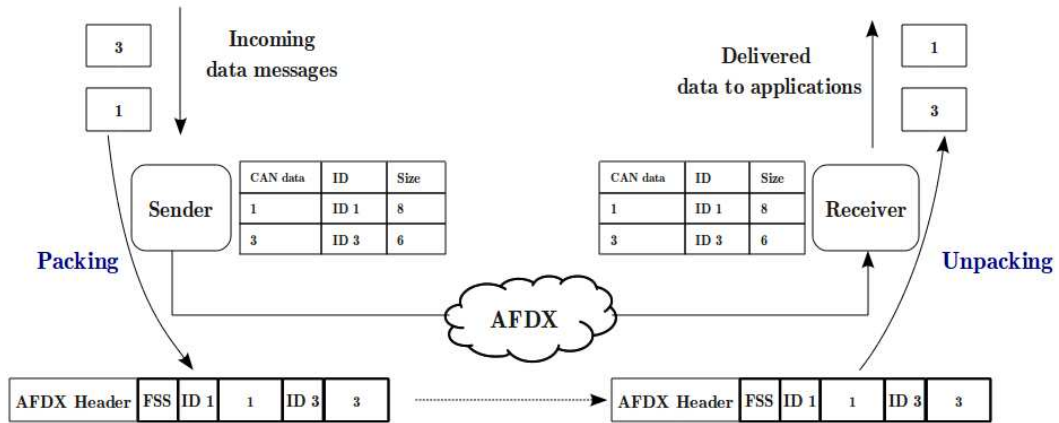


Figure 3.13: *Explicit AFDX frame structure*

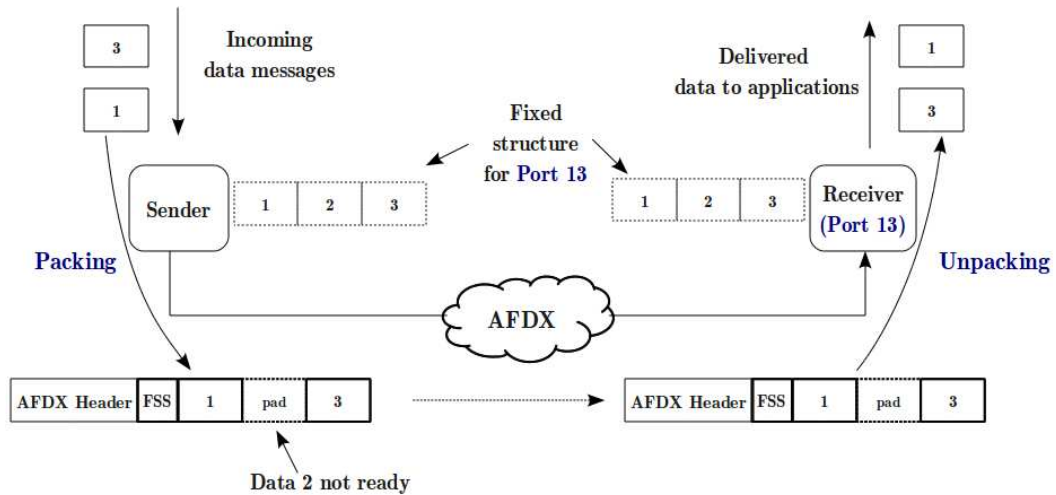


Figure 3.14: *Implicit AFDX frame structure*

An implicit structure is shown in Figure 3.14 where the frame formats are affected to port numbers. For each destination port receiving an AFDX frame, the corresponding structure defines the maximum size of the AFDX frame, and the elementary data fields in a predefined order where each data has a specific type and size. Padding may be used in the source to keep the same structure of the AFDX frame between successive transmissions, and to allow destinations to correctly decode included data. The information about frame structure is shared between senders and receivers.

The appropriate formatting structure which minimizes the induced communication overhead while guaranteeing correct identification of data, should be selected during the network design. This choice will mainly depend on the avionics applications and the knowledge of the AFDX frames composition during execution time. In our case, this choice depends also on the frame packing strategy. Hence, the frame structure is chosen as follows:

- **Under FWT:** we do not know a priori the set of data to pack in each AFDX frame since packing is done on-the-fly according to the waiting time parameter. Hence, the explicit structure is considered as more adequate under FWT packing strategy. Then, the only parameter to fix in this case is the maximum AFDX frame size, which is generally the maximum size of all possible resulting AFDX frames under FWT packing strategy. Thus, we compute the worst-case scenario in terms of gathered data size during the waiting time to define payload size of the explicit structure of AFDX frames.
- **Under MSP:** the composition of the AFDX frames is fixed and is known a priori. Therefore, using an implicit structure is more adequate in this case to identify packed data into the AFDX frames.

## 3.5 Traffic Shaping Mechanism

In this section, we first review the main related work to traffic shaping mechanism. Then, we introduce a traffic shaping technique, called Hierarchical Traffic Shaping (HTS), adapted to our CAN-AFDX RDC device to isolate upstream and downstream flows and control contention between them on I/O CAN buses.

### 3.5.1 Related Work

Traffic shaping is a traffic management technique which consists in delaying some packets to be conform with a desired traffic profile. It is a widely used technique in communication networks in general, and especially in real-time networks. It is used to guarantee performances and to improve latencies by bounding packets interference.

The Hierarchical Traffic Shaping (HTS) is a part of general Hierarchical Server-Based

(HSB) Scheduling where each traffic shaper in the hierarchy structure is considered as a server which will bound the traffic burstiness sent within a limited time window. HSB scheduling is a common approach that has been used in many network applications to control interference between various traffic classes with different real-time requirements, i.e., Soft Real-Time (SRT) and Hard Real-Time (HRT) traffic. Concerning industrial application and especially Real-Time Ethernet, one of the most relevant approaches based on HSB framework to guarantee a dynamic adaptation of servers was proposed in [36]. The authors presented a multi-level HSB architecture for Ethernet, implemented on commercial switches and based on FTT-SE (Flexible Time Triggered Switched Ethernet) paradigm [40]. Schedulability analysis was detailed and validated using experimentation. This approach is efficient in dynamic environment, and typically open networks. However, it assumes that servers parameters verify a priori traffic temporal constraints.

In automotive applications, various approaches based on traffic shaping and HSB scheduling were proposed to improve CAN bus performances. In [38], traffic shaping algorithm based on leaky bucket method, and particularly greedy method [37], was integrated within gateways to reduce the jitter on the destination network and improve the schedulability of lower priority messages. However, this approach is considered as a limited form of HTS approach implementing only one level of traffic shapers to control individual input messages. In [35], HSB scheduler, based on Earliest Deadline First (EDF) algorithm, was detailed to use CAN in a more flexible way compared to native CAN. This approach improved bandwidth isolation among aperiodic traffic and was validated using simulation. However, no analytical approach was proposed to provide worst-case response times of messages and to guarantee messages schedulability.

In avionics application, traffic shaping is integrated in AFDX end-systems to guarantee a reserved bandwidth for each application and is standardized as Virtual Link concept. This approach guarantees bandwidth isolation between traffic flows and improves the predictability of the AFDX network. In our case, we extend this approach by implementing HTS scheduling within RDC devices to interconnect the backbone AFDX with I/O CAN buses. The main idea is to minimize the interference due to downstream flows on the transmission of upstream flows on CAN, and consequently the WCRTs on CAN of upstream flows. This will favor frame packing mechanism for upstream frames within RDC device, and thus will reduce bandwidth utilization on the AFDX.

Our proposal consists of two traffic shaping levels and a root server to implement native CAN scheduler. The idea of the first level of traffic shapers is very similar to the

one detailed in [38] where we consider greedy method, which does not increase maximum end-to-end delays as proved in [37], and induced jitter by the AFDX network. However, we extend this implementation by adding a second level of traffic shapers to substantially reduce the number of flows introducing interference on upstream flows on CAN. The schedulability analysis of upstream and downstream flows is proved and validated through a realistic avionic case study. Furthermore, unlike [36], a tuning process of the HTS parameters is proposed to minimize as much as possible bandwidth utilization on the AFDX, while guaranteeing at the same time upstream and downstream flows requirements.

### 3.5.2 HTS Algorithm

The HTS mechanism is based on a set of traffic shapers and servers connected in a tree structure and defined in a static manner a priori, as shown in Figure 3.15. This latter is organized into three levels: leaf, inner and root.

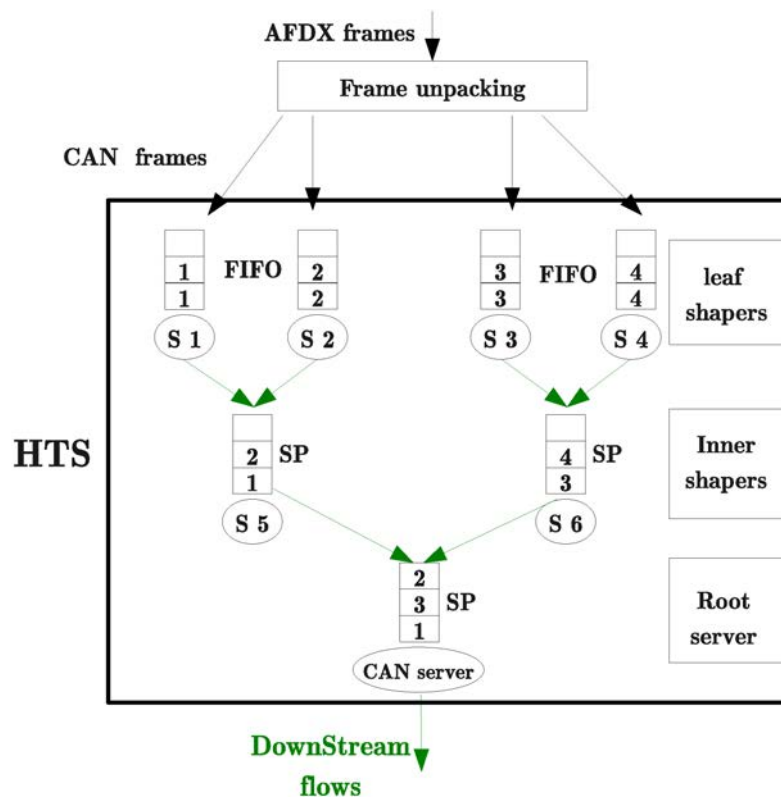


Figure 3.15: Hierarchical Traffic Shaping structure

- **Leaf traffic shapers:** are implemented to control the flow of received packets from the AFDX network. They are based on greedy method [8]. A greedy shaper is a special traffic shaper, that not only ensures an output stream that conforms to a given traffic specification, but that also guarantees that no packets get delayed any longer than necessary. In our case, leaf shapers ensures the same minimal inter-arrival time as in AFDX sources for each downstream flow. Hence, do not increase maximum end-to-end delays, however, they reduce efficiently the observed jitter in the RDC device. This fact enhances lower priority messages schedulability on CAN [9].
- **Inner traffic shapers:** each one is based on leaky bucket method to shape aggregate downstream flows of outgoing packets from leaf shapers after being classified and scheduled according to a fixed priority non-preemptive policy. The aim of these shapers is to substantially reduce the number of flows introducing interference on upstream flows, and to guarantee bandwidth isolation on CAN. One or many inner traffic shapers can be implemented depending on the incoming traffic rate. Indeed, shaping all the incoming flows using the same inner traffic shaper will induce small inter-arrival time between packets at the output, and consequently important interference with upstream flows. The tuning process of these inner shapers will be detailed in next chapters.
- The **root server** implements simply fixed priority non-preemptive scheduling which represents the CAN native behavior. All the packets will be multiplexed at the root server according to their corresponding priorities.

## 3.6 Conclusion

In this chapter, we presented an enhanced RDC device which is capable of: (i) connecting multiple I/O CAN networks to AFDX; (ii) saving AFDX bandwidth by reducing communication overheads induced by the RDC. Compared to the currently used RDC, our proposed RDC implements a set of additional functions: (i) frame packing based on dynamic or static strategy; (ii) frame unpacking; (iii) Hierarchical Traffic Shaping (HTS). The upstream flows, i.e., flows sent from CAN to AFDX, are processed by the frame packing strategy in the RDC; while the downstream flows, i.e., flows sent from CAN to AFDX, are first unpacked to extract elementary CAN data, then they are processed by the HTS unit. Furthermore, a partitioning process, ARINC 653-compliant, is used in the

RDC to isolate communication from different I/O CAN buses. A partition in the RDC is affected to each I/O CAN bus connected to the AFDX network. This choice reduces the number of required RDC hardware units, and thus reduces the system weight and cost.

The proposed RDC device presents several advantages such as modularity, configurability and resource management efficiency. However, introduced functions imply additional complexity in the performance analysis and RDC configuration task. As the RDC device inherits from the avionics system requirements, we have to prove that it meets real-time requirements. In the next chapter, we will introduce adequate timing analysis approach to validate the real-time behaviour of our proposed RDC device, while enhancing network resource savings.

# Chapter 4

## Modeling and Timing Analysis of the Enhanced RDC

In this chapter, we first model the CAN-AFDX network interconnected using our enhanced RDC device and the supported data flows. Afterwards, a timing analysis method is proposed and detailed to verify the system schedulability under different RDC's configurations. A performance evaluation through a small scale CAN-AFDX network is then provided.

### 4.1 CAN-AFDX RDC Modeling

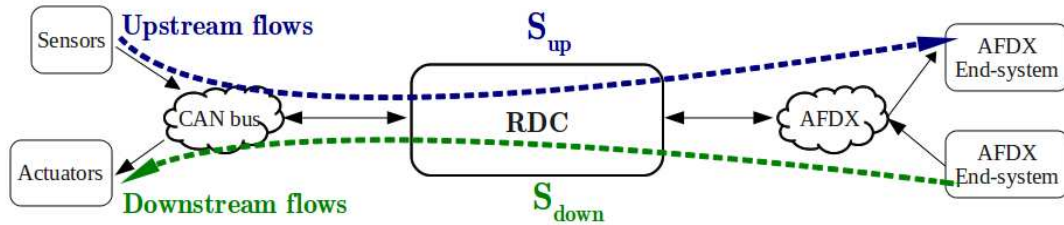


Figure 4.1: *CAN-AFDX network architecture*

As shown in Figure 4.1, the traffic supported by the RDC device can be organized into two types of flows: (i) upstream flows received from sensors connected to CAN bus and destined to calculators on AFDX; (ii) downstream flows received from calculators connected to AFDX and destined to actuators connected to CAN bus. We consider  $S_{up}$  and  $S_{down}$  for upstream and downstream flow sets, respectively. For each stream flow  $m \in S_{up} \cup S_{down}$ , we associate four characteristics  $\{T_m, L_m, Dl_m, P_m\}$  which represent the

period, maximum payload, deadline and priority on CAN bus, respectively. We consider a strict order of CAN priorities, i.e. for any two messages  $m_k$  and  $m_j$ ,  $P_{m_k} < P_{m_j}$  means that message  $m_k$  has higher priority than  $m_j$ .

When upstream and downstream flows cross the RDC device, they are processed as follows:

- **Upstream flows:** as shown in Figure 4.2, the RDC device maps CAN messages set  $S_{up}$  onto AFDX VLs set to support the upstream flows on AFDX network. This mapping process is called *VLs allocation*. To check the network temporal constraints, the allocated VLs need to be completely characterized. The VLs allocation is detailed for each proposed frame packing strategy, i.e., FWT and MSP, in Section 4.1.1;

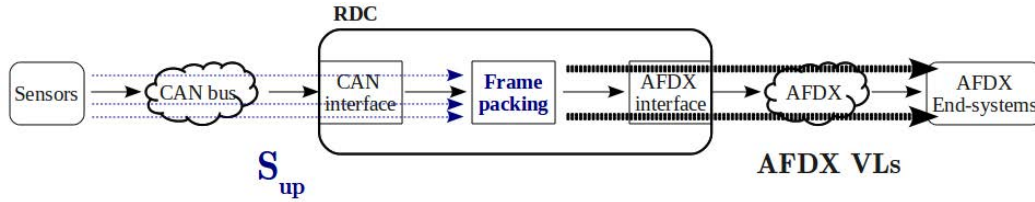


Figure 4.2: Upstream flows modeling from end-to-end

- **Downstream flows:** as shown in Figure 4.3, the RDC device will first extract the CAN messages set  $S_{down}$  from the AFDX VLs. Then, the obtained CAN messages are processed by the set of shapers in the HTS structure. To prove the network temporal guarantees, these shapers have to be completely characterized. The mapping of downstream flows  $S_{down}$  onto the shapers of the HTS structure is detailed in Section 4.1.2.

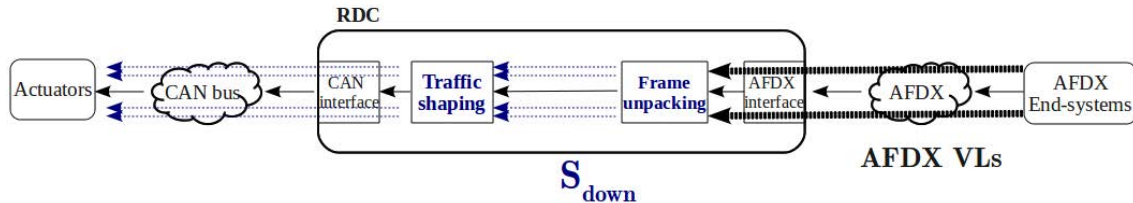


Figure 4.3: Downstream flows modeling from end-to-end



### 4.1.1 Frame Packing Strategies Modeling

The frame packing process consists in building a set of AFDX VLs  $V = \{v_1, v_2, \dots, v_m\}$  to define the output traffic from the RDC to the AFDX network, knowing the set of CAN-messages  $M = \{m_1, m_2, \dots, m_n\}$  at the input.

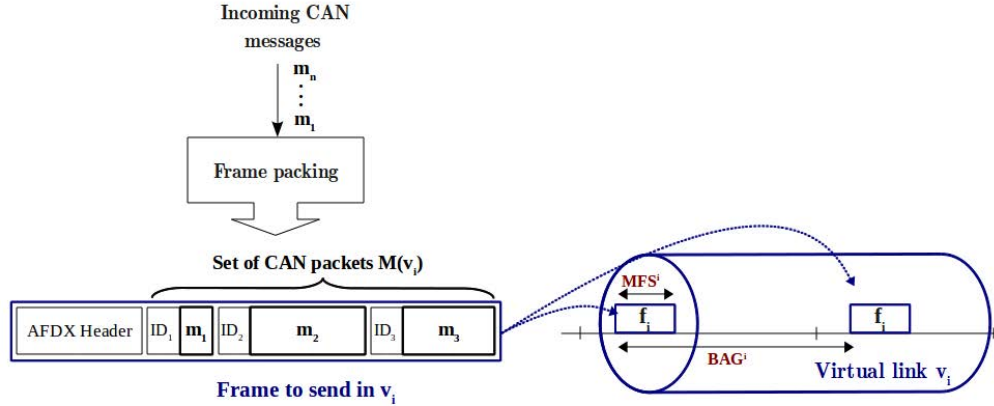


Figure 4.4: Example of CAN messages mapping onto AFDX VLs

As we can see through the example of Figure 4.4, after the frame packing process, each AFDX frame  $f_i$  within the VL  $v_i \in V$  will contain a subset of CAN messages  $M(v_i) \subset M$ . This subset of messages which can be static under MSP strategy, i.e., does not change over successive transmissions, or dynamic under FWT strategy, i.e., may vary from a transmission to another. Each VL  $v_i$  is characterized by  $\{BAG^i, MFS^i, D^i, DES_{AFDX}^i\}$  which represent the bandwidth allocation gap, the maximum frame size, the deadline and the set of AFDX end-system destinations, respectively. These characteristics will clearly depend on the implemented frame packing strategy in the RDC, and will be developed in the rest of this section.

#### 4.1.1.1 FWT Strategy

For an RDC device implementing the FWT strategy with a waiting timer  $\Delta$ , we define a set of AFDX VLs to support the AFDX frames resulting from FWT packing process. The number of VLs is defined considering that the RDC can forward as much AFDX frames as timer  $\Delta$  occurrences during the smallest period of the CAN messages set  $M$ . Hence, we define the number of VLs to support CAN messages under FWT strategy as

follows:

$$N_{vls}(\Delta) = Card(V) = \left\lceil \frac{\min_{m_j \in M} T_j}{\Delta} \right\rceil \quad (4.1)$$

In the worst-case scenario, any defined virtual link may support the most urgent CAN data and may include the maximum number of elementary CAN data accumulated during the FWT packing process. Hence, the allocated VLs  $V$  to the CAN traffic under FWT strategy which cover the worst-case scenario are considered as identical in terms of their composing elementary data, and their characteristics are defined as following.

For any  $v_i \in V$ ,

- $BAG^i$ : since any allocated VL  $v_i$  needs to transmit the message having the smallest period within the messages set  $M$ , we define the BAG as the closest value in power of 2 to the smallest period of messages in  $M$ :

$$BAG^i = 2^k, \quad k = \left\lceil \frac{\log(\min_{m_j \in M} T_j)}{\log(2)} \right\rceil \quad (4.2)$$

- $MFS^i$ : is considered as the sum of all data payloads in the messages set  $M$  and the induced overhead imposed by the AFDX structure. Padding may be used to guarantee a minimum AFDX frame size of 84 bytes (IFG (Inter Frame Gap) included). The largest AFDX frame generated by the RDC depends on the waiting time  $\Delta$ . According to the explicit structure detailed in the previous chapter, a bound on the maximal frame size (in bits) is as follows:

$$MFS^i = \max(84 * 8, \min(S_i, \Delta * \frac{8}{17} * 10^6) + (67 + N_{lb}(\Delta)) * 8) \quad (4.3)$$

where,

- $S_i$  is the sum of all data payloads in  $M$  (in bits);
- $\Delta * \frac{8}{17} * 10^6$  is the maximal payload (in bits) that can be accumulated in the RDC during  $\Delta$ . The typical CAN parameters are integrated where 8 bytes correspond to the maximum CAN payload size, and 17 bytes the size of a maximum frame size including payload and CAN protocol overhead and a transmission capacity of  $10^6 Mbps$ ;

- $(67 + N_{lb}(\Delta)) * 8$  is the overhead (in bits) imposed by the AFDX explicit structure, where  $N_{lb}(\Delta)$  is the maximal number of CAN identifiers received during  $\Delta$ ;
- Padding may be used to ensure a minimum AFDX frame size of 84 bytes.
- $Dl^i$ : is the relative deadline of the obtained AFDX frame. This relative deadline will be detailed in Section 4.2.
- $DES_{AFDX}^i$ : since any VL  $v_i$  in  $V$  can include any CAN message in  $M$ , then  $v_i$  can be received by any AFDX end-system that initially consumes at least one of these data. Therefore,  $DES_{AFDX}^i$  is as follows:

$$DES_{AFDX}^i = \cup_{m_j \in M} DES_{AFDX}^j \quad (4.4)$$

An example of AFDX VLs allocation under FWT strategy is shown in Figure 4.5. In this example, a set of 4 CAN messages is mapped onto 2 AFDX VLs. The choice of VL to support packed data is done during the execution time among VLs 1 and 2.

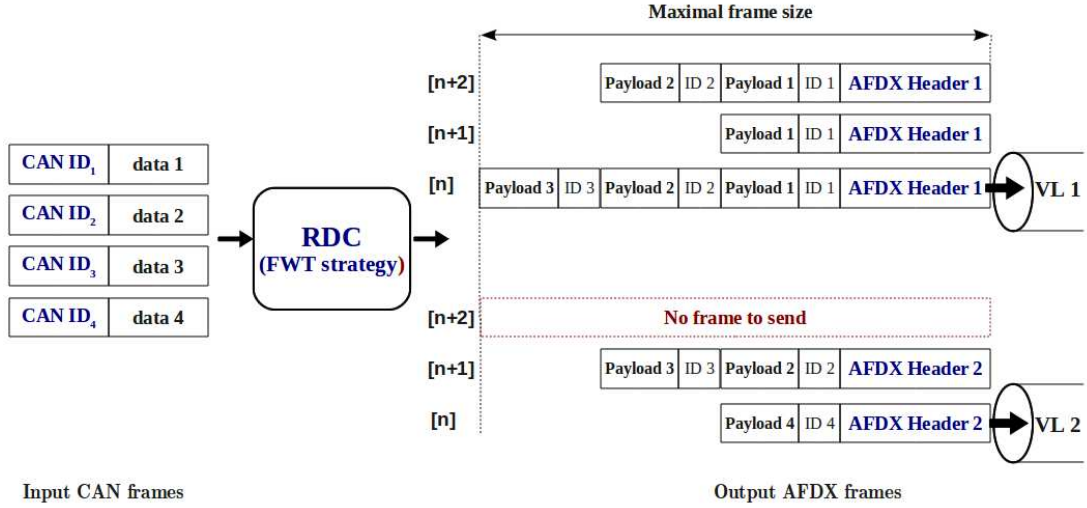


Figure 4.5: Example of AFDX VLs allocation under FWT strategy

#### 4.1.1.2 MSP Strategy

The MSP strategy for CAN-AFDX RDC is defined using a partitioning process of CAN messages set  $M$ . Each AFDX VL  $v_i \in V$  consists of a sub-set  $M(v_i)$  of CAN mes-

sages obtained after the partitioning process and it is characterized as follows:

- $BAG^i$ : unlike FWT strategy, under the MSP strategy the subset  $M(v_i)$  is fixed. Therefore, for a AFDX VL  $v_i$  the BAG is computed as follows:

$$BAG^i = 2^k, \quad k = \left\lceil \frac{\log(\min_{m_j \in M(v_i)} T_j)}{\log(2)} \right\rceil \quad (4.5)$$

- $MFS^i$ : unlike FWT, under MSP strategy an implicit AFDX frame structure is used and the sub-set of CAN messages  $M(v_i)$  to pack is known a priori. Therefore, an accurate MFS (in bits) for AFDX VL  $v_i$  is computed as follows:

$$MFS^i = \max \left( 84, \sum_{m_j \in M(v_i)} L_j + 67 \right) * 8 \quad (4.6)$$

- $DL^i$ : is the relative deadline of the obtained AFDX frame which depends on its associated CAN-messages subset  $M(v_i)$ . Unlike FWT strategy, under MSP strategy only the impact of CAN messages in  $M(v_i)$  needs to be taken into account instead of all CAN messages set  $M$  with FWT;
- $DES_{AFDX}^i$ : under MSP strategy, the sub-set  $M(v_i)$  is known a priori. Therefore, the set of AFDX destination end-systems is more accurate than under FWT:

$$DES_{AFDX}^i = \cup_{m_j \in M(v_i)} DES^j \quad (4.7)$$

An example of AFDX VLs allocation under MSP strategy is illustrated in Figure 4.6. In this example, a set of 4 CAN messages is mapped onto 2 AFDX VLs. VL 1 supports the successive transmission of frames containing messages 1 and 3, whereas VL 2 supports the successive transmission of frames 2 and 4.

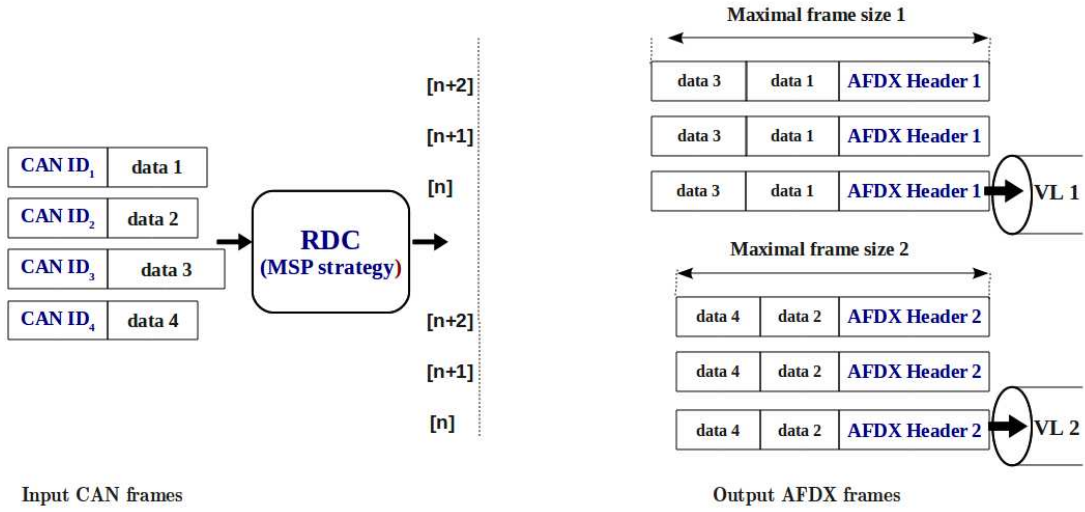


Figure 4.6: Example of AFDX VLs allocation under MSP strategy

### 4.1.2 HTS Mechanism Modeling

The HTS is used to manage downstream flows to minimize interference with upstream flows on CAN. Each leaf traffic shaper is applied for only one type of downstream flow and consequently admits the same period and authorized maximum payload than its associated flow. However, an inner traffic shaper is applied to a group of outgoing flows from leaf shapers. Then, each inner shaper  $sh$  in the set of inner shapers  $S_{h_{inner}}$ , applied for a set of downstream flows  $S_{sh}$ , is characterized by  $\{T_{sh}, L_{sh}, P_{sh}\}$ , where:

- $T_{sh}$  is the period. This value is comprised between  $T_{\min_{sh}}$  and  $T_{\max_{sh}}$  depending on the characteristics of  $S_{sh}$ . To support the aggregate flow rate,  $T_{\max_{sh}}$  is at most equal to  $\frac{1}{\sum_{i \in S_{sh}} \frac{1}{T_i}}$ . Furthermore, to avoid overflowing the CAN bus, we consider that  $T_{\min_{sh}}$  is at least equal to 1ms, which is an arbitrary choice that integrates CAN transmission capacity and typical production periods of CAN sources. If  $\frac{1}{\sum_{i \in S_{sh}} \frac{1}{T_i}} > 1\text{ms}$ , than this configuration is possible; else we should investigate other HTS configurations;
- $L_{sh}$  is the maximum payload size where  $L_{sh} = \max_{i \in S_{sh}} L_i$ ;
- $P_{sh}$  is the associated priority to the inner shaper. This value depends on the considered communication way and is equal to  $P_{\min_{sh}}$  or  $P_{\max_{sh}}$ . To cover the worst-case from the downstream flows point of view, this priority is considered as the lowest

priority among all its input downstream flows set, and  $P_{sh} = P \max_{sh} = \max_{i \in S_{sh}} P_i$ . However, the worst-case from the upstream point of view corresponds to considering the highest priority among all its input downstream flows set and  $P_{sh} = P \min_{sh} = \min_{i \in S_{sh}} P_i$ .

## 4.2 Timing Analysis

In this section, we first introduce a schedulability test based on end-to-end latencies to analyze the timing guarantees offered by our enhanced RDC to the crossed flows. Afterwards, an adequate timing analysis is provided to compute end-to-end latencies and evaluate the timing performance of the RDC.

### 4.2.1 Sufficient Schedulability Test

For avionics embedded applications, it is essential that the communication network fulfills certification requirements, e.g. predictable behavior under hard real-time constraints and temporal deadline guarantees. The use of a frame packing process and traffic shaping within the RDC may increase communication latencies and real-time constraints have to be checked. To deal with the worst-case performance analysis of such networks, we consider as a metric the worst-case end-to-end delay that will be compared to the temporal deadline for each frame.

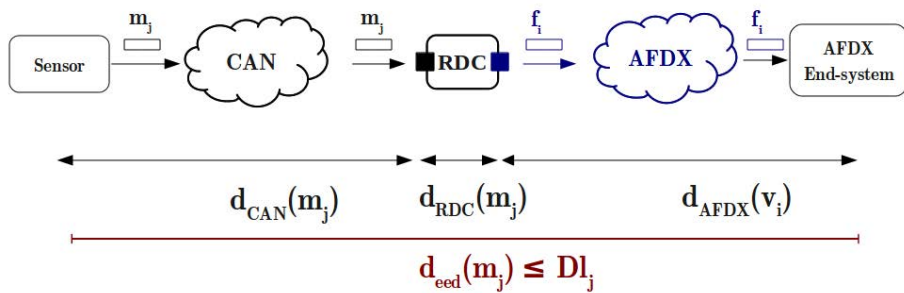


Figure 4.7: End-to-end delay metric definition

The end-to-end delay  $d_{eed}(m_j)$  of each CAN message  $m_j \in M(v_i)$ , where  $M(v_i)$  is the subset of CAN-messages associated with the VL  $v_i \in V$ , consists of three parts as shown

in Figure 4.7:

- $d_{CAN}(m_j)$ : is the maximal response time of a CAN frame. A schedulability analysis for native CAN bus has been introduced in [11], where the CAN bus is modeled as a static priority non-preemptive scheduler. This analysis will be adapted in the case where the HTS mechanism is applied in the RDC.
- $d_{RDC}(m_j)$ : is the maximal duration the message  $m_j$  might be delayed in the RDC. This delay depends mainly on the implemented frame packing strategy in the RDC device for upstream flows, and on the HTS mechanism implemented for downstream flows. For upstream flows, this delay is the sum of: (i) a technological latency, denoted by  $\epsilon$ , which is due to payload extraction/encapsulation and reading the mapping table; (ii) waiting time in the RDC between the reception instant of the CAN message and the transmission instant of its associated AFDX frame, denoted by  $WT(m_j)$ , then

$$d_{RDC}(m_j) = \epsilon + WT(m_j) \quad (4.8)$$

In this section, we will provide bounds on the RDC traversal latency for both upstream and downstream flows.

- $d_{AFDX}(v_i)$ : is the upper bound on the delay experienced by the AFDX VL including  $m_j$ . Delay bounds computation for the AFDX network, based on *Network Calculus* formalism, has been introduced in [17]. The tool *WoPANets* presented in [6] and based on Network Calculus formalism, will be used throughout this work to analyze AFDX delay bounds (see Appendix A for more details about the Network Calculus concepts and *WoPANets tool*).

The proposed schedulability test is as follows:

$$\forall v_i \in V, \forall m_j \in M(v_i),$$

$$d_{CAN}(m_j) + d_{RDC}(m_j) + d_{AFDX}(v_i) \leq Dl_j \quad (4.9)$$

## 4.2.2 Timing Analysis for Upstream Flows

First, we provide a method to compute a bound on RDC traversal delay  $d_{RDC}(m)$ . Afterwards, we provide a method to compute a bound on worst-case response time on CAN bus  $d_{CAN}(m)$ . The AFDX delay bound  $d_{AFDX}$  is computed using WoPANets tool given the set of allocated VLs obtained according to the implemented frame packing strategy, as provided in Section 4.1.1.

### 4.2.2.1 RDC Traversal Delay Computation

The RDC device delay imposed to upstream flows is due to the frame packing unit. Under FWT strategy, the worst-case waiting time in the RDC is equal to  $\Delta$ . As shown in Figure 4.8, this occurs when a CAN message is not completely received at the FWT packing queue before the expiration of an already started timer of duration  $\Delta$ . In this case, the received CAN message has to be transmitted within the next AFDX frame which is built after the expiration of a timer of duration  $\Delta$ .

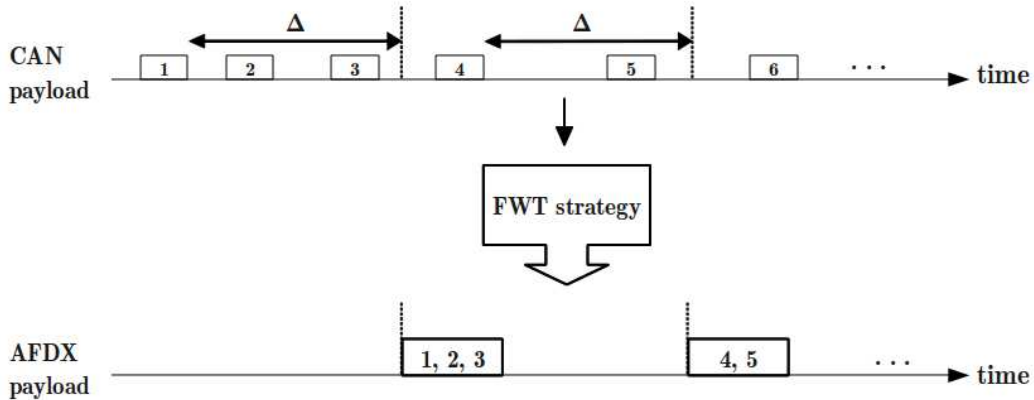


Figure 4.8: *Worst-case waiting time under FWT strategy*

Hence, a bound on the waiting time for message  $m_j$  in the RDC device under FWT strategy is given as follows:

$$WT(m_j) = \Delta \quad (4.10)$$

Under MSP packing strategy, the worst-case waiting time of a CAN-message  $m_j \in M(v_i) \setminus \{m_s\}$ , where  $m_s$  is the message with the smallest period, occurs when it arrives



immediately after the end of  $m_s$  reception in the RDC. In this case, the message  $m_j$  has to wait for the next reception of  $m_s$  to be packed in the same AFDX frame, as illustrated in Figure 4.9. Therefore, an upper bound of the waiting time in the RDC of  $m_j \in M(v_i)$  is:

$$WT(m_j) = \begin{cases} 0 & \text{if } j = s \\ T_s + d_{CAN}(m_s) & \text{otherwise} \end{cases} \quad (4.11)$$

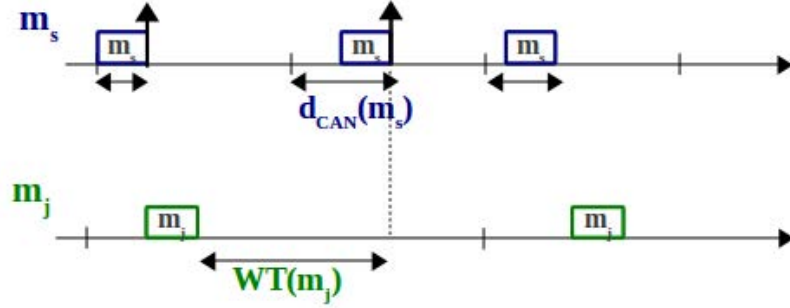


Figure 4.9: Worst-case waiting time under MSP strategy

#### 4.2.2.2 CAN Worst Case Response Time Computation

In [11], the CAN bus was modeled as a **static priority non-preemptive scheduler** and the Worst Case Response Time (WCRT) for a message  $m$  was provided:

$$\begin{aligned} d_{CAN}(m) &= R_m \\ &= \max_{q=0..Q_m-1} R_m(q) \end{aligned} \quad (4.12)$$

where  $Q_m$  is the number of instances of message  $m$  that become ready to transmission before the end of the busy period relative to  $m$ , and  $R_m(q)$  is the WCRT of instance  $q$  of message  $m$ .  $R_m(q)$  is given by:

$$R_m(q) = C_m + J_m + w_m(q) - qT_m \quad (4.13)$$

where,

- The transmission time  $C_m$ , corresponding to the longest time that the message can take to be transmitted;

- The queuing jitter  $J_m$ , corresponding to the longest time between the initiating event and the message being queued, ready to be transmitted on the bus;
- The queuing delay  $w_m(q)$ , corresponding to the longest time that the instance  $q$  of message  $m$  can remain in the CAN controller queue, before commencing transmission on the bus.
- $T_m$  is the period of message  $m$ .

$w_m(q)$  is computed using the following iterative expression:

$$w_m^{n+1}(q) = B_m + qC_m + \sum_{k \in hp(m)} \left\lceil \frac{w_m^n(q) + J_k + \tau_{bit}}{T_k} \right\rceil * C_k \quad (4.14)$$

where  $hp(m)$  corresponds to the set of messages with priority higher than  $m$ ,  $\tau_{bit}$  the transmission time of one bit and  $B_m$  the maximum blocking time due to the set of messages with lower priority than  $m$ , denoted by  $lp(m)$ . The recurrence relation starts with a value of  $w_m^0(q) = B_m + qC_m$ , and ends when  $w_m^n(q) = w_m^{n+1}(q)$ , or when  $R_m(q) = C_m + J_m + w_m^{n+1}(q) - qT_m > Dl_m$  in which case the message is unschedulable. For values of  $q > 0$  an efficient starting value is given by  $w_m^0(q) = w_m(q - 1) + C_m$ .  $B_m$  is given by:

$$B_m = \max_{k \in lp(m)} C_k \quad (4.15)$$

The number of instances that need to be examined  $Q_m$  is given by:

$$Q_m = \left\lceil \frac{t_m + J_m}{T_m} \right\rceil \quad (4.16)$$

where  $t_m$  corresponds to the length of the priority level- $m$  busy period is given by the following recurrence relation, starting with an initial value of  $t_m = C_m$ , and finishing when  $t_m^{n+1} = t_m^n$ :

$$t_m^{n+1} = B_m + \sum_{k \in hep(m)} \left\lceil \frac{t_m^n + J_k}{T_k} \right\rceil * C_k \quad (4.17)$$

$hep(m)$  is the set of messages with priority higher or equal to  $m$ .

The response time computed using equations 4.12 to 4.17 corresponds to the exact WCRT on CAN. However, it may induce a high computing complexity since it potentially requires the computation of multiple response times for each CAN message. In [11], authors presented a simpler but more pessimistic schedulability test which computes an upper bound on the WCRT on CAN, which is **only valid for CAN messages with**

**deadlines less or equal to periods.** An upper bound on WCRT on CAN for message  $m$  can be thus given by:

$$d_{CAN}(m) = C_m + w_m + J_m \quad (4.18)$$

where,  $w_m$  is an upper bound on the queuing delay of any instance  $q$  of message  $m$ , which is obtained using the following iterative expression:

$$w_m^{n+1} = \max(B_m, C_m) + \sum_{k \in hp(m)} \left\lceil \frac{w_m^n + J_k + \tau_{bit}}{T_k} \right\rceil * C_k \quad (4.19)$$

We denote by  $lep(m)$  the set of flows with priority lower or equal to  $m$ , then, 4.19 can be written as follows:

$$w_m^{n+1} = \max_{k \in lep(m)} (C_k) + \sum_{k \in hp(m)} \left\lceil \frac{w_m^n + J_k + \tau_{bit}}{T_k} \right\rceil * C_k \quad (4.20)$$

To check the schedulability of message  $m$  on CAN, we start with an initial value  $w^0(m) = C_m$  and continue until obtaining one of these two situations: (i)  $w^{n+1}(m) + C_m + J_m > Dl_m$ , then stop but no conclusion on the schedulability of message  $m$ ; (ii)  $w^{n+1}(m) = w^n(m)$ , then stop and conclude  $m$  is schedulable with an upper bound on its WCRT of  $w_m + C_m + J_m$ .

In order to compute the exact WCRT on CAN using equations 4.12 to 4.17, we define for an upstream flow  $m$  the set of messages  $hp(m)$  and  $lp(m)$  required for this timing analysis:

- $hp(m) = \{k \in S_{up} \cup Sh_{inner} / P_k < P_m\}$ : set of messages with priorities higher than  $m$  among upstream flows and the set of inner shapers in HTS structure by considering  $P \min_{sh}$  for each inner shaper  $sh \in Sh_{inner}$ ;
- $lp(m) = \{j \in S_{up} \cup Sh_{inner} / P_k > P_m\}$ : set of messages with priorities lower or equal than  $m$  among upstream flows and the set of inner shapers in the HTS structure by considering  $P \min_{sh}$  for each inner shaper  $sh \in Sh_{inner}$ .

To apply the sufficient schedulability test using equation 4.18 and 4.19, we define for an upstream flow  $m$  the set of messages  $hp(m)$  and  $lep(m)$  required for this timing analysis:

- $hp(m) = \{k \in S_{up} \cup Sh_{inner} / P_k < P_m\}$ : set of messages with priorities higher than  $m$  among upstream flows and the set of inner shapers in HTS structure by considering  $P \min_{sh}$  for each inner shaper  $sh \in Sh_{inner}$ ;
- $lep(m) = \{j \in S_{up} \cup Sh_{inner} / P_k \geq P_m\}$ : set of messages with priorities lower or equal than  $m$  among upstream flows and the set of inner shapers in the HTS structure by considering  $P \max_{sh}$  for each inner shaper  $sh \in Sh_{inner}$ .

In Section 4.2.2.3, we conduct a comparison between the upper bound on the WCRT on CAN bus and the exact WCRT to evaluate the degree of pessimism of the upper bound. The schedulability test 4.9 can be verified for each message  $m$  using equation 4.10, 4.11, 4.12 (or 4.18 under the assumption that the deadline of a message is equal to its period) and the obtained AFDX delay bounds using WoPANets tool.

#### 4.2.2.3 CAN analysis: upper bound vs exact WCRT

To illustrate the proposed timing analysis on CAN and assess the pessimism of the upper bound on the WCRT on CAN, we consider the following examples of flows on CAN:

- **Example 1:** we consider three messages corresponding to the example of Table 3 in [11], which was used to highlight the flaw in the analysis introduced by Tindell and al. in [25], as described in Table 4.1. The CAN message’s payload leading to a transmission time of 1 ms is equal to 116 bytes, which largely exceeds the maximum payload of 8 bytes allowed by CAN and the deadline of each message is equal to its production period. Even if this traffic is non realistic for a CAN bus, we use it to compare WCRT and the proposed upper bound on WCRT for CAN-like schedulers.

Table 4.1: Example 1: traffic characterization

Message	Priority	Period (ms)	Tx time (ms)	Deadline (ms)
A	1	2.5	1	2.5
B	2	3.5	1	3.5
C	3	3.5	1	3.5

- **Example 2:** we randomly generate a set of CAN messages with periods in 4,8,16ms and payloads in the interval [2,8]bytes. We consider several messages sets with a CAN utilization rate between 15% and 70%. The priorities are assigned to messages

such as  $P_i < P_j$  if  $T_i < T_j$ , i.e. the lower the period of  $m_i$  is the higher its priority is. For messages with the same period we arbitrary associated distinct priorities. The deadline of each CAN message is considered equal to its production period.

To evaluate the pessimism of the upper bound on the WCRT on CAN, for each of the previous CAN flows examples, we compute the exact WCRT using equation 4.12 and the upper bound on the WCRT using equation 4.18. Afterwards, we compare the obtained results and conclude on the degree of pessimism of our schedulability test.

For **example 1**, the obtained WCRT and upper bound on WCRT on CAN are reported in Table 4.2.

Table 4.2: Example 1: exact WCRT vs upper bound

Message	Deadline (ms)	WCRT (ms)	Upper Bound (ms)
A	2.5	2	2
B	3.5	3	3
C	3.5	3.5	7

The upper bounds obtained for messages A and B are equal to the exact WCRT. However, for message C we obtain a pessimistic upper bound of 7 ms compared to the exact WCRT which is equal to 3.5 ms. For this example, the CAN utilization is equal to 97% and messages utilization rates ( $C_m/T_m$ ) are relatively high, 40% for A and 28% for B and C.

For **example 2**, we consider the generated CAN traffic with the utilization rate 70%. The obtained WCRT and upper bound for each CAN message are reported in Figure 4.10. As can be seen, the obtained upper bounds for CAN messages are equal to the exact WCRT for all the messages except message 42 where the upper bound is slightly higher than the exact WCRT. The results obtained for generated CAN messages sets with low CAN utilization rates show very tight upper bounds. In this case, the number of instances obtained using Equation 4.17 is equal to 1 and the difference between computed WCRT and the upper bound is due to considering  $\max(B_m, C_m)$  (for the upper bound) instead of  $\max(B_m)$  (for the exact WCRT).

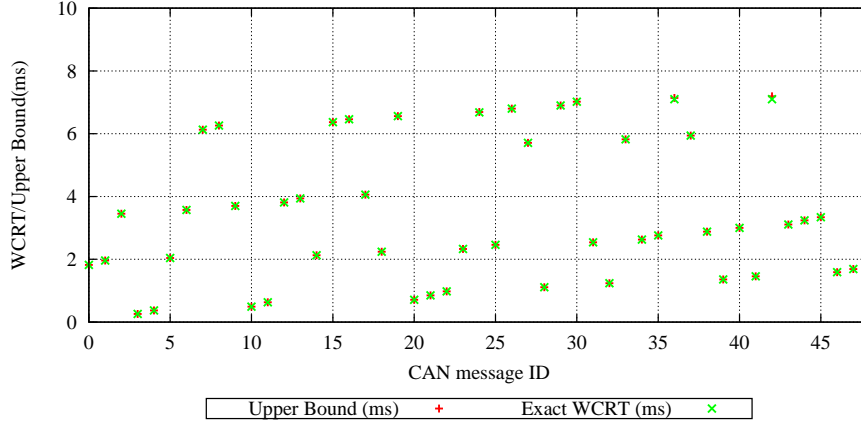


Figure 4.10: Comparison between exact WCRT and upper bound (Example 2)

The example 1 shows that under some extreme conditions (a very high CAN load, high individual utilization rates) the analysis using the upper bound may lead to large upper bound compared to the exact WCRT. However, for example 2, which represents a realistic CAN traffic in terms of payload size, periods and CAN bus utilization, the obtained results showed tight upper bounds on the WCRT. In our study, we consider realistic CAN traffic with similar properties as those of example 2 and we use the upper bound on WCRT for timing analysis on CAN bus to simplify the computation.

### 4.2.3 Timing Analysis for Downstream Flows

Downstream flows are subject to HTS when crossing the RDC device. In this section, we provide a method to compute a bound on RDC traversal delay,  $d_{RDC}(m)$ . Afterwards, we provide a method to compute a bound on worst-case response time on CAN bus  $d_{CAN}(m)$ .

#### 4.2.3.1 RDC Traversal Delay Computation

The RDC delay  $d_{RDC}(m)$  for a downstream flow  $m$  is composed of: (i) a technological latency, denoted by  $\epsilon$  due to payload extraction, unpacking and data encapsulation process; (ii) a blocking time due to the HTS structure, denoted by  $B_{shaper}(m)$ . The RDC delay can be written as follows:

$$d_{RDC}(m) = \epsilon + B_{shaper}(m) \quad (4.21)$$

For each downstream message  $m$ , first the leaf shaper, based on greedy method, absorbs the jitter due to AFDX network without increasing the maximal AFDX delay. The impact of this shaper on end-to-end delay is thus included in the AFDX delay. Furthermore, the input flows of inner shapers are considered as jitter free. An inner shaper, as we defined in the HTS structure, can be modeled as a static priority non-preemptive scheduler for downstream flows outcoming from leaf shapers. Each message  $m \in S_{sh}$  will occupy the shaper during  $T_{sh}$  units of time since the shaper does not send more than one packet per  $T_{sh}$ . Then, the worst-case blocking time at shaper  $sh$  is derived:

$$B_{shaper} = \max_{q=0..Q_m-1} B_{shaper}(q) \quad (4.22)$$

where  $Q_m$  is the number of instances of message  $m$  that become ready to transmission before the end of the busy period relative to  $m$ , and  $B_{shaper}(q)$  is the maximal blocking time in shaper  $sh$  of instance  $q$  of message  $m$ . Considering jitter free downstream flows at the entry of inner shapers,  $B_{shaper}(q)$  is derived as follows:

$$B_{shaper}(q) = Csh_m + w_m(q) - qT_m \quad (4.23)$$

where,

- $Csh_m$ , corresponding to the longest time that the message can take to be forwarded by the inner shaper;
- The queuing delay  $w_m(q)$ , corresponding to the longest time that the instance  $q$  of message  $m$  can remain in the inner shaper queue, before being forwarded;
- $T_m$  is the period of message  $m$ .

$w_m(q)$  is computed using the following iterative expression:

$$w_m^{n+1}(q) = B_m + q * T_{sh} + \sum_{k \in hp_{inner}(m)} \left\lceil \frac{w_m^n(q) + \tau_{bit}}{T_k} \right\rceil * T_{sh} \quad (4.24)$$

where  $hp_{inner}(m)$  corresponds to the set of messages with priority higher than  $m$  crossing the shaper  $sh$  and  $B_m$  the maximum blocking time due to the set of messages with lower priority than  $m$  sharing the shaper  $sh$ , denoted by  $lp_{inner}(m)$ :

$$B_m = \begin{cases} 0 & \text{if } lp_{inner}(m) = \emptyset \\ T_{sh} & \text{otherwise} \end{cases} \quad (4.25)$$

- $hp_{inner}(m) = \{k \in S_{sh} / P_k < P_m\}$ : set of messages shaped with the same inner shaper  $sh$ , with priorities higher than  $m$ ;
- $lp_{inner}(m) = \{j \in S_{sh} / P_j > P_m\}$ : set of messages shaped with the same inner shaper  $sh$ , with priorities lower than  $m$ .

The number of instances that need to be examined  $Q_m$  is given by:

$$Q_m = \left\lceil \frac{t_m}{T_m} \right\rceil \quad (4.26)$$

where  $t_m$  corresponds to the length of the priority level- $m$  busy period is given by the following recurrence relation, starting with an initial value of  $t_m = T_{sh}$ , and finishing when  $t_m^{n+1} = t_m^n$ :

$$t_m^{n+1} = B_m + \sum_{k \in hep_{inner}(m)} \left\lceil \frac{t_m^n}{T_k} \right\rceil * T_{sh} \quad (4.27)$$

$hep_{inner}(m)$  is the set of messages with priority higher or equal to  $m$  sharing the shaper  $sh$ .

#### 4.2.3.2 CAN Worst Case Response Time Computation

A bound on the worst-case response time on CAN for a downstream flow can be computed using equation 4.12 to equation 4.17 by considering the output flows of inner shapers as CAN flows with the same characteristics as the associated inner shaper (period, maximal size and priority) and by define the  $lp(m)$ ,  $hp(m)$  and  $hep(m)$  sets for each message  $m \in S_{down}$  as follows:

- $hp(m) = \{k \in S_{up} \cup Sh_{inner} / P_k < P_m\}$ : set of messages with priorities higher than  $m$  among upstream flows and inner shapers by considering  $P \max_{sh}$  for each inner shaper  $sh \in Sh_{inner}$ ;
- $hep(m) = \{k \in S_{up} \cup Sh_{inner} / P_k \leq P_m\}$ : set of messages with priorities higher than  $m$  among upstream flows and inner shapers by considering  $P \max_{sh}$  for each inner shaper  $sh \in Sh_{inner}$ ;
- $lp(m) = \{j \in S_{up} \cup Sh_{inner} / P_k < P_m\}$ : set of messages with priorities lower or equal than  $m$  among upstream flows and inner shapers by considering  $P \min_{sh}$  for



each inner shaper  $sh \in Sh_{inner}$ .

Hence, the schedulability test 4.9 can be verified for each message  $m$  using equation 4.12 and equation 4.21 and the obtained AFDX delay bounds using WoPANets tool.

## 4.3 Preliminary Performance Analysis

To evaluate the performance of our enhanced RDC CAN-AFDX device in terms of temporal guarantees and bandwidth utilization, we consider a small scale CAN-AFDX network with different upstream and downstream traffic scenarios. The impact of the RDC's functions on the communication latencies is assessed. Furthermore, the bandwidth utilization rates are computed to evaluate the efficiency of our enhanced RDC device to save network resources.

### 4.3.1 Considered Test Cases

#### 4.3.1.1 Test Case 1

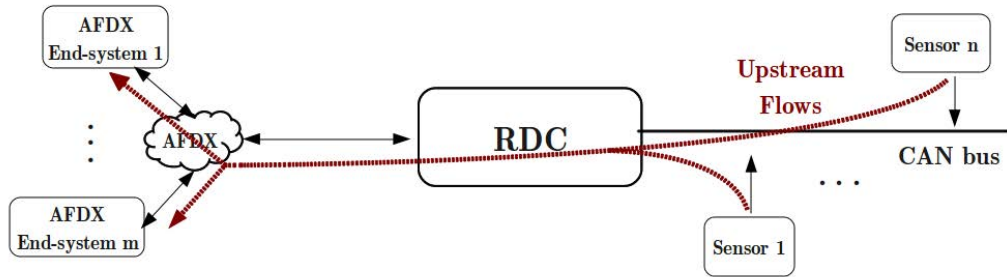


Figure 4.11: *Test case 1: one sensors CAN bus interconnected to the AFDX*

To illustrate the VLs allocation methodology and the schedulability analysis test for each proposed frame packing strategy, namely FWT and MSP, we consider the test case shown in Figure 4.11. In this considered test case, one sensors CAN bus is connected to the AFDX backbone using our enhanced RDC device. Hence, there is no contention between upstream and downstream flows on the CAN bus and the HTS mechanism can be deactivated within the RDC device. The considered CAN bus supports a set of upstream flows, with characteristics described in Table 4.3. The deadline of each message in Table 4.3 is assumed to be equal to its production period. A background AFDX traffic, i.e., AFDX flows exchanged between AFDX end-systems, is considered. The impact of the

AFDX flows on upstream flows is integrated in the AFDX delays  $d_{AFDX}$  computed using WoPANets tool.

Table 4.3: Upstream flows description

Messages	Number	Payload(bytes)	Period(ms)
$m_1$	3	8	4
$m_2$	2	8	8
$m_3$	16	2	16
$m_4$	4	2	32

#### 4.3.1.2 Test Case 2

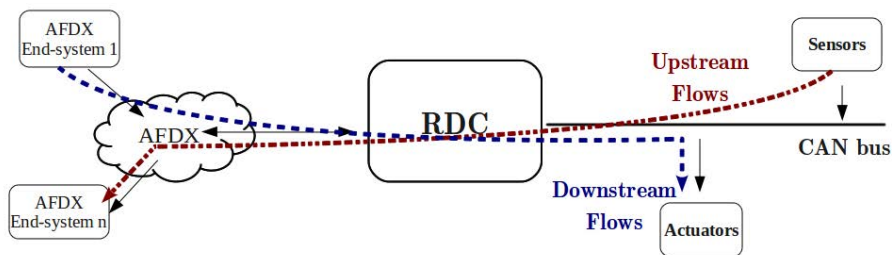


Figure 4.12: Test case 2: one sensors/actuators CAN bus interconnected to the AFDX

To evaluate the impact of the HTS algorithm integrated into the RDC device on the system performance, we consider the CAN-AFDX network architecture described in Figure 4.12. A sensors/actuators CAN bus is connected to the AFDX backbone using our enhanced RDC device, as shown in Figure 4.12. The CAN flows are described in Tables 4.4 and 4.5. Upstream and downstream flows consist both of 24 CAN messages with a payload size of 8 bytes and periods between 8ms and 32ms. We assume the deadline of each message is equal to its production period. We also assume that downstream flows have higher priorities than upstream flows. The same background AFDX traffic as Test Case 1 is considered to compute the AFDX delay  $d_{AFDX}$ .

Table 4.4: Downstream flows description

Message	Period (ms)	size (bytes)	Priority
$m_1 - m_8$	8	8	1 - 8
$m_9 - m_{16}$	16	8	9 - 16
$m_{17} - m_{24}$	32	8	17 - 24

Table 4.5: Upstream flows description

Message	Period (ms)	size (bytes)	Priority
$m_{25} - m_{32}$	8	8	25 - 32
$m_{33} - m_{40}$	16	8	33 - 40
$m_{41} - m_{48}$	32	8	41 - 48

### 4.3.2 Impact of Frame Packing Strategy

To evaluate the impact of frame packing strategies on network performance, we consider **Test Case 1**.

#### 4.3.2.1 Under FWT

Induced VLs characteristics and corresponding AFDX bandwidth consumption under FWT strategy, obtained with different values of waiting time  $\Delta$  varying between  $1ms$  to  $3ms$ , are reported in Table 4.6. These values have been chosen less than the smallest period among upstream flows, i.e.,  $T_1 = 4ms$ , otherwise the configuration is obviously not feasible. The (1:1) strategy is used as a reference to show the performance enhancements offered by our proposed FWT strategy.

As it can be noticed, implementing (1:1) strategy in the CAN-AFDX RDC leads to a significant number of VLs with a high induced AFDX bandwidth rate. This is essentially due to the high overhead when sending each CAN data (less than or equal to 8 bytes) in one AFDX frame (at least 84 bytes, including inter-frames gap). On the other hand, the FWT strategy offers a noticeable amelioration on the number of allocated VLs in the RDC, but also on the consumed AFDX bandwidth where a reduction of roughly 50% is obtained with  $\Delta_2$  and  $\Delta_3$ .

These results show a decreasing bandwidth consumption when the waiting time  $\Delta$  increases. However, from a given value, the obtained bandwidth consumption becomes stable even if the waiting time increases. In this case, we observe no improvement in terms of induced AFDX bandwidth rate for  $\Delta_3 = 3ms$  compared to  $\Delta_2 = 2ms$ . It is worth to note that a non-optimal choice of waiting time can lead to a poor bandwidth utilization rate, which is the case for  $\Delta_1 = 1ms$ . In fact, this value reduces the number of allocated VLs, but the induced bandwidth consumption is still comparable to the one obtained with (1:1) strategy. This is mainly due to the over-dimensioning of the allocated BAG and MFS for each VL. For waiting times  $\Delta_2$  and  $\Delta_3$ , important bandwidth savings are achieved compared to (1:1) strategy and this is mainly due to the reduction of the number of AFDX VLS allocated to upstream flows.

Table 4.6: VLs characteristics under FWT

Strategy	BAG (ms)	MFS (bytes)	VLs number	rate (Mbps)
(1:1)	4	84	25	1.42
$\Delta_1 = 1ms$	4	167	4	1.3
$\Delta_2 = 2ms$	4	172	2	0.69
$\Delta_3 = 3ms$	4	172	2	0.69

The end-to-end delay bound is computed for each message and then compared to its respective deadline to check its schedulability condition. The obtained delay bounds under the (1:1) strategy and the FWT with the different waiting times are described in Tables 4.7 and 4.8, respectively. The technological latency in the RDC device is assumed to be bounded by  $\epsilon = 0.05ms$ .

Table 4.7: End-to-end delay bounds under (1:1) strategy

Msgs	$d_{AFDX}(ms)$	$d_{CAN}(ms)$	$T(ms)$	$d_{eed}^{1:1}(ms)$
$m_1$	1.1	0.54	4	1.69
$m_2$	1	0.8	8	1.85
$m_3$	1.1	1.95	16	3.1
$m_4$	1.4	2.23	32	3.68

Table 4.8: End-to-end delay bounds under FWT strategy with  $\Delta_1$ ,  $\Delta_2$  and  $\Delta_3$ 

Message class	$T(ms)$	$d_{eed}^{\Delta_1}(ms)$	$d_{eed}^{\Delta_2}(ms)$	$d_{eed}^{\Delta_3}(ms)$
$m_1$	4	2.9	3.75	4.75
$m_2$	8	3.15	4	5
$m_3$	16	4.3	5.15	6.15
$m_4$	32	4.58	5.4	6.4

As it can be noticed from Table 4.7, the set of CAN messages is schedulable under (1:1) strategy since all obtained delays respect their associated deadlines, chosen equal to periods in our example. Under FWT strategy, as reported in Table 4.8,  $\Delta_1$  and  $\Delta_2$  lead to a schedulable configurations. However, when  $\Delta$  increases the schedulability condition is compromised as it can be seen with  $\Delta_3$ . Hence, increasing the waiting time inside the gateway is not always the best solution to enhance the performances while satisfying the temporal constraints.

#### 4.3.2.2 Under MSP

Different MSP configurations may be defined by partitioning the set of CAN messages and defining the resulting allocated AFDX VLs into the RDC device. A direct MSP configuration consists in affecting all CAN messages to one AFDX VL. This configuration is not schedulable in practice and is therefore discarded.

For upstream flows described in Table 4.3, we introduce the MSP configurations of Table 4.9.

Table 4.9: MSP configurations considered for upstream flows in Table 4.3

Configurations	VL allocation
$conf_1$	$v_1 : \{3 * m_1\}, v_2 : \{2 * m_2\}, v_3 : \{16 * m_3\}, v_4 : \{4 * m_4\}$
$conf_2$	$v_1 : \{3 * m_1, 2 * m_2\}, v_2 : \{16 * m_3, 4 * m_4\}$
$conf_3$	$v_1 : \{1 * m_1, 2 * m_2\}, v_2 : \{1 * m_1, 16 * m_3\}, v_3 : \{1 * m_1, 4 * m_4\}$

The configuration  $conf_1$  corresponds to packing all the messages of type  $m_i$  within the same AFDX frame supported by the virtual link  $v_i$ . In Table 4.10, we reported the

characteristics of the allocated AFDX VLs for each MSP configuration,  $conf_1$ ,  $conf_2$  and  $conf_3$ . Furthermore, the end-to-end delay bounds under the different MSP configuration are described in Table 4.11.

As we can see from Tables 4.10 and 4.11, MSP configurations  $conf_1$  and  $conf_2$  offer high AFDX bandwidth reduction. However, they imply high end-to-end delays and do not meet schedulability constraints of upstream flows. For example under  $conf_1$ , message  $m_1$  has a delay bound about  $5.8ms$ , which is higher than its deadline equal to  $4ms$ . Hence, these two configurations are not schedulable and have to be discarded.

Table 4.10: Induced VLs characteristics under MSP configurations

Strategy	VLs number	rate (Mbps)
(1:1)	25	1.42
$conf_1$	4	0.34
$conf_2$	2	0.27
$conf_3$	3	0.56

MSP configuration  $conf_3$  offers an AFDX bandwidth consumption reduction of roughly 60% compared to (1:1) strategy, and it meets timing constraints for all CAN messages, as shown in Table 4.11. Hence,  $conf_3$  is schedulable and can be implemented within the RDC device to process the upstream messages.

Table 4.11: End-to-end delay bounds under MSP strategy

Message class	$T(ms)$	$d_{eed}^{conf_1}(ms)$	$d_{eed}^{conf_2}(ms)$	$d_{eed}^{conf_3}(ms)$
$m_1$	4	5.7	5.8	1.95
$m_2$	8	10	6.1	6.2
$m_3$	16	19.2	19.1	7.35
$m_4$	32	35.4	19.5	7.6

#### 4.3.2.3 Comparative Analysis

As we have seen through results of Test Case 1, frame packing mechanism offers significant reduction of consumed AFDX bandwidth by upstream flows on AFDX network

under well-configured strategy. The comparison between the two proposed frame packing strategies, in terms of consumed AFDX rate, is in favour of MSP strategy where the AFDX rate is about  $0.56Mbps$  instead of  $0.69Mbps$  under FWT.

However, the comparison between these two frame packing strategies should also take into account the complexity of implementation. The FWT strategy requires only one queue and a fixed timer to be implemented within the RDC, whereas MSP strategy needs several queues and a timer per queue to be set up within the RDC.

On the other hand, the choice of accurate frame packing strategy parameters, for both FWT and MSP strategies, could be a hard task. This fact is due to the high number of possible configurations and the verification of the temporal constraints. Therefore, a tuning process to select accurate frame packing configurations for both FWT and MSP strategies is required, and it will be detailed in the next chapter.

### 4.3.3 Impact of HTS Mechanism

To evaluate the impact of HTS mechanism, we consider the **Test Case 2**. We first compute the CAN WCRT for upstream flows and the delay bounds integrating the RDC and CAN delays for downstream flows to show the impact of traffic shaping process on timing performance. Then, we compute consumed AFDX bandwidth by the RDC device when using MSP packing strategy to process upstream flows, combined to HTS mechanism for downstream flows. Indeed, MSP strategy is selected herein since it showed better enhancements in terms of bandwidth consumption than FWT strategy in Section 4.3.2

As can be seen in Figure 4.13, the use of HTS in RDC device reduces upstream flows delays on CAN by almost 50%. Consequently, as reported in Table 4.12, the consumed AFDX bandwidth by upstream flows has also decreased when using HTS mechanism with reference to a naive (1:1) strategy and the case where HTS is deactivated. We can see that using HTS offers a significant bandwidth saving, of roughly 40% and 33%, respectively. This is due to the reduction of upstream flows CAN delays which favors the frame packing process. On the other hand, as shown in Figure 4.14, the improvement of upstream flows delays and AFDX bandwidth saving comes with the degradation of downstream flows delays. In this case, messages 7 and 8 do not respect their respective timing constraints, and consequently the RDC configuration is non schedulable.

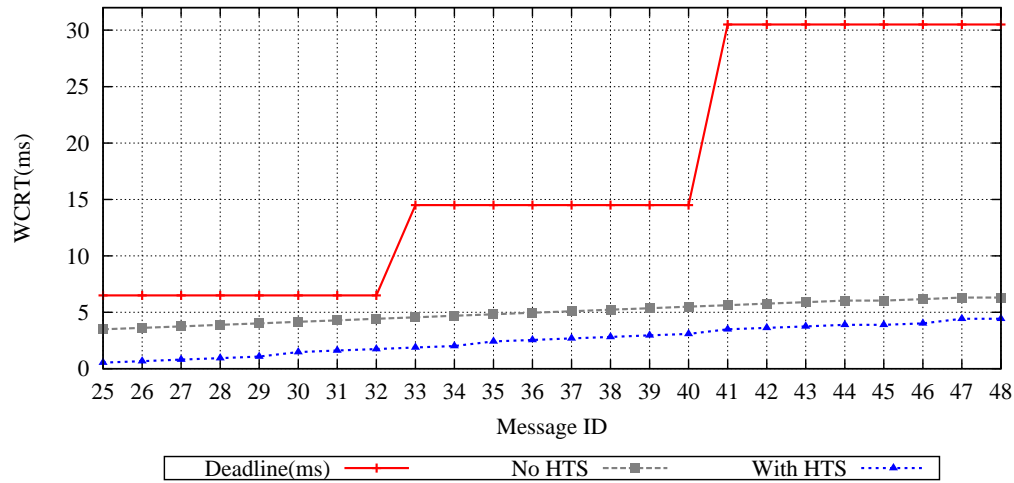


Figure 4.13: CAN WCRT of upstream flows

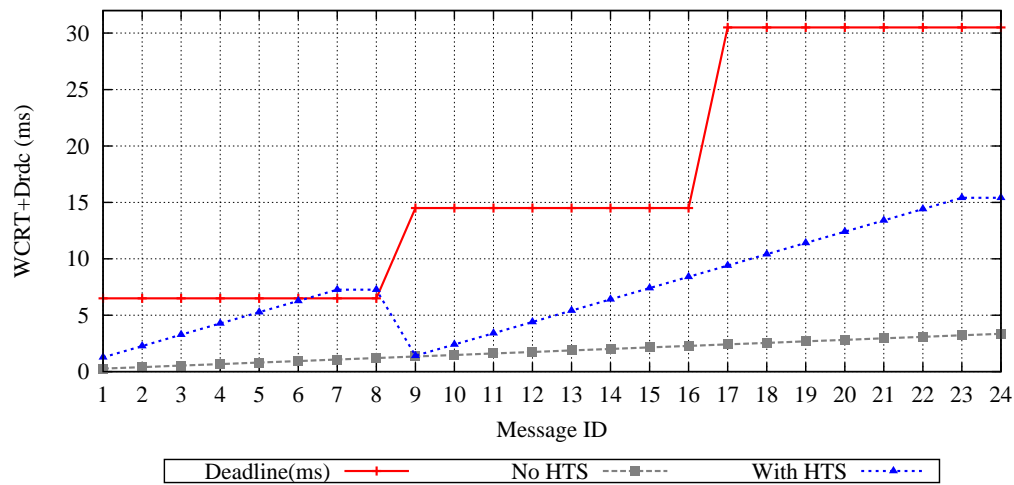


Figure 4.14: CAN WCRT of downstream flows

Table 4.12: Example 1: AFDX bandwidth consumption

Configuration	AFDX Bandwidth (in Mbps)
(1:1)	1.15
MSP + NO HTS	1.05
MSP + HTS	0.7

Various configurations of HTS can be explored to find an accurate shaping in the



CAN-AFDX RDC, i.e., offering a significant reduction of AFDX bandwidth consumption and meeting timing constraints for both upstream and downstream flows. However, as this will be shown in the next chapter, the selection of traffic shaping parameters is a hard task, and a method for RDC parameters tuning is needed to find the best configuration.

## 4.4 Conclusion

In this chapter, the frame packing and traffic shaping functions applied on the upstream and downstream flows, respectively, have been modeled. Furthermore, a timing analysis approach has been introduced to verify the temporal constraints when using our enhanced RDC device. The analytical results with simple test cases have shown the efficiency of the frame packing approaches in saving AFDX bandwidth, especially the static strategy MSP. The HTS shaping approach has also shown an important role on guaranteeing isolation on CAN between upstream and downstream flows. Moreover, it improves the efficiency of the frame packing process applied on the upstream flows in terms of AFDX bandwidth consumption.

The first results have also shown that there are various CAN-AFDX RDC configurations, i.e., various frame packing strategy and HTS mechanism parameters, which offer a feasible communication and different network utilization levels. Therefore, a major challenge consists in tuning the RDC device parameters to maximize the network's resource savings. This RDC tuning problem will be addressed in the next chapter, and adequate solving approaches will be provided.



# Chapter 5

## Performance Optimization of the Enhanced RDC

In this chapter, the tuning of our proposed RDC device, i.e., selection of the frame packing and traffic shaping configurations, is performed to maximize network resource savings. First, the RDC tuning problem is formulated as an optimization problem. Afterwards, since finding the exact optimal solution is a hard task in practice, we have introduced heuristic approaches to find accurate solutions in a polynomial time. Finally, preliminary performance evaluation of the optimized CAN-AFDX RDC device is conducted through a small scale case study under various traffic loads and RDC configurations.

### 5.1 Problem Formulation

To enhance the avionic networks scalability and let margins for future function addition, an adequate optimization process is required to define the best RDC configuration maximizing resource savings and respecting system timing constraints. We select the AFDX bandwidth consumption as a relevant metric to assess network resource savings when using the enhanced RDC device for CAN-AFDX interconnection.

Our objective consists in finding the RDC configuration, i.e., parameters of frame packing and HTS functions, minimizing the bandwidth consumption on AFDX network and meeting system's time constraints. This can be formulated as an optimization problem as follows:

$$\underset{V}{\text{minimize}} \quad Bw(V) \tag{5.1}$$

$$\text{subject to} \quad \forall m_i \in S_{up} \cup S_{down}, d_{eed}(m_i) \leq Dl_i \tag{5.2}$$

where,

- $Bw(V) = \sum_{v_i \in V} \frac{MFS^i}{BAG^i}$  is the AFDX bandwidth consumption of allocated VLs set  $V$  originating at the RDC;
- the constraint corresponds to the schedulability condition of upstream and downstream flows;

This optimization problem will be studied following an incremental approach:

- **First**, we consider the case where the enhanced RDC device interconnects specific CAN buses for either sensors or actuators to the AFDX backbone network. Hence, we focus on the impact of the RDC on upstream flows by activating the frame packing process and deactivating the HTS mechanism.
  - As a first step, we select the **FWT packing strategy** in the RDC and we vary the waiting timer  $\Delta$ . Then, the optimization problem becomes equivalent to tuning the parameter  $\Delta$  of the FWT strategy to minimize the AFDX bandwidth consumption induced by the RDC device while fulfilling timing constraints. This study is detailed in Section 5.2;
  - Then, we select the **MSP packing strategy** in the RDC and we vary the partition of the upstream flows set. Then, the optimization problem becomes equivalent to the selection of the best partition which minimizes the AFDX bandwidth consumption induced by the RDC device while fulfilling timing constraints. This study is detailed in Section 5.3;
- **Second**, we consider the general case where the enhanced RDC device interconnects sensors/actuators CAN buses to the AFDX backbone. Hence, we integrate the HTS mechanism effect when the frame packing process is activated in the RDC and we vary the parameters of the shapers in the HTS structure. Then, the optimization problem becomes equivalent to the selection of the best configuration of

the HTS mechanism, combined with the best frame packing strategy that minimizes the AFDX bandwidth consumption induced by the RDC device while fulfilling timing constraints. This study is detailed in Section 5.4;

## 5.2 Optimization Process under FWT Strategy

For FWT strategy, we consider the waiting time duration as the parameter to tune, as shown in Figure 5.1, to enhance the AFDX bandwidth consumption efficiency. Therefore, we introduce a solving approach to find the most accurate value of  $\Delta$ .

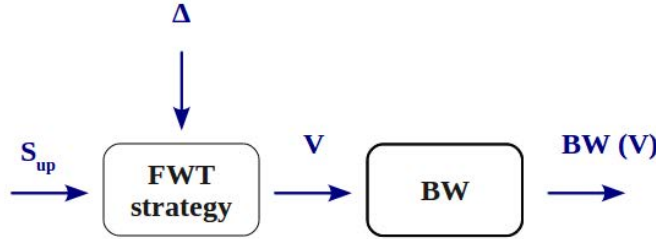


Figure 5.1: Optimization for FWT strategy

The main difficulty to solve the optimization problem 5.1 for FWT strategy is due to the fact that the schedulability constraints cannot be expressed using closed-form expressions depending on the waiting time  $\Delta$ , since iterative algorithms based on Network Calculus formalism are used to compute bounds on AFDX delays. To cope with this problem, we start by analyzing the impact of the parameter  $\Delta$  on the induced RDC bandwidth consumption on the AFDX.

This latter is expressed as follows where the characteristics of the allocated VLs  $V$  associated to each waiting time  $\Delta$  are determined as explained in the previous chapter in Section 4.1.1.1:

$$BW(\Delta) = \sum_{v_i \in V(\Delta)} \frac{MFS^i}{BAG^i} \quad (5.3)$$

The function  $BW(\Delta)$  obtained for the example described in Table 4.3 in the previous chapter is illustrated in Figure 5.2. The AFDX bandwidth consumption obtained with

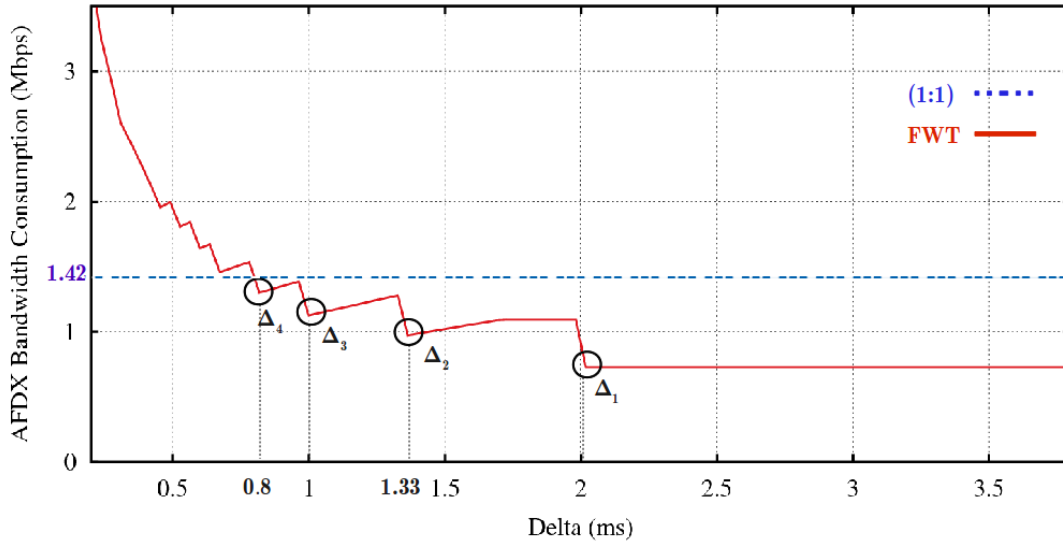


Figure 5.2: Impact of the waiting timer  $\Delta$  on the AFDX bandwidth consumption

the (1:1) strategy, denoted by (1:1) in the Figure 5.2, is considered as a reference. This latter corresponds to the sum of allocated VLs rates obtained when sending each CAN message of the set  $M$  in a separate VL and it is as follows:

$$BW_{(1:1)} = \sum_{m_j \in M} \frac{84 * 8}{T_j} \quad (5.4)$$

As shown in Figure 5.2, implementing (1:1) strategy in the RDC device induces an AFDX bandwidth equal to  $1.42 Mbps$ . However, the FWT strategy offers a better bandwidth consumption compared to the (1:1) strategy, for all waiting times greater than 0,8ms. Furthermore, as it can be noticed in Figure 5.2, there are many local minima of RDC bandwidth consumption corresponding to the waiting times equal to integer divisors of  $T_{min}$ , which is the smallest period among upstream flows. The list  $L_{\Delta}$  containing the values of  $\Delta$  corresponding to these minima is considered and sorted in a decreasing order as follows:

$$L_{\Delta} = \left\{ \Delta_1 = \frac{T_{min}}{2}, \Delta_2 = \frac{T_{min}}{3}, \dots, \Delta_K = \frac{T_{min}}{K+1} \right\} \quad (5.5)$$

where  $K$  is the maximum integer giving a better bandwidth consumption than the strategy (1:1). For instance, in Figure 5.2,  $T_{min} = 8ms$  and  $K = 4$ .

According to the plotted curve in Figure 5.2, the induced bandwidth rate decreases when the waiting time increases. However, we could not simply consider the biggest waiting time duration because there is no guarantee of the schedulability constraints. Hence, we propose to explore this waiting time list to check for each value of  $\Delta$  the temporal constraints. If the constraints are verified, then the exploration is stopped and the current value of  $\Delta$  is considered as the accurate waiting time to implement in the RDC.

Therefore, we introduce FWT heuristic to solve this problem. This heuristic takes the upstream flows set as input data and returns as output the accurate waiting time  $\Delta$  that guarantees the minimum AFDX bandwidth consumption and the temporal constraints. The different steps of the proposed FWT heuristic are as follows:

1. Compute  $BW(\Delta)$  and  $BW_{(1:1)}$  for the input upstream messages set  $M$ , using expressions 5.3 and 5.4, respectively.
2. Find  $\Delta_{min}$  corresponding to the smallest local minima leading to lower bandwidth consumption compared to (1:1) strategy. As  $\Delta_{min} = \frac{T_{min}}{K+1}$ , this is equivalent to finding  $K$  which is the maximum integer leading to the lowest AFDX bandwidth consumption compared to (1:1) strategy.
3. Define the list  $L_{\Delta}$  of waiting times to explore. This list contains local minima of bandwidth consumption as explained in expression 5.5 for the example shown in Figure 5.2. To be inserted in  $L_{\Delta}$ , a local minima has to be in the interval  $[\Delta_{min}, \frac{T_{min}}{2}]$  and equal to integer divisors of  $T_{min}$ . Then, the list  $L_{\Delta}$  is sorted in decreasing order to find the highest waiting time which offers the lowest bandwidth consumption.
4. Consider the next value of  $\Delta$  from the list  $L_{\Delta}$ , then check the schedulability condition, i.e., the timing constraints of upstream flows are met, :
  - (a) If the condition is verified, then SUCCESS.
  - (b) If not and there is at least one value of  $\Delta$  to explore, go to step (4). If all values of  $\Delta$  are already explored, then FAILURE.

### 5.3 Optimization Process under MSP Strategy

Using MSP strategy, the AFDX VLs allocation for upstream flows is directly defined using a partitioning process as shown in Figure 5.3. Therefore, the choice of the partition in the RDC is the main parameter to tune, to achieve the lowest AFDX bandwidth consumption. For the MSP strategy, the optimization problem 5.1 can be modeled as a Bin-Packing (BP) problem.

For the BP problem, items have to be assigned to bins. Each item is assigned to exactly one bin and the total size of each bin does not exceed its maximal capacity. Then, the number of used bins has to be minimized. The BP problem has been considered as a NP-hard problem in [41] and many algorithms have been introduced to find approximate solutions in a polynomial execution time.

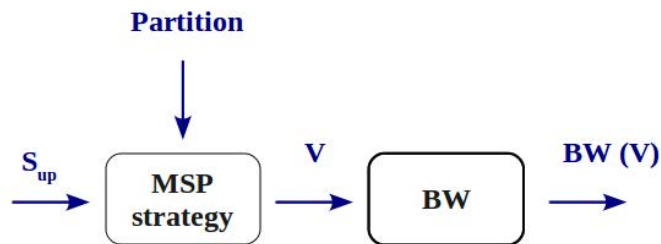


Figure 5.3: Optimization for MSP strategy

Hence, to solve the optimization problem for the MSP strategy, we formulate it as a BP problem where:

- AFDX VLs are considered as the bins;
- CAN data are modeled as the items to pack into bins;
- The objective is to minimize the AFDX bandwidth consumption induced by the RDC device.

However, unlike the BP problems where the number of used bins has to be minimized, in our case we are looking for minimizing the AFDX bandwidth consumption and not the AFDX frames number. Indeed, minimizing the number of AFDX frames is not necessary



the best choice in terms of AFDX bandwidth consumption which depends on multiple parameters such as the frames number, sizes and periods. Furthermore, the BP problem considers only the bin capacity constraint, whereas in our case, in addition to AFDX frame size constraint, we have timing constraints. Therefore, the introduced algorithms to solve classic BP problems need some adaptations to be used for MSP tuning problem.

In this section, we investigate different optimization approaches that can be used to find a feasible MSP strategy, i.e., frame set partition respecting the schedulability constraints and minimizing the induced AFDX bandwidth. The proposed approaches are as follows:

- The first approach is based on Exhaustive Search that considers all possible partitions to find the best feasible one. However, the partition number of a set with a size  $n$  is known as Bell number  $B$  that grows exponentially with  $n$ , i.e., for a set of 20 frames,  $B \sim 5.10^{14}$ . Hence, this approach will certainly lead to the best frame partition in terms of bandwidth consumption, but at the same time it is a time-consuming approach due to solutions-space explosion;
- The second approach consists in building a specific heuristic, inspired by the classical Best-Fit-Decreasing (BFD) algorithm [41], to reach an approximate solution in terms of bandwidth consumption within a polynomial time;
- The third approach is based on the Branch & Bound algorithm [42] to bridge the gap between the Exhaustive Search and the Heuristic approach by reducing the size of explored solutions-space compared to the former and enhancing the quality of the obtained solution compared to the latter.

A comparative analysis between the three approaches in terms of complexity and solution quality is shown in Table 5.1. As can be noticed, the Heuristic approach and the Branch & Bound algorithm are the most adapted approaches for our optimization problem.

Therefore, an adapted heuristic approach, called *Bandwidth-Best-Fit Decreasing* (BBFD) heuristic, and an adequate algorithm based on the *Branch & Bound* (B&B) concept are proposed to solve our MSP tuning problem within the RDC device.

Table 5.1: Comparative analysis of Optimization approaches

Approach	Complexity	Solution Quality
Exhaustive Search	high	high
Branch & Bound	medium	high
Heuristic	low	medium

### 5.3.1 Bandwidth Best Fit Decreasing Heuristic

Several heuristics were introduced to compute an approximate solution for the classical Bin-Packing problem [41]. The simplest heuristic is *First-Fit Decreasing (FFD)* which is based on sorting items according to a decreasing order of sizes, and then inserting each item in the first bin with enough space to include that item. A more effective heuristic is *Best-Fit Decreasing (BFD)* which differs from the first one by selecting the most suitable bin among the list of bins instead of the first possible bin. Our objective is to minimize bandwidth consumption instead of the number of used VLs, corresponding to the bins in the BP problem, while guaranteeing the temporal constraints of all the transmitted AFDX frames. Thus, we introduce the Bandwidth-Best-Fit Decreasing (BBFD) heuristic described in Figure 5.4, and we describe in the following sections the main steps of this heuristic.

#### 5.3.1.1 Initialization

The heuristic sorts the input messages set  $M$  to pack into AFDX VLs in the increasing order of their respective deadlines. The heuristic starts by packing first the messages with the smallest deadlines to build partitions favoring the most constrained messages.

#### 5.3.1.2 Iterative partitioning

The set of AFDX VLs is built iteratively. At the beginning, the first message in set  $M$  is inserted in a new VL that is added to the set  $V$ . Then, the BBFD heuristic is conducted for each selected message  $m_i \in M$  as follows:

- (a) if there is at least one existent VL in  $V$  that can support message  $m_i$ , i.e. the temporal deadline and the maximal MFS size of 1518 bytes are respected, then it builds the subset  $V(m_i)$  that corresponds to the obtained VLs sets including  $m_i$ .

Afterwards, it selects the VL in  $V(m_i)$  that minimizes the obtained AFDX bandwidth consumption and adds it to the set  $V$ ;

- (b) if there is no existent VL in  $V$  that can support  $m_i$ , because the maximal MFS size of 1518 bytes is exceeded or its deadline constraint is not respected, then it builds a new VL including  $m_i$  and adds it to the set  $V$ .

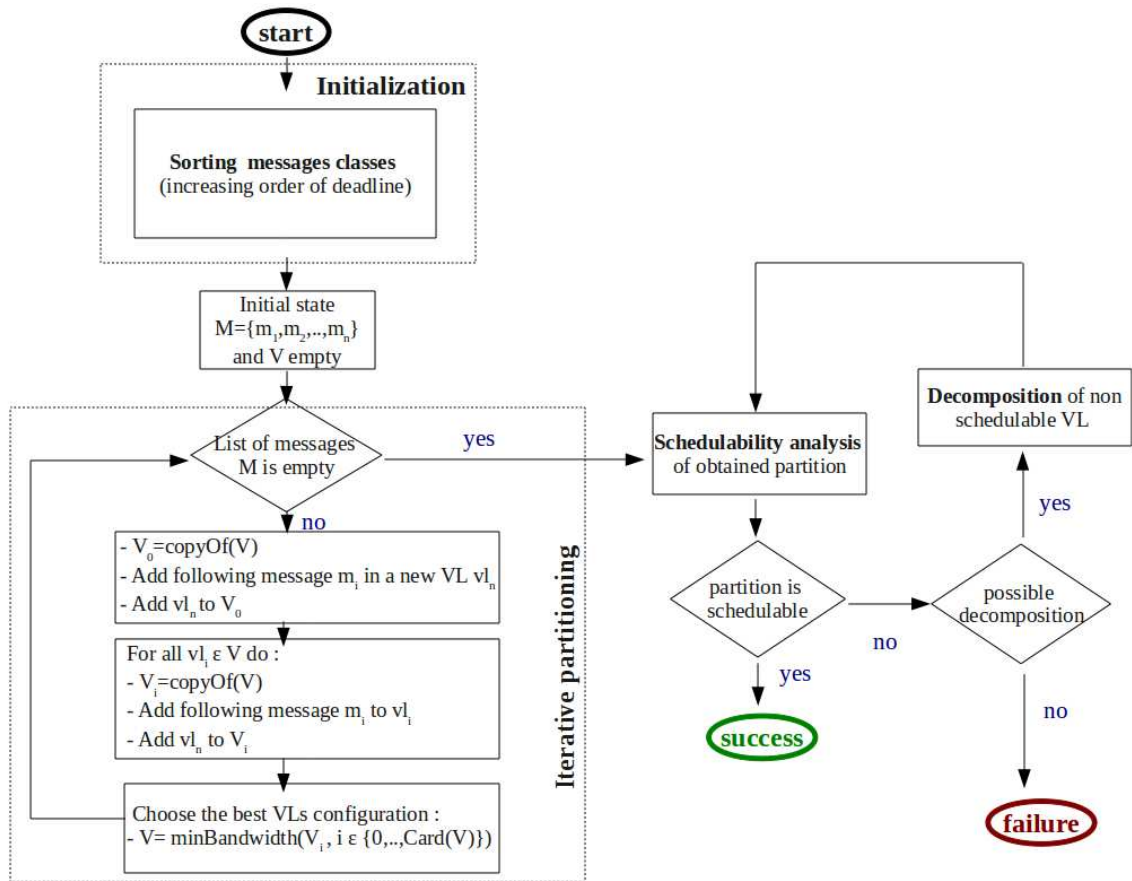


Figure 5.4: *Bandwidth-Best-Fit Decreasing heuristic*

At the end of this step, an AFDX VLs set  $V$  is obtained such that bandwidth consumption is minimized. However, the schedulability analysis of this configuration needs to be checked.

### 5.3.1.3 Schedulability analysis

This step consists in conducting the schedulability analysis of the obtained configuration. If the schedulability condition is verified, then this configuration is considered as the solution of our optimization process and the heuristic stops successfully. Otherwise, a decomposition process is launched.

### 5.3.1.4 Decomposition

The main idea of decomposition process consists in identifying the VLs subset  $V^* \subset V$ , which does not meet the schedulability condition. Then, to relax this constraint, the heuristic is based on unpacking the most urgent messages included in the identified VLs. Therefore, for each VL  $v_k \in V^*$ :

- (a) if  $v_k$  contains at least two messages, then unpack the most critical one and include it in a new VL. Afterwards, update the VL set  $V$  and go back to the step Schedulability analysis of the heuristic;
- (b) if  $v_k$  consists of one CAN message, then there is no possible improvement of VLs schedulability using our decomposition process. In this case, the heuristic returns a failure.

## 5.3.2 Branch & Bound Algorithm

The main idea of Branch & Bound algorithm [42] is based on the definition of upper and lower bounds for an objective function to explore the most promising subspace of potential solutions, and consequently to reduce the computation's complexity. The two main operations to process the Branch & Bound algorithm are: (i) a Branching-Strategy that consists in generating the new states from an existing one; (ii) a Discarding-Policy that consists in eliminating the subspace of solutions admitting their lower bound of the objective function exceeding the upper bound of the reference solution.

This general algorithm is adapted to our MSP tuning problem to build a schedulable set of AFDX VLs within the gateway, while minimizing the bandwidth consumption. To explore the subspace of potential solutions, we identify each state by  $(V, \mathcal{M})$ , where  $V$  is the set of VLs already created and  $\mathcal{M}$  the set of input messages not yet processed, i.e. not yet allocated to VLs in  $V$ . The upper and lower bounds of our objective function

i.e. bandwidth consumption, the Branching-Strategy and Discarding-Policy are defined in the following sections.

### 5.3.2.1 Upper bound

The main idea consists in enhancing the quality of the solution obtained with the BBFD heuristic. Hence, the CAN-messages partition obtained with this latter solution is considered as a reference solution and the induced bandwidth consumption of the obtained VLs set is identified as the upper bound of the bandwidth consumption to launch the exploration of the most promising solutions. If BBFD fails to find a feasible solution, then any schedulable partition of messages can be considered as the reference solution, such as the partition obtained with (1:1) strategy. However, it is worth noting that the better is the reference solution, the faster an optimal solution is obtained with the B & B algorithm. Each time we find a CAN-messages partition with a bandwidth consumption lower than this upper bound, the reference solution is updated.

### 5.3.2.2 Lower bound

For each state  $s$  characterized by  $V(s)$  and  $M(s)$ , a lower bound on the consumed bandwidth is defined as follows:

$$\text{lowerBound}(s) = Bw(V(s)) + Bw(M(s)) \quad (5.6)$$

where,

$$Bw(M(s)) = \sum_{m_i \in M(s)} \frac{L_i}{T_i}$$

### 5.3.2.3 Branching-Strategy

For each state, we consider all possible states that can be obtained by selecting a message  $m_i$  from  $M$  and packing it in an existing VL in  $V$ , or by creating a new VL including only  $m_i$ .

#### 5.3.2.4 Discarding-Policy

Three conditions must be verified in our case to discard a state or to keep it in the potential solutions space. The first concerns the validity of the state, i.e., the generated VLs meet the schedulability condition and maximal frame size constraint of 1518 Bytes. The second is that the obtained lower bound of the state has to be smaller than the reference's upper bound. Finally, the third concerns the schedulability of the state which is applicable only for final states that define a complete CAN-messages partition.

#### 5.3.2.5 Algorithm process & example

The different steps of this optimization method are as follows:

- First, input messages set  $M$  is sorted in the increasing order of periods. Then, a reference solution is obtained using the BBFD heuristic.
- Afterwards, we apply iteratively the Branching-Strategy and Discarding-Policy:
  - if a state corresponds to a complete partition, i.e. all input messages are assigned to AFDX VLs, we proceed to an update of the reference solution only if it enhances the bandwidth consumption and it is schedulable, otherwise this state is discarded;
  - if the state is intermediary, which means that it corresponds to a partial partition of input messages set, then we generate all possible new states by including the next CAN message in  $M$  in an existing VL or putting it in a new VL. For each valid created state, we evaluate the lower bound. If its lower bound is smaller than the bandwidth consumption of the reference solution, then this state is added to the list to explore;
  - the set of states to explore is sorted in the increasing order of lower bound values to consider the most bandwidth-efficient states first.

In Figure 5.5, our proposed B&B approach is applied to an abstracted frame packing example with 3 messages. Only a part of the exploration tree is presented in this figure to illustrate how our proposed Branch & Bound algorithm is applied. For each considered state, we update the set of CAN messages  $M$  that is not yet affected to AFDX VLs,

VLs set  $V$  and the lower bound value. By comparing the lower bound to the bandwidth consumption of the reference solution, we make one of the following decisions:

- if lower bound is higher, then **discard** the state, which is the case for state number 5 in the exploration tree of Figure 5.5;
- if lower bound is smaller and the state is intermediate, then **branch** from that state, i.e., generate all child states originating at the considered state, which is the case of state 4;
- if lower bound is smaller and the state is a leaf in the tree, then **update** the reference solution, which is the case of state 14.

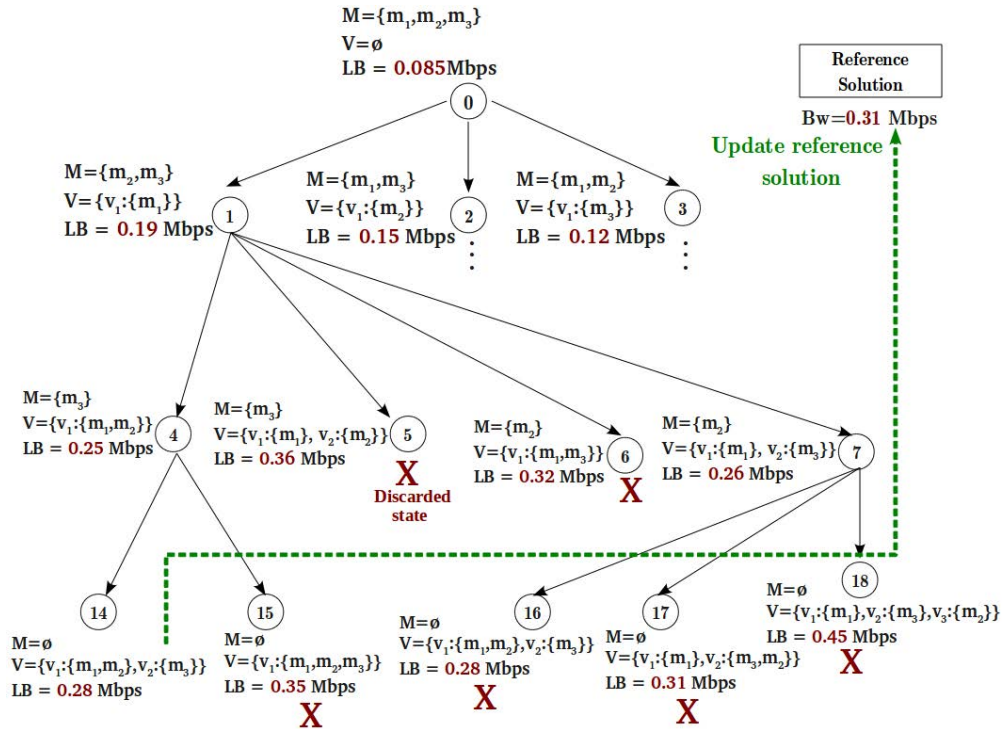


Figure 5.5: BB based algorithm example

## 5.4 Optimization process under HTS Mechanism

A HTS configuration can be seen as a partition of the set of downstream flows, defining the set of inner shapers that have to be implemented in the RDC to control the rate of downstream flows, as shown in Figure 5.6. Each obtained sub-set of downstream flows from the partitioning process will share the same inner shaper. This problem can be modeled as a bin-packing problem, where downstream flows are modeled as items and inner shapers as bins that will include items.

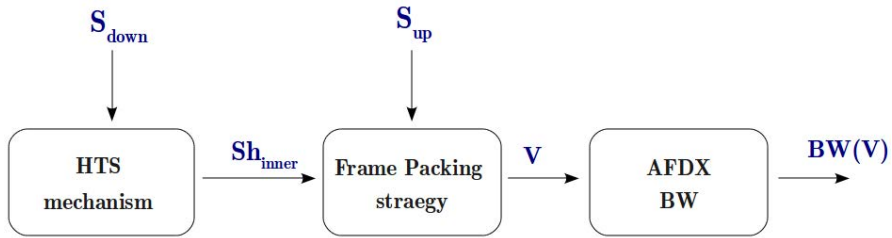


Figure 5.6: Optimization for HTS mechanism

Our objective is to find the best HTS structure, i.e. the number and parameters of inner shapers in  $Sh_{inner}$  combined with the frame packing strategy configuration, which minimizes as much as possible the AFDX bandwidth consumption while guaranteeing the temporal constraints of upstream and downstream flows.

Hence, to solve this NP-hard problem, we introduce an adequate heuristic approach.

### 5.4.1 Heuristic Approach

The different steps of our proposed heuristic for the HTS tuning are as follows:

1. **Initialization:** First, the heuristic sorts downstream messages set  $S_{down}$  in non-decreasing order of periods. At this step, the set of inner shapers is empty,  $Sh_{inner} = \emptyset$ . The heuristic will start by allocating the first message in  $S_{down}$ .
2. **Iterative construction of inner shapers:** Then, the set  $Sh_{inner}$  is built iteratively. At the beginning, the first message in  $S_{down}$  is inserted in a new shaper  $sh$  that would be added to the list of HTS configurations  $List_{Sh_{inner}}^0$ . Then, for the next selected message in  $S_{down}$ , the heuristic is conducted as follows for each iteration



$k \geq 1$ :

- (a) we add the selected message to each inner shaper in each HTS configuration in the list  $List_{Sh_{inner}}^{k-1}$  and we build a new configuration by adding a new inner shaper containing only the selected message. Then, we update the inner shaper characteristics of each HTS configuration as defined in Section 4.1.2 of the previous chapter. Furthermore, for each HTS configuration, we verify the schedulability condition of each upstream flow in  $S_{up}$  and of each selected downstream flow. Only feasible configurations (if any) are considered to form the list  $List_{Sh_{inner}}^k$  and then go to step (b) until the stop condition is verified, i.e. each message in  $S_{down}$  has an associated inner shaper in the final HTS configuration. For  $k \geq 2$ , if there is no feasible configuration, go to step (c).
- (b) for each configuration of inner shapers in the list  $List_{Sh_{inner}}^k$ , we compute the sum of WCRTs of upstream flows on CAN. Then, we sort the list  $List_{Sh_{inner}}^k$  in non-decreasing order of associated sum of WCRTs obtained for upstream flows. Afterwards, we select the first inner shaper configuration  $Sh_{inner}$  in the sorted list  $List_{Sh_{inner}}^k$  and we come back to step (a) by considering  $List_{Sh_{inner}}^{k-1} = Sh_{inner}$  for the next selected message in  $S_{down}$ .
- (c) for each inner shaper configuration in  $List_{Sh_{inner}}^{k-1}$ , we compute the sum of WCRTs of upstream flows on CAN. Then, we sort the list  $List_{Sh_{inner}}^{k-1}$  in non-decreasing order of associated sum of WCRTs obtained for upstream flows. Then, we select the next not yet selected inner shaper configuration  $Sh_{inner}$  in the sorted list  $List_{Sh_{inner}}^{k-1}$  and we come back to step (a) by considering  $List_{Sh_{inner}}^{k-1} = Sh_{inner}$  for the next selected message in  $S_{down}$ .

### 5.4.2 Example

Figures 5.7 and 5.8 illustrate the proposed heuristic to find the optimal configuration of HTS, through two possible execution scenarios on an abstracted example with 3 downstream flows. These scenarios consider the same set of downstream flows  $S_{down}$  but illustrate two complementary cases of the proposed heuristic execution. State 0 corresponds to the initialization step. The set of inner shapers is then iteratively constructed by generating states 1 to 5. For example for scenario 1, in state 1 message  $m_1$  is inserted into shaper  $sh_1$ . Then following *step 1.a)* states 2 and 3 are generated by inserting message  $m_2$  in shaper  $sh_1$  or putting it into shaper  $sh_2$ . Afterwards, *step 1.b)* selects state 2

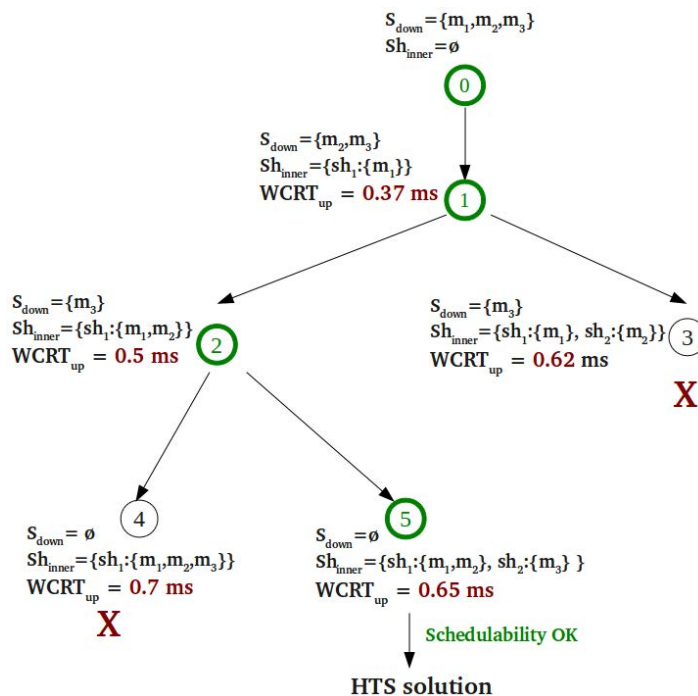


Figure 5.7: Example with the HTS heuristic approach (scenario 1)

and the exploration of the tree is carried from state 2. Then states 4 and 5 are generated by affecting message  $m_3$  to shaper  $sh_1$  and  $sh_2$  respectively. In scenario 1, the state 5 corresponds to a complete partition of the set of downstream flows  $S_{down}$  and is selected in *step 1.a)* as the best configuration of shapers. In scenario 2, states 4 and 5 are non schedulable, therefore, *step 1.c)* is processed, and the exploration of the tree is carried from state 3 following *step 1.a)*.

## 5.5 Preliminary Performances Analysis

As a first step, to illustrate the optimization process for frame packing strategies, we consider the **Test Case 1** described in Section 4.3 of the previous chapter. We implement FWT and MSP packing strategies in the RDC, and we apply our proposed optimization approaches to select the best RDC configuration for each implemented strategy.

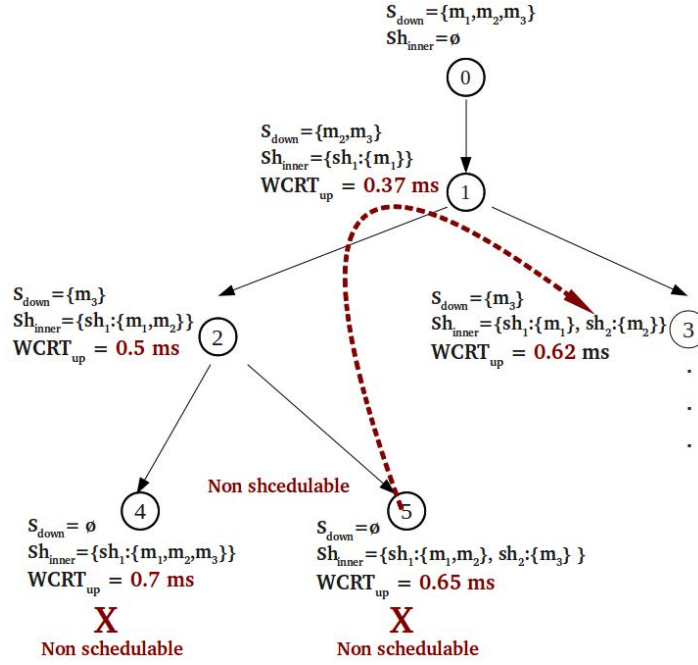


Figure 5.8: Example with the HTS heuristic approach (scenario 2)

### 5.5.1 Results under Optimized FWT Strategy

To find the best waiting time  $\Delta$  for FWT strategy, we process as follows:

1.  $BW_{(1:1)} = 1.42$  and  $BW(\Delta)$  is plotted as in Figure 5.2;
2.  $\Delta_{min} = 0.8ms$  is the smallest local minima leading to a better bandwidth compared to (1:1) strategy. Thus, the exploration interval for  $\Delta$  is  $[0.8ms, 2ms]$  since the minimum period is equal to 4 ms;
3.  $L_{\Delta} = \{2ms, 1.3ms, 1ms, 0.8ms\}$  is the list to explore, sorted in the decreasing order of  $\Delta$ ;
4.  $\Delta = 2ms$  is the first value to test and  $BW(2ms) = 0.69Mbps$ . Schedulability test is positive, and consequently FWT heuristic returns  $\Delta = 2ms$  as the optimal solution for FWT optimization problem.

It is worth noting that for this example with 24 upstream flows the size of the list  $L_{\Delta}$  to explore is equal to 4. The size of this list depends on the timing characteristics of

messages and not on their number which reduces the complexity of the FWT heuristic.

### 5.5.2 Results under Optimized MSP Strategy

Table 5.2 illustrates a comparative analysis between the MSP configurations obtained with the two introduced optimization approaches, BBFD heuristic and B&B algorithm, in terms of solution accuracy and approach complexity. Different test scenarios with CAN messages number increasing from 2 to 7 and periods in  $[4, 128]ms$  and payload size in  $[1, 8]bytes$  are considered.

The number of explored states with each approach are described in Table 5.2 to show their respective complexities with reference to Exhaustive Search (ES) approach. Only the scenarios leading to the best enhancements in terms of bandwidth consumption are presented when applying B&B algorithm compared to *BBFD* heuristic.

Table 5.2: Comparison between the optimization approaches for MSP configuration

Messages number	2	3	4	5	6	7
States (Heuristic)	3	5	8	11	15	19
States (B&B)	6	45	340	4110	67165	$\geq 1.6 \cdot 10^6$
States (Exhaustive Search)	6	45	508	8285	190000	$\geq 5.6 \cdot 10^6$
$\frac{Bw(BB) - Bw(H)}{Bw(BB)}$ (%)	0	0.2	0.7	0.3	0.1	0.1

As can be seen, the enhancements obtained in terms of bandwidth consumption when applying the B&B algorithm instead of the *BBFD* heuristic approach are very small (less than 1%), whereas the number of explored states with the former is inherently higher compared to the number obtained with the latter. For example, test scenario in Table 5.2 with 5 messages required the exploration of 4110 states to return an MSP configuration with B&B algorithm while it required only 11 with *BBFD* heuristic. The obtained solution with *BBFD* heuristic offers very similar bandwidth saving compared to B&B algorithm (0.3% of difference).

Although B&B algorithm allows to reduce the number of explored states compared to Exhaustive Search to find an optimal MSP configuration, it induces high complexity even for small input messages size, e.g., it requires  $1.6 \cdot 10^6$  state explorations for 7 messages.

In addition, it induces high execution time and it is not simple to use with big upstream flows number. Therefore, our introduced BBFD heuristic approach is considered as an accurate approach to find a valid solution with low computing complexity. This heuristic is then selected to find the best MSP configuration and the following performance analysis are based on this heuristic.

To find the best MSP configuration for upstream flows for the **Test Case 1** described in Section 4.3 of the previous chapter, we applied our proposed BBFD heuristic which returns the following MSP configuration:

$$- \text{conf}_{BBFD}: v_1 : \{1 * m_1, 2 * m_2, \}, v_2 : \{1 * m_1, 16 * m_3\}, v_3 : \{1 * m_1, 4 * m_4\}$$

This configuration induces a bandwidth consumption on the AFDX of  $0.56\text{Mbps}$  and offers a reduction of almost 60% compared to (1:1) strategy.

The obtained results under FWT and MSP strategies are described in Table 5.3.

Table 5.3: Impact of frame packing strategies

Strategy	VLs number	AFDX bandwidth (Mbps)	Schedulability
(1:1)	25	1.42	OK
FWT ( $\Delta = 2ms$ )	2	0.69	OK
MSP ( $\text{conf}_{BBFD}$ )	3	0.56	OK

As we can see, optimized FWT and MSP strategies lead to significant enhancement of network resource savings in terms of AFDX bandwidth consumption, compared to (1:1) strategy. For instance, they offer a reduction of AFDX bandwidth consumption of 50% and 60% with reference to (1:1) strategy, respectively. Moreover, MSP strategy offers a reduction of 20% compared to FWT strategy. This fact is mainly due to the communication overhead reduction under MSP strategy, which explicitly defines the CAN messages-set packed in each AFDX frame transmitted by the RDC, unlike FWT strategy. This leads to an accurate VL allocation and avoids VLs over-dimensioning problem that can occur under FWT strategy. Hence, in the following section, to evaluate the performance of the HTS mechanism, we will consider the MSP strategy.

### 5.5.3 Results under Optimized HTS Mechanism

To illustrate our HTS heuristic, we consider the **Test Case 2** described in Section 4.3 of the previous chapter. When applying the introduced heuristic approach, the obtained inner shapers set consists of 7 shapers where each shaper has a shaping period of  $4ms$  and the following composition:

- $Sh_1 : \{m_1, m_2\}$
- $Sh_2 : \{m_3, m_4\}$
- $Sh_3 : \{m_5, m_6\}$
- $Sh_4 : \{m_7, m_8\}$
- $Sh_5 : \{m_9, m_{10}, m_{11}, m_{12}\}$
- $Sh_6 : \{m_{13}, m_{14}, m_{15}, m_{16}\}$
- $Sh_7 : \{m_{17}, m_{18}, m_{19}, m_{20}, m_{21}, m_{22}, m_{23}, m_{24}\}$

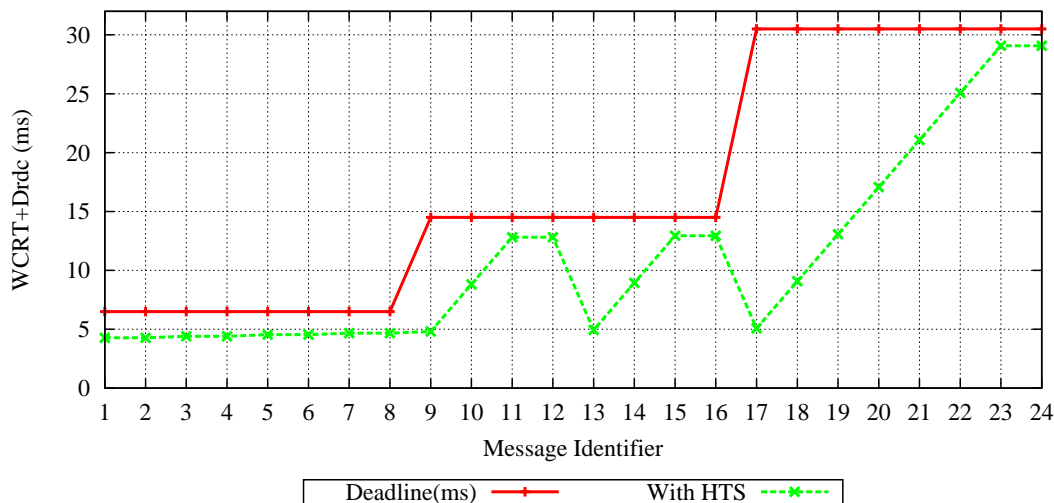


Figure 5.9: CAN WCRT of downstream flows

This HTS configuration is feasible and leads to a bandwidth consumption of 0.75 Mbps. Compared to (1:1) strategy and the configuration where MSP packing is used and HTS is deactivated, it offers a significant bandwidth saving while ensuring the schedulability of both upstream and downstream flows, as can be seen in Table 5.4. Unlike the HTS configuration considered in Section 4.3.3, the optimized HTS configuration obtained with our proposed heuristic builds a set of inner shapers which respects the downstream flows deadlines as shown in Figure 5.9.

Hence, the obtained RDC configuration based on the optimized HTS mechanism, combined with MSP strategy offers:

- feasible upstream flows;
- feasible downstream flows;
- low AFDX bandwidth consumption.

Table 5.4: Impact of HTS mechanism

Configuration	Bandwidth (in Mbps)	Schedulability
(1:1)	1.42	OK
MSP + NO HTS	1.05	OK
MSP + HTS ( heuristic)	0.75	OK

## 5.6 Conclusion

In this chapter, we formulated a general CAN-AFDX RDC optimization problem to maximize network resource savings. Particularly, we selected the AFDX bandwidth consumption as a relevant metric since it lets margins for future evolutions of avionics systems. The schedulability constraints are integrated to guarantee certification requirements. As the general RDC tuning problem is too complex, we followed an incremental approach. First, we considered specific CAN buses, i.e., either for sensors or actuators, to focus on the frame packing process and its impact on upstream flows. Each of the proposed frame packing strategies, FWT and MSP, was considered and a frame packing optimization problem was addressed. Second, we considered the general case with sensors/actuators CAN buses and contention between upstream and downstream flows to show the impact of the HTS mechanism, combined with the frame packing process on the AFDX bandwidth consumption. The HTS mechanism applied to downstream flows was optimized to achieve efficient AFDX bandwidth consumption. This latter was combined with the best optimized frame packing strategy, for instance MSP strategy.

Since the RDC parameters tuning problem turned to be a NP-hard, we introduced heuristics to solve it. Obtained results confirmed the efficiency of the frame packing func-

tion to save AFDX bandwidth consumption and reduce the number of allocated AFDX VLs induced by the RDC device. Moreover, the HTS mechanism, applied to downstream flows, showed an important role in improving frame packing efficiency when applied to upstream flows. This is due to the capacity of HTS mechanism to isolate downstream and upstream flows and to avoid interference.

The proposed approaches to enhance the RDC device performances for CAN-AFDX multi-cluster networks while meeting the real-time constraints are extended to other CAN-like protocols such as TTCAN [43]. The frame packing strategies and the timing analysis are adapted to suit the specificities of this CAN-like bus, and the details are provided in Appendix B. The validation of the enhanced RDC device for CAN-AFDX network will be conducted in the next chapter through a realistic avionics case study.



# Chapter 6

## Avionics Case Study

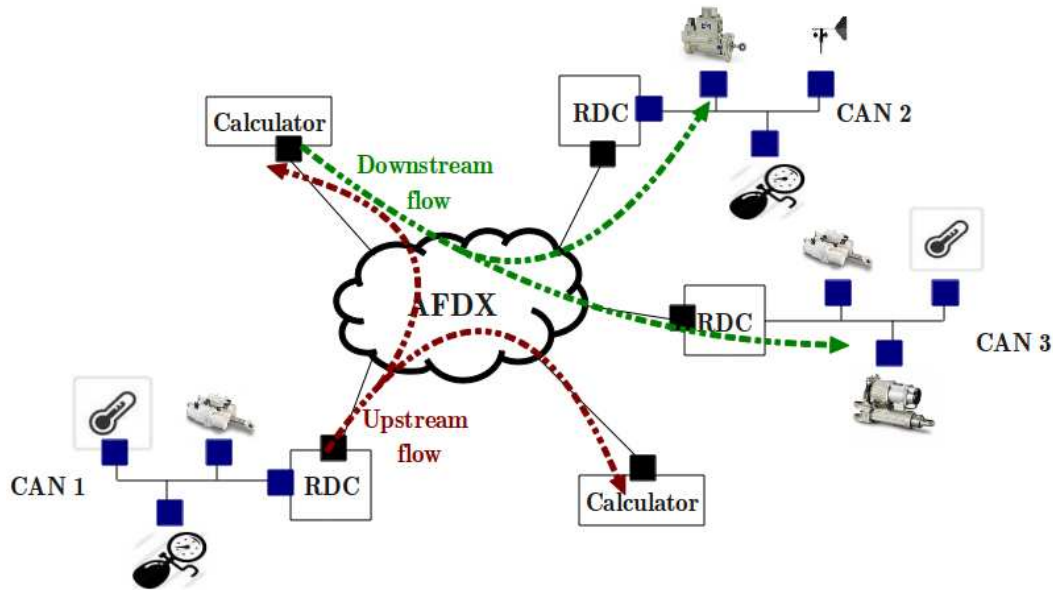
In this chapter, the validation of our proposed CAN-AFDX RDC performance is conducted through a realistic avionics case study. First, the avionics case study is described and the considered test scenarios are presented. Then, the computation and analysis of the end-to-end latencies and the network bandwidth utilization are detailed, to verify the first conclusions of the previous chapters, and to highlight the ability of our enhanced RDC device to improve system's performance, with reference to the currently used RDC device.

### 6.1 Description

#### 6.1.1 CAN-AFDX Architecture

We consider the multi-cluster CAN-AFDX avionic network shown in Figure 6.1. This network architecture consists of 3 I/O CAN buses with a transmission capacity of 1 Mbps, and a high speed AFDX backbone with a transmission capacity of 100 Mbps.

The communication between sensors/actuators and the avionics calculators is performed using RDC devices. In our case, we will consider the proposed RDC device integrating frame packing and HTS mechanism instead of the currently used RDC device. The figure 6.2 shows the details of the AFDX backbone network which interconnects 56 end-systems using a switched topology with 9 AFDX switches. This network architecture supports the flight control, the cabin functions and the management of engines, fuel and energy.

Figure 6.1: *CAN-AFDX case study*

## 6.1.2 Communication Traffic

Data flows supported by architecture of Figure 6.1 can be organized into three classes:

- the **upstream flows**, i.e., the sensors flows destined to AFDX calculators;
- the **downstream flows**, i.e., the calculators flows destined to actuators;
- **AFDX flows**, i.e., flows exchanged between AFDX calculators.

Upstream and downstream flows have to cross the I/O network, the RDC device and the AFDX backbone to reach their destinations, whereas AFDX flows are circulating only on the AFDX network.

### 6.1.2.1 AFDX Flows

As can be seen in Table 6.1, AFDX flows consists of 450 VLs with BAG values ranging in  $\{4, 16, 32\}$ ms and MFS values in  $\{16, 226, 482\}$  bytes. This table represents the VL distribution according to BAG and frame size values.



guarantee CAN bus schedulability.

### 6.1.3 Test Scenarios

The performance evaluation of our enhanced CAN-AFDX RDC device is conducted through the following test scenarios:

- **Test Scenario 1:** in this case, each CAN bus is used exclusively either for sensors or actuators to avoid contention between upstream and downstream flows. As a first step, we activate the frame packing function in the RDC device applied to upstream flows and we deactivate the HTS mechanism since there is no contention on CAN bus with downstream flows. In addition to the AFDX flows described in Table 6.1, we generate upstream flows as described in Section 6.1.2.2 for non shared I/O CAN buses;
- **Test Scenario 2:** in this case, each CAN bus is shared between sensors and actuators and supports upstream and downstream flows communication. The generated upstream and downstream flows share equitably the CAN bus load, i.e., half of CAN load is due to upstream flows and the other half to downstream flows. Frame packing and HTS mechanism are both activated within the RDC device to minimize communication overheads on the AFDX and interferences on CAN. In addition to the AFDX flows described in Table 6.1, we generate upstream and downstream flows as described in Section 6.1.2.2 for the shared I/O CAN buses.

## 6.2 Benefits of Frame Packing Strategies

As a first step, we consider the **Test Scenario 1**. The aim of this performance evaluation is to show the impact of the frame packing process within our proposed RDC device on AFDX bandwidth consumption and end-to-end latencies for the considered CAN-AFDX network architecture. First, for each CAN load, we conduct the optimization process for the FWT frame packing strategy within each CAN-AFDX RDC device of the considered network architecture. Afterwards, we verify the timing constraints of the system and we compute the induced AFDX bandwidth utilization by the RDC device. Then, we proceed in the same way under MSP strategy. Finally, we compare obtained results in terms of network resource savings and offered real-time guarantees.

### 6.2.1 Under FWT

To analyze the efficiency of the FWT packing strategy, we compute the maximum AFDX bandwidth consumption among the three RDC device of our case study. The obtained values for the different CAN loads are illustrated in Figure 6.3. Each plotted point on Figure 6.3 corresponds to the optimal configuration obtained following the optimization process described in the previous chapter, which meets the schedulability condition for both upstream and downstream flows. As can be seen, the (1:1) strategy leads to an important bandwidth consumption, essentially due to the overhead of sending each sensor message (less or equal to 8 bytes) in one AFDX frame (at least 64 bytes). However, under the FWT strategy, we can notice an interesting reduction of the consumed AFDX bandwidth compared to the (1:1) strategy. For instance, for a CAN load around 50%, FWT strategy induces 2Mbps while (1:1) strategy induces 3.4Mbps. This fact represents a reduction up to 40% of the consumed AFDX bandwidth under FWT strategy. However, it is worth noticing that under low CAN loads the bandwidth utilization reduction is less important compared to high CAN loads. This is mainly due to the over-dimensioning effect of VLs characterisation under FWT strategy which is a consequence of its dynamic nature where the frame structure is defined "on-the-fly" during execution time.

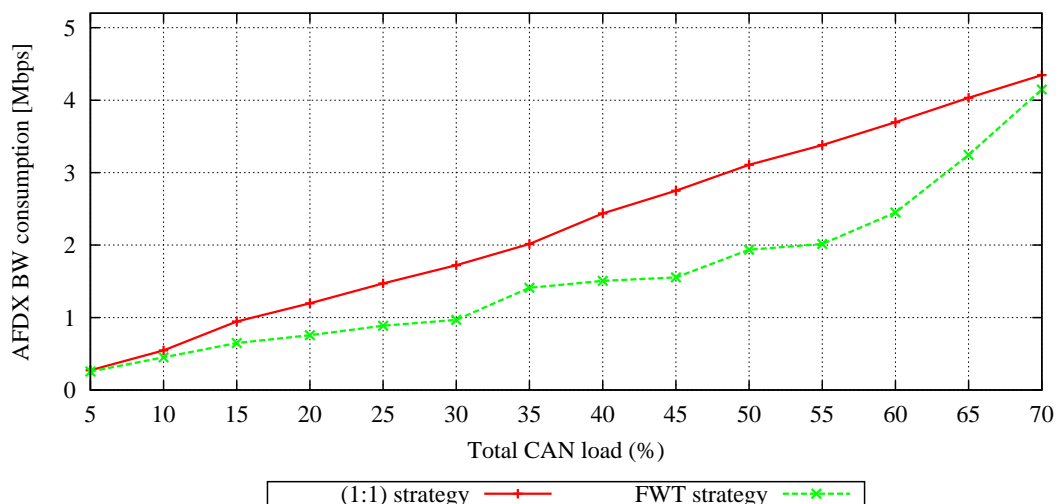


Figure 6.3: Impact of FWT frame packing strategy on AFDX bandwidth consumption

### 6.2.2 Under MSP

The obtained results with MSP strategy are illustrated in Figure 6.4. We can notice further enhancements under MSP strategy compared with (1:1) strategy and FWT strategies. For instance, we observe a reduction of AFDX bandwidth consumption under MSP of 47% and 15% with reference to (1:1) and FWT strategies, respectively. Unlike FWT, the explicit structure of the AFDX frames under MSP reduces the communication overheads, and consequently the induced AFDX bandwidth consumption on the AFDX. This fact clearly leads to an accurate VL allocation induced by the RDC device and avoids the relative VLs over-dimensioning problem of the FWT strategy.

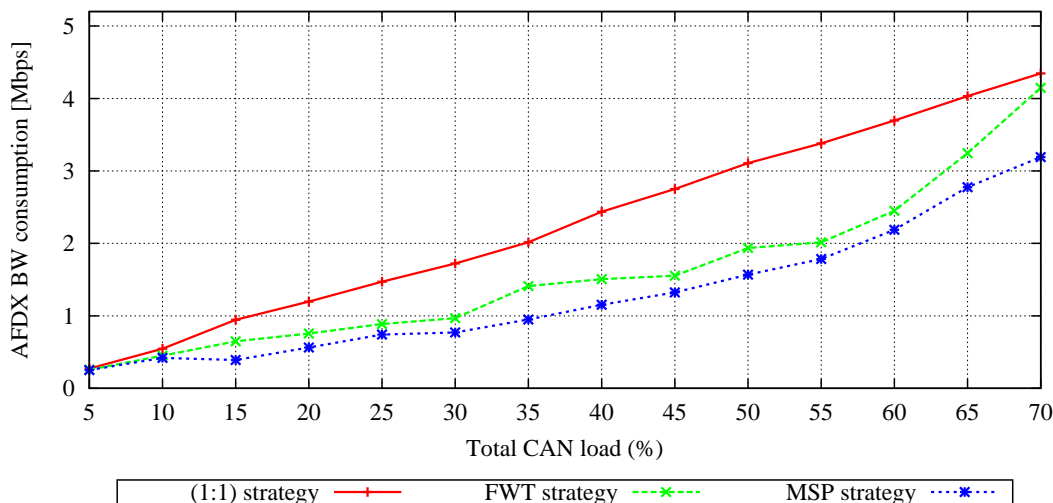


Figure 6.4: Impact of MSP frame packing strategy on AFDX bandwidth consumption

### 6.2.3 Comparative Analysis and Conclusion

MSP strategy leads to better performances than FWT strategy under all tested CAN load conditions. This is due to the schedulability condition under FWT strategy for high CAN loads. Under FWT strategy, all CAN data are subject to additional waiting delay, even the most urgent ones, to be packed into an AFDX frame. However, when CAN load increases, the response times on CAN bus increase, and consequently the admissible waiting time decreases. This fact is not in favor of the packing process under FWT strategy, and the induced bandwidth consumption will be similar to the one under (1:1) strategy. On the other hand, MSP strategy does not delay the most urgent messages since packed frames transmission is synchronized with the reception of these messages. This allows

MSP strategy to be more efficient under high CAN loads.

Hence, the obtained results in this section have shown the efficiency of the proposed RDC device, including frame packing strategies and the optimization process, to reduce AFDX bandwidth consumption. Further, the comparative analysis of our two proposed packing strategies, namely FWT and MSP, has shown that the MSP frame packing strategy integrated into the CAN-AFDX RDC offers better bandwidth savings on the AFDX network, compared to the FWT strategy. However, it is worth noting that the comparison of these two strategies should consider implementation and configuration complexity of each strategy. From this perspective, FWT is simpler to implement since it requires one packing queue and a timer to be integrated into CAN-AFDX RDC; whereas, MSP strategy requires one queue per a group of messages to pack and a processor unit capable of handling specific messages reception to trigger the packing process.

## 6.3 Benefits of HTS Mechanism

To show the impact of the HTS mechanism within our proposed RDC device on the AFDX bandwidth consumption and end-to-end latencies for the considered CAN-AFDX network, we consider the **Test Scenario 2**. Based on the previous results, we consider the most efficient frame packing strategy, MSP strategy to pack upstream flows and reduce communication overheads, and the HTS mechanism for downstream flows to minimize interferences on CAN bus between upstream and downstream flows. First, we process the optimization approaches for MSP strategy and HTS mechanism. Then, we compute the induced AFDX bandwidth consumption for each optimal configuration when varying the CAN load.

### 6.3.1 Impact of I/O CAN Bus Sharing on Frame Packing

As priority assignment on CAN bus is an important parameter for upstream and downstream flows, we consider two configurations of priority assignment:

- **Configuration 1:** upstream flows have higher priority than downstream flows;
- **Configuration 2:** downstream flows have higher priority than upstream flows.

The main idea here is to show the behavior of the proposed RDC device, when only the frame packing process is activated within the RDC. The obtained results will highlight the importance of the HTS mechanism integration within the RDC device.

We consider a bound on RDC traversal delay for downstream flows equal to  $0.05ms$  which takes into account the unpacking process, the extraction of data from AFDX frame and the encapsulation of an actuator data into a CAN frame. Then, the induced bandwidth consumption by the RDC is shown in Figure 6.5. For each configuration, the CAN load is varying from 5% to 70% and the MSP strategy applied on upstream flows is configured to respect the schedulability condition. The bandwidth consumption under (1:1) strategy is considered as a reference.

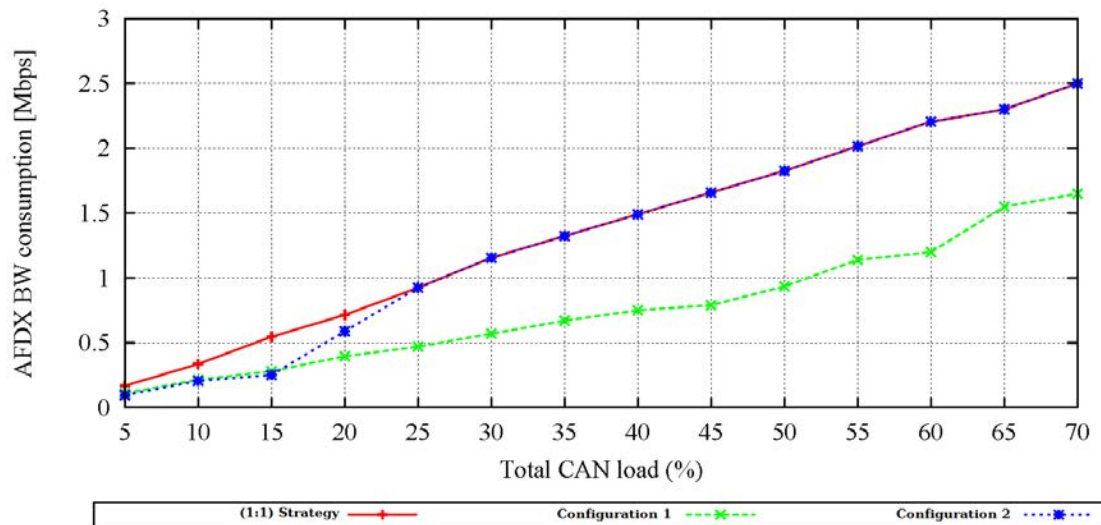


Figure 6.5: Bandwidth Utilization on the AFDX with shared I/O network

Under configuration 1, we still observe a significant reduction of the bandwidth consumption on the AFDX when using the optimized RDC device implementing MSP strategy, compared to the basic one with (1:1) strategy. Hence, under this priority assignment configuration, the proposed RDC device deactivating the HTS mechanism is still efficient, since only one downstream message at maximum can interfere with the upstream flows. However, under configuration 2, the performance of the optimized RDC device is degraded and becomes equivalent to the performance of the RDC device implementing a (1:1) strategy under CAN load more than 25%. To understand the reasons of this degradation, consider the Worst-Case Response Times (WCRT) on CAN of upstream flows. In Figure 6.6, we report WCRTs for upstream messages with period equal to  $16ms$  to show the



impact of HTS mechanism on WCRT on CAN bus. As can be noticed, WCRTs increase significantly under configuration 2 because of the important contentions due to the higher priority downstream flows. However, increasing upstream flows delays on CAN is not in favor of performing frame packing within RDC device, and consequently of reducing bandwidth consumption on the AFDX. Hence, if it is possible, then it would be better to select the configuration 1, which is more bandwidth efficient compared to configuration 2.

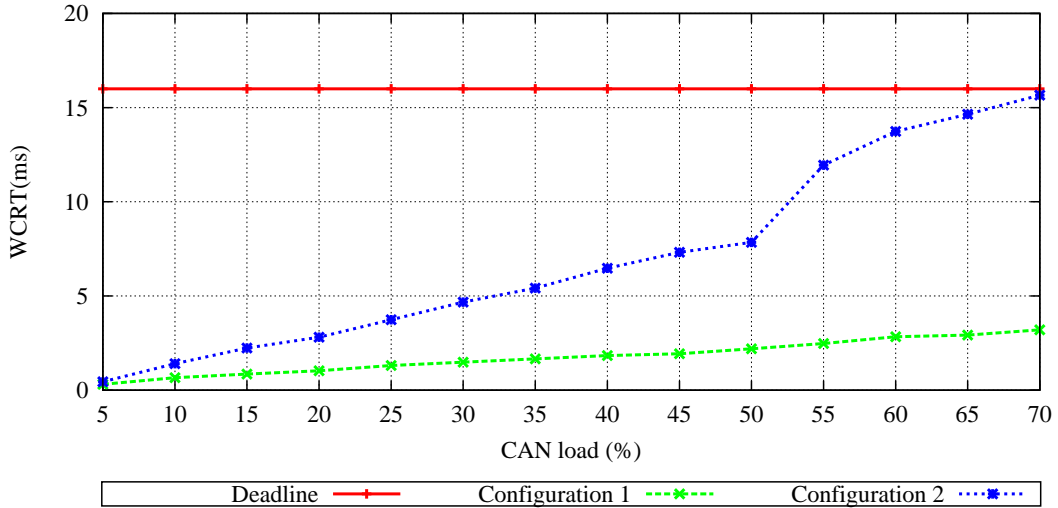


Figure 6.6: *WCRT on CAN of upstream flows with shared I/O network*

However, in avionics context, the modification of application specifications can ramify maintenance efforts and incremental design process. Therefore, revising priority assignment of different flows to improve system performances can be a complicated task for designers. Our aim consists in reducing as much as possible bandwidth consumption on the AFDX induced by the RDC device, even in the worst-case configuration of priority assignment for upstream flows, i.e., upstream flows have lower priority than downstream flows. Therefore, to overcome the limitations highlighted with these first results, the key idea consists in favoring frame packing mechanism for upstream flows within the RDC device to reduce bandwidth consumption on the AFDX network. This fact consists in minimizing as much as possible WCRTs on CAN of upstream flows when having the low priority, and ensuring at the same time the temporal constraints of downstream flows. To achieve this aim, we will activate the HTS mechanism on downstream flows in our proposed RDC device, to reduce interference on CAN and to isolate upstream and downstream flows.

### 6.3.2 On the Effects of HTS Mechanism

To evaluate the performance of our enhanced CAN-AFDX RDC, we compute AFDX bandwidth consumption for each RDC when activating both the HTS mechanism and MSP frame packing strategy. The maximum AFDX bandwidth consumption induced by RDC devices are illustrated in Figure 6.7 when varying CAN loads. The cases where only (1:1) strategy or MSP strategy without HTS mechanism is implemented are considered as references to highlight the efficiency of HTS mechanism.

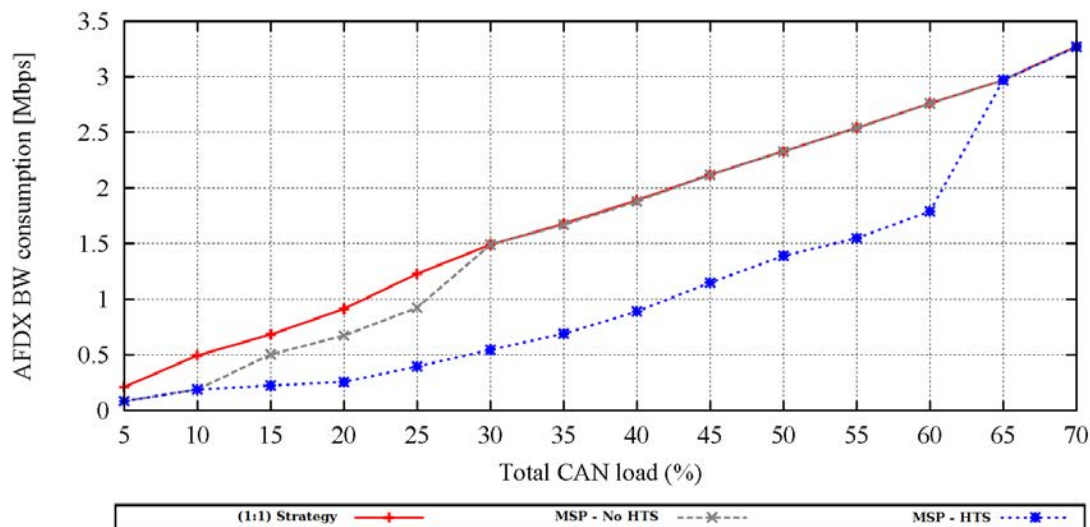


Figure 6.7: Impact of HTS mechanism on AFDX bandwidth consumption

As can be seen in Figure 6.7, the use of the HTS mechanism combined with the MSP strategy within the RDC device offers significant AFDX bandwidth consumption savings, compared to the case where only MSP strategy is activated. For instance, for a CAN load of 40%, we got an AFDX bandwidth consumption of roughly  $1.7Mbps$  under (1:1) strategy and of  $0.7Mbps$  under MSP strategy combined with the HTS mechanism. Further, we can notice that when only the frame packing process is activated within the RDC device, the performances converge quickly to the ones under (1:1) strategy. This is mainly due to the high upstream flows delays on CAN because of the contention with the higher priority downstream flows. For CAN loads higher than 65%, we notice that the use of the HTS mechanism does not improve the AFDX bandwidth consumption, compared to (1:1) strategy and the case where no HTS is used. This is due to the fact that even if the HTS mechanism is applied within the RDC device, the enhancements of the WCRT on CAN of upstream flows are not that noticeable to favor the frame packing process.

## 6.4 Conclusion

In this chapter, the validation of the enhanced RDC device was conducted through a realistic avionics case study. Obtained results confirm our first conclusions from the preliminary performance evaluation in Chapters 4 and 5, and have shown significant AFDX bandwidth savings under various CAN loads conditions. For instance, for specific CAN bus, i.e., either for sensors or actuators, the MSP strategy has shown a high efficiency in saving network bandwidth with reductions of almost 50% and 20%, with reference to (1:1) and FWT strategies, respectively. Furthermore, we notice that sharing CAN buses between sensors and actuators may limit bandwidth savings that can be achieved by our proposed frame packing process. However, the use of the Hierarchical Traffic Shaping mechanism combined with the MSP strategy within the proposed RDC device shows better efficiency to limit the AFDX bandwidth consumption. This fact is due to the isolation between upstream and downstream flows on CAN bus, which improves upstream flows worst-case response times on CAN, and consequently favors the frame packing process.



# Conclusions and Prospectives

## Conclusions

The current avionic communication architecture consists of an AFDX network to connect the avionic computing systems and several I/O data buses, such as CAN bus, to connect sensors and actuators. Clusters are then interconnected via specific devices, called Remote Data Concentrators (RDCs), standardized as ARINC 655 [4]. RDC devices are modular gateways distributed throughout the aircraft to handle heterogeneity between the AFDX backbone and I/O data buses. For certification reasons, the timing constraints of the avionics system have to be guaranteed. Furthermore, the avionics system have to meet emerging requirements for resource utilization efficiency to let margins for future evolution and limit system weight and costs. Although the RDC device has been introduced as the standard for interconnection devices for avionics use, the existing implementations of RDC do not consider network resource savings. In this thesis, we proposed an enhanced CAN-AFDX RDC device which maximizes resource savings, while meeting real-time constraints.

**First**, we proposed **the design of an enhanced CAN-AFDX RDC device** in terms of network bandwidth utilization. Our proposed RDC is compliant with the ARINC 655 specifications. From a functional perspective, our proposed RDC is composed of elementary functions. The main functions integrated into the RDC are:

- frame packing applied on upstream flows, i.e., flows generated by sensors and destined to AFDX, to reduce communication overheads required to transmit CAN traffic on AFDX network, and consequently decrease the AFDX bandwidth utilization. Two frame packing strategies have been proposed: (i) a dynamic strategy, called FWT strategy; (ii) a static strategy, called MSP strategy;
- Hierarchical Traffic Shaping (HTS) applied on downstream flows, i.e., flows generated by AFDX sources and destined to actuators on CAN buses, to guarantee

isolation between upstream and downstream flows on each I/O CAN bus, and consequently to favor the frame packing process.

These functions can be activated and configured to fulfill real-time and resource efficiency requirements. From an architectural perspective, our proposed RDC connects multiple I/O CAN buses and uses a partitioning process compliant with ARINC 653 [5] specifications to guarantee isolation between different criticality levels. This fact reduces the number of RDC devices required for the multi-cluster network architecture, and consequently the system weight and costs.

**Second**, to analyze the performance offered by our proposed RDC, we proceeded as following:

- First, we proposed the modeling of the CAN-AFDX architecture with a focus on the RDC device and its implemented functions;
- Then, we introduced a **timing analysis** for CAN-AFDX network integrating the impact of our enhanced RDC device to verify the schedulability of communication. Furthermore, to prove the efficiency of our RDC to save avionics resources utilization, we considered the AFDX bandwidth consumption induced by the RDC device as a relevant metric. The introduced timing analysis approach combines results of Network Calculus theory and worst-case response time analysis for CAN bus, and computes bounds on the end-to-end latencies for CAN-AFDX network. Moreover, the impacts of the elementary functions activated in the RDC device were integrated within the maximum RDC traversal delay;
- Preliminary performance analysis for our proposed RDC device has been conducted through a CAN-AFDX case study with different scenarios of upstream and downstream flows. The AFDX bandwidth consumption was considered as a relevant metric to assess system's resource utilization, whereas the end-to-end latency was used to verify the schedulability of the used RDC configuration. Obtained results have shown significant AFDX bandwidth consumption savings when using frame packing strategies, namely FWT and MSP, while meeting time constraints. A comparison between these two packing strategies in terms of AFDX bandwidth savings has shown that MSP strategy is more efficient than FWT strategy. However, the former is more complex to implement within the RDC device. Furthermore, using the HTS mechanism within the RDC device for downstream flows has shown its

---

efficiency to reduce interference on upstream flows. This fact favors frame packing process, and consequently maximizes the AFDX bandwidth savings. To be more specific, the HTS mechanism improves the worst-case response times on CAN for upstream flows, and thus it offers margins to perform packing of upstream data in the RDC device.

**Third**, an **RDC optimization process** to minimize network resource utilization while ensuring flows schedulability has been performed. As this RDC tuning problem turned to be combinatorial, we proposed adapted approaches to solve this problem under different frame packing strategies and traffic shaping configurations. For instance, we proposed:

- an heuristic to find the best FWT configuration defined using the parameter  $\Delta$  representing the waiting timer used to accumulate data to pack;
- Moreover, we proposed an heuristic approach, called Best-Bandwidth-Fit-Decreasing (BBFD), to find the most resource efficient MSP strategy in a polynomial time. Furthermore, a Branch & Bound algorithm to find the optimal MSP configuration has been investigated. A comparative performance analysis to select the most adapted solving approaches was conducted. The obtained results have shown the accuracy of our proposed heuristic with lower computational complexity compared to Branch & Bound algorithm for industrial scale case study. Therefore, BBFD heuristic was selected as the most efficient approach, among our proposed ones, for MSP frame packing strategy optimization.
- Furthermore, to find the best HTS shapers parameters, i.e., minimizing the AFDX bandwidth consumption and meeting time constraints, we proposed an heuristic approach which iteratively partitions the set of downstream flows to build the set of shapers of the HTS structure used within our proposed RDC device.

The application of these proposed heuristic approaches to tune our enhanced RDC configuration was illustrated through various test scenarios. The obtained results of the RDC device with optimal configurations have confirmed the role of frame packing process combined with HTS mechanism to maximize network resource saving, i.e., AFDX bandwidth consumption in our case.

**Finally**, to validate the performance of our optimized RDC, we considered an

industrial scale avionics case study. The performance guarantees of this network architecture were analyzed when considering various I/O CAN bus loads to check the scalability of our proposed RDC functions. We proceeded as following:

- First, we conducted a comparative analysis between the two proposed frame packing strategies in terms of AFDX bandwidth consumption savings in the case of specific I/O CAN buses either for sensors or actuators, to focus on the role of frame packing process applied for upstream flows. The obtained results have shown that MSP strategy is more efficient and offers up to 15% of bandwidth consumption reduction with reference to FWT. Furthermore, these results have confirmed the capacity of our proposed RDC device to save avionics resources under different traffic load conditions, while meeting the real-time requirements of avionics networks. For instance, frame packing process used within the RDC device showed an AFDX bandwidth consumption reduction of up to 40%, with reference to the (1:1) strategy used within the currently used RDC device.
- In the case of shared I/O CAN buses between sensors and actuators, the contention between upstream and downstream flows has shown negative impact on the efficiency of frame packing, and consequently there is less AFDX bandwidth savings. The activation of the HTS mechanism in the RDC combined with MSP strategy has shown better performance and increases AFDX bandwidth savings.

Hence, the use of frame packing process combined with HTS mechanism within the RDC device has shown significant network resource savings with reference to the currently used RDC device, i.e., up to 40% of AFDX bandwidth utilization.

## Prospectives

- **CAN-AFDX RDC Implementation and Testing:** the hardware implementation of our enhanced RDC device introduced to connect I/O CAN buses to AFDX is necessary to confirm its real-time guarantees and its capacity to improve AFDX bandwidth management. The ARINC 655 specifications [4] provides guidelines for RDC hardware implementation. This latter offers a starting point for our CAN-AFDX RDC device implementation with frame packing and traffic shaping functions. Then, a testing phase should consider analyzing the robustness of the enhanced RDC device implementing new elementary functions, i.e., frame packing



---

and hierarchical traffic shaping, to improve AFDX bandwidth utilization.

- **Extension of the RDC to CAN-like buses:** TTCAN [43] and ARINC 825 [31] are two CAN-like buses which present some dissimilarities with the native CAN. Therefore, it could be interesting to extend our proposed RDC device to fit the characteristics of these technologies. For instance, a preliminary analysis of a possible extension of the frame packing strategies, namely FWT and MSP and HTS mechanism, for TTCAN is proposed in Appendix B. Unlike the native CAN, TTCAN is based a Time-Triggered communication with a precise schedule of messages transmissions. To take into account this aspect, we revised our proposed frame packing strategies. Then, the HTS mechanism is deactivated, as the isolation between upstream and downstream flows is already supported by the time-triggered scheme. For instance, the triggering of the packing process, the virtual link allocation and the impact on the end-to-end delay are revised. On the other hand, the ARINC 825 introduces a bandwidth management mechanism which impacts the transmission scheme of CAN messages compared to the case of native CAN. Therefore, the extension of the RDC functions to fit the specificities of ARINC 825 may be more complex than TTCAN.
- **Generalization of the RDC design to the MIL-STD-1553B:** MIL-STD-1553B is a master/slave avionics data-bus used especially for military aircraft. The MIL-STD-1553B present many dissimilarities with native CAN bus. First, it has a master/slave communication scheme which is a centralized transmission control, unlike the distributed control mechanism (CSMA/CA) of CAN bus. Then, it admits bigger frame size with up to 64 bytes of payload, unlike the maximum payload of 8 bytes with CAN. Hence, the generalization of our enhanced RDC device requires revising the RDC functions, especially the frame mapping, frame packing process and the HTS mechanism. For instance, the efficiency of the frame packing strategies may be affected by the relatively big size of MIL-STD-1553B frames. Moreover, the timing analysis has to take into account the communication overheads due to the master node. The selection of the RDC as the master node may be considered to evaluate the impact of such a design choice on the RDC efficiency and the end-to-end communication performance.



# Appendix A

## Network Calculus Overview

The Network Calculus (NC) is a framework extensively used to model and analyze communication networks. This theory is based on Min-Plus algebra [20]. Network calculus has been used for analyzing performance guarantees for different types of computer networks. For instance, it was applied to AFDX network to prove the determinism of communication in [17] [21]. This leads to the certification of AFDX network for A380 aircraft. Network Calculus theory and its main results are presented in this appendix and more details can be found in [20].

### A.1 Network Calculus Theory

To provide performance guarantees for flows crossing a network, the network must guarantee resources to process data flows and sources of traffic have to guarantee a maximum traffic emission. Using Network Calculus, the data generated by network elements (sources) is modeled using *arrival curve* concept. Then, the network element capacity guaranteed for its crossing data flows is modeled using the *service curve* concept. The service curve takes into account the packet scheduling used by the network element. Then, given the arrival and service curves, Network Calculus provides maximum bounds on delays and backlogs.

#### A.1.1 Cumulative Functions

Network Calculus describes data flows by means of the cumulative function  $R(t)$ , defined as the number of transmitted bits during the time interval  $[0, t]$ . Function  $R(t)$  is always a non-decreasing function of time and it is generally assumed that  $R(0) = 0$ .

Consider a system  $S$  receiving input data with cumulative function  $R(t)$ , called input function. The received data is processed and then transmitted at the output. The output data is described using another cumulative function  $R^*(t)$ , called output function. In Figure A.1, two examples of input and output functions are shown. The horizontal distance  $d(t)$  between the input and output function graphs represents the delay that an input data received at time  $t$  will experience in the system. The vertical distance  $x(t)$  between input and output function graphs represents the backlog, i.e., total number of bits present in the system at time  $t$ . Cumulative functions  $R_1(t)$  and  $R_1^*(t)$  correspond to a fluid model, i.e., we assume that packets arrive bit by bit. Functions  $R_2(t)$  and  $R_2^*(t)$  show packetized model, i.e., we assume that a packet is received only when the last bit is received.

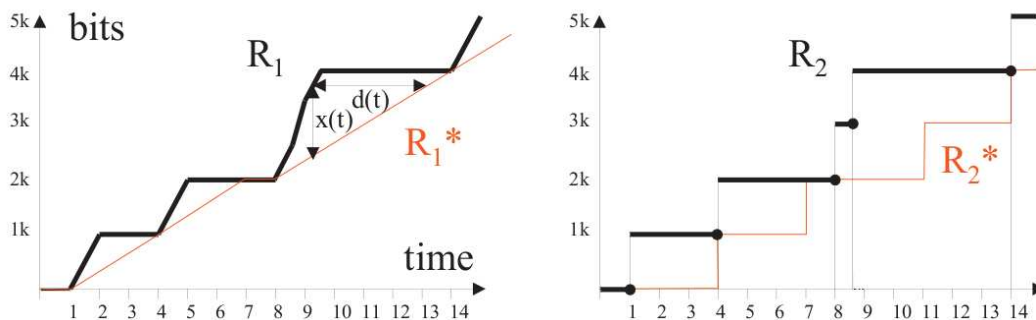


Figure A.1: Examples of Input and Output cumulative functions

### A.1.2 Arrival Curve

To model the traffic sent by a network source, Network Calculus introduces the concept of arrival curve. An arrival curve constrains the traffic emission for a network element, as shown in Figure A.2. Given a wide-sense increasing function  $\alpha$  defined for  $t \geq 0$ , we say that function  $\alpha$  is an arrival curve for flow with cumulative function  $R(t)$ , if and only if for all  $s \leq t$ :

$$R(t) - R(s) \leq \alpha(t - s) \quad (\text{A.1})$$

A very useful example of arrival curve is a leaky bucket curve  $\gamma_{r,b}$  illustrated in Figure A.3, where  $b$  represents the maximum data burst and  $r$  represents the steady rate of data

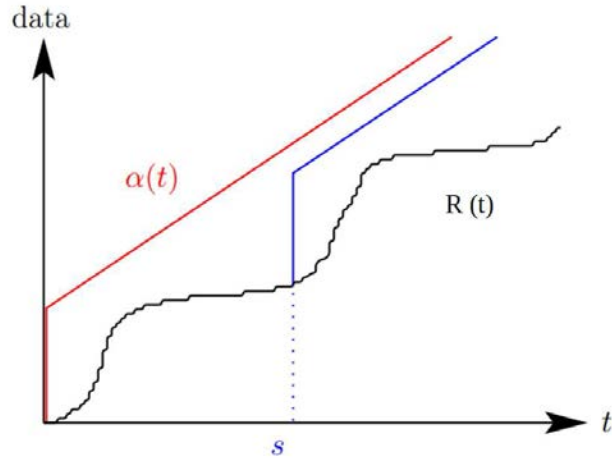


Figure A.2: Arrival curve

emission by the source node. This leaky bucket function is defined as follows:

$$\gamma_{b,r}(t) = \begin{cases} 0 & \text{if } t < 0 \\ rt + b & \text{if } t \geq 0 \end{cases} \quad (\text{A.2})$$

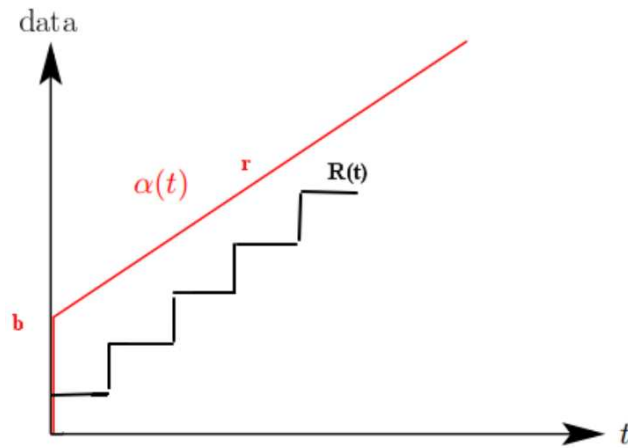


Figure A.3: Example of leaky bucket arrival curve

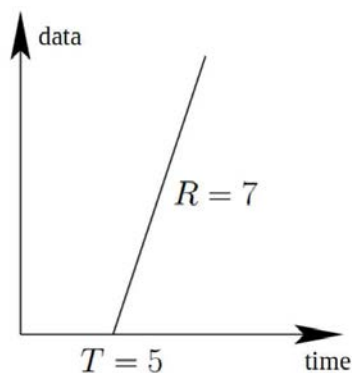


Figure A.4: Example of rate latency service curve

### A.1.3 Service Curve

For a network element  $S$  and a flow  $f$  crossing  $S$  with an input function  $R$  and an output function  $R^*$ , to model the service guarantees offered by the node  $S$  to flow  $f$ , Network Calculus introduces the concept of service curve. We say that  $S$  offers a service curve  $\beta$  to flow  $f$ , if and only if  $\beta$  is a wide sense increasing function and  $\beta(0) = 0$  for all  $s \leq t$ :

$$R^*(t) \geq (R(s) + \beta(t - s)) \quad (\text{A.3})$$

This latter condition can be written as  $R^* \geq R \otimes \beta$  using the  $\otimes$  min-plus convolution operator defined as following:

$$f \otimes g(t) = \inf_{s \leq t} (f(s) + g(t - s))$$

This means that the system  $S$  offers a minimum guaranteed service to input flow  $f$  and the guaranteed service is characterized by the function  $\beta$ . A very useful service curve is the rate latency curve  $\beta_{R,T}$  illustrated in Figure A.4, where  $R$  represents the minimum guaranteed rate and  $T$  represents the maximum initial latency. This rate latency function is defined as follows:

$$\beta_{R,T}(t) = \begin{cases} 0 & \text{if } t < T \\ R(t - T) & \text{if otherwise} \end{cases} \quad (\text{A.4})$$

### A.1.4 Network Calculus Bounds

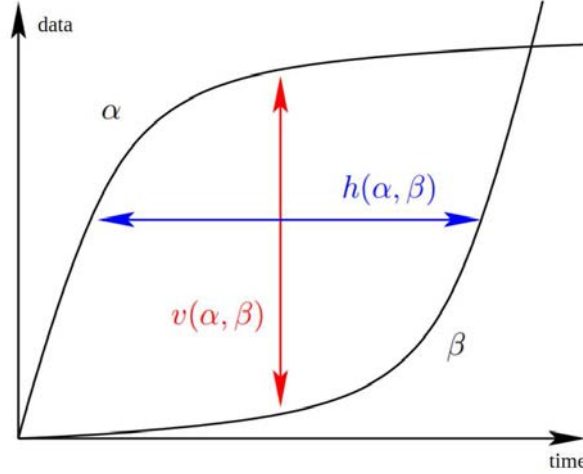


Figure A.5: *Backlog and delay bounds*

For a network system  $S$  offering a service curve  $\beta$  to a data flow  $f$  characterized by arrival curve  $\alpha$ , Network Calculus provides three main results:

- **Backlog bound:** an upper bound on backlog in system  $S$  processing flow  $f$  is equal to the vertical distance (denoted by  $v(\alpha, \beta)$ ) between arrival curve  $\alpha$  and service curve  $\beta$ , as shown in Figure A.5. If flow  $f$  has a cumulative function  $R$  and an output function  $R^*$ , then the backlog  $R(t) - R^*(t)$  in  $S$  satisfies the following inequality:

$$R(t) - R^*(t) \leq v(\alpha, \beta) = \sup_{s \geq 0} (\alpha(s) - \beta(s)) \quad (\text{A.5})$$

- **Delay bound:** an upper bound on the traversal delay of system  $S$  by flow  $f$  is equal to the horizontal distance (denoted by  $h(\alpha, \beta)$ ) between arrival curve  $\alpha$  and service curve  $\beta$ , as shown in Figure A.5. The delay  $d(t)$  for all values of time  $t$  satisfies the following inequality;

$$d(t) \leq h(\alpha, \beta) = \sup_{z \geq 0} (\beta^{-1}(z) - \alpha^{-1}(z)) \quad (\text{A.6})$$

- **Output arrival curve:** the output flow is constrained by the arrival curve  $\alpha^*$ , obtained by min-plus deconvolution of arrival curve  $\alpha$  and service curve  $\beta$ :

$$\alpha^* \geq \alpha \circledast \beta \tag{A.7}$$

where, the operator  $\circledast$  is defined as following :

$$f \circledast g(t) = \sup_{s \geq 0} (f(t+s) + g(t))$$

### A.1.5 Concatenation and Blind Multiplexing

An important result of Network Calculus introduced in [20] is about concatenation of the services of network systems:

**Theorem 1:** *assume a flow with arrival curve  $\alpha(t)$  traverses systems  $S_1$  and  $S_2$  in sequence where  $S_1$  offers service curve  $\beta_1(t)$  and  $S_2$  offers  $\beta_2(t)$ . Then, the concatenation of these two systems offers the following single service curve  $\beta(t)$  to the traversing flow:*

$$\beta(t) = \beta_1 \otimes \beta_2(t) \tag{A.8}$$

There is also another interesting result introduced in [20] concerning the blind multiplexing:

**Theorem 2:** *assume flows 1 and 2 with arrival curves  $\alpha_1(t)$  and  $\alpha_2(t)$  traverse system  $S$  which offers a strict service curve  $\beta(t)$ . Then, the minimal service curve offered to flow 1 is:*

$$\beta_1(t) = \max(0, \beta(t) - \alpha_2(t)) \tag{A.9}$$

However, this result has to be used carefully because the strict service curve assumption is essential and it is not verified in the general case except when the crossed node has a constant rate service or a FIFO multiplexing service. Further explanations can be found in [20].

### A.1.6 Application to AFDX

As described in Section 1.2.1 from Chapter 1, AFDX network connects a set of end-systems using a set of AFDX switches. Traffic flows are constrained using virtual links (VLs) which are mono-sender multicast channels with a minimum frame size  $MFS$  and a



minimum interval between two consecutive frames called *BAG*. To use Network Calculus theory to analyze the performance guarantees of AFDX network, we model AFDX data flows and network elements as following:

- a VL is modeled as a leaky bucket arrival curve  $\gamma_{\frac{MFS}{BAG}, MFS}$ ;
- a source end-system is modeled as a rate latency service curve  $\beta_{R,0}$ , where  $R$  the throughput of the output AFDX link;
- each switch input port is modeled using  $\delta_{\frac{L_{max}}{C}}$  for Store & Forward technique as shown in Figure A.6;
- each switch output port is modeled as a rate latency service curve  $\beta_{R,T}$ , where  $R$  is the throughput of the output AFDX link and  $T$  the technological latency.

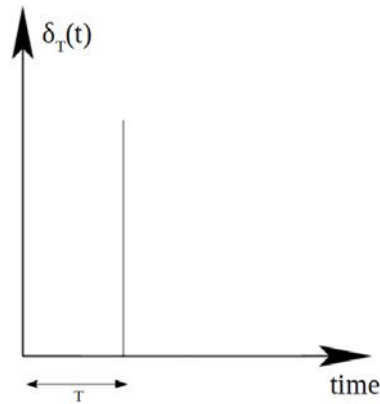


Figure A.6:  $\delta_T$  service curve

## A.2 WoPANets Performance Analysis Tool

WoPANets (Worst case Performance Analysis of embedded Networks) [6] is a design aided-decision tool developed for embedded networks. This tool offers an interface to the designer to describe the network and the circulating traffic and embodies a static performance evaluation technique based on the Network Calculus theory combined with optimization analysis to support early system design exploration for embedded networks.

In what follows, we present the main features of the WoPANets tool and we provide analysis in the case of a realistic Switched Ethernet to illustrate the use of WoPANets tool for network performance analysis.

### **A.2.1 WoPANets Features and Structure**

The WOPANets tool can handle the following parameters:

- Traffic types: periodic and aperiodic traffic with jitter or not.
- Different communication types: unicast, multicast and broadcast.
- Technology types: Ethernet, AFDX and CAN.
- Different scheduling policies: First Come First Served (FCFS), Static Priority (SP), Weighed Fair Queuing (WFQ), Round robin (RR); and many control mechanisms like TDMA and Master/Slave.
- Different performance metrics: end-to-end delays, backlog, network load and loss rate.

WOPANets tool consists of three main modules as described in the Figure [A.7](#): the Graphical User Interface, the Network Calculus Analyzer and the Optimization Analyzer.

First, the network to analyze is defined using the Graphical User Interface of WoPANets. For instance, the used network elements, the topology of the network and the communication flows have to be defined by the network designer. Then, the performance metrics to work with in WoPANets have to be selected. Second, the performance analyzer defines the arrival curve of each flow according to its characteristics and the service curve of each node in the network according to its policy or its control mechanism. Then, the performance analysis is done using Network Calculus algorithms. Third, the Optimization Analyzer allows network designer to find the optimal network configuration given a specific objective function, a set of variables corresponding to the network elements parameters that can be tuned by the network designer and a set of constraints. The obtained results after an analysis or an optimization process in WoPANets are displayed in the Graphical User Interface.

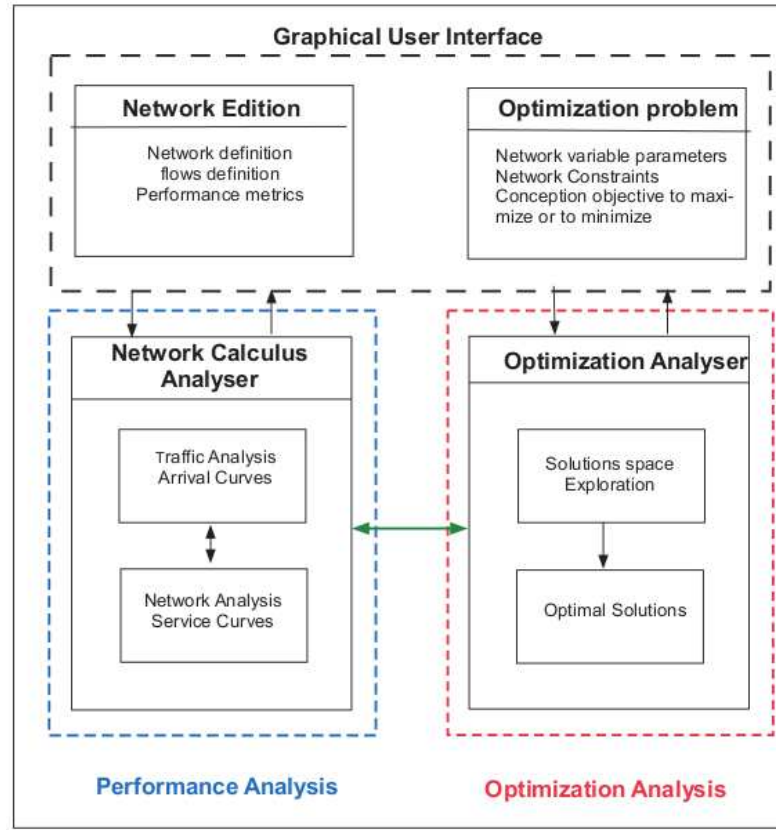


Figure A.7: WOPANETS Structure

### A.2.2 Propagation Analysis Algorithm

To compute the metric selected by the user, which could be either the maximal end-to-end delay bound, the maximal backlog bound or the maximal loss rate bound, there are mainly two possible performance analysis algorithms: Propagation Analysis algorithm and PBOO (Pay Burst Only Once) algorithm. The former is the easiest one where the flows are analyzed as a whole in each crossed node and the calculus is propagated from one node to another; whereas the latter gives less pessimistic bounds for each individual flow using the concatenation (A.8) and the blinding multiplexing (A.9) theorems.

The propagation analysis algorithm is described in Algorithm 1. First, the sets of received flows at each terminal are identified (line 6). Then, for each flow in the identified set, it determines its initial arrival curve (line 9), its associated path (line 10) and the service curves offered by crossed components along that path according to their processing mechanism (line 11). Afterwards, the delay bound calculation is propagated from one crossed component to another by resolving the burstiness constraint evolution of each flow. Knowing the arrival curve and service curves, the submitted delay and backlog

---

**Algorithm 1** Propagation Analysis Algorithm

---

```

1:  $T \leftarrow \{T_1, T_2 \dots T_{n_{terminals}}\}$ 
2:  $S \leftarrow \{s_1, s_2 \dots s_{n_{streams}}\}$ 
3:  $EED_{DEST} \leftarrow \text{HashMap} \langle \text{Terminal}, \text{List} \langle \text{double} \rangle \rangle$ 
4:  $Backlogs \leftarrow \text{HashMap} \langle \text{Terminal}, \text{double} \rangle$ 
5: for  $i = 1$  to  $n_{terminals}$  do
6:    $R \leftarrow \text{Vector-rcv-streams}(T_i, S)$ 
7:    $EDD_{streams} \leftarrow \text{List}(R.length)$ 
8:   for  $j = 1$  to  $R.length$  do
9:      $\alpha \leftarrow \text{Initial-arrival-curve}(R(j))$ 
10:     $\text{Path} \leftarrow \text{Vector-crossed-components}(R(j))$ 
11:     $\beta \leftarrow \text{Vector-service-curves}(\text{Path})$ 
12:    for  $k = 1$  to  $\text{Path.length}$  do
13:       $D \leftarrow \text{Delay-calculus}(\alpha, \beta(k))$ 
14:       $B \leftarrow \text{Backlog-calculus}(\alpha, \beta(k))$ 
15:       $\alpha \leftarrow \text{ShiftLeft}(\alpha, D)$ 
16:       $EDD_{streams}(j) \leftarrow EED_{streams}(j) + D$ 
17:    end for
18:  end for
19:   $EED_{DEST}(i) \leftarrow \langle T_i, EED_{streams} \rangle$ 
20:   $Backlogs(i) \leftarrow \langle T_i, B \rangle$ 
21: end for

```

---

bounds are calculated for each flow (lines 13-14) and then its output arrival curve (line 15). This latter curve will be the input arrival curve for the next network component and so on until the last component. Since submitted delay bounds are known for each flow and in each point of the network, a maximal end-to-end delay bound can be determined for each flow along its path (line 16).

### A.2.3 Illustrative Example

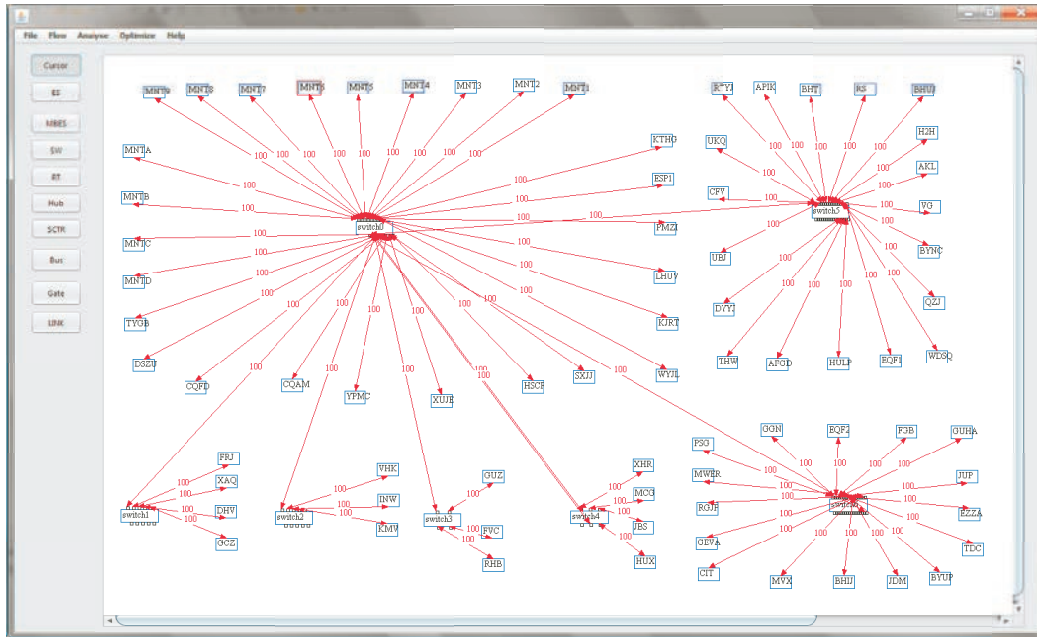


Figure A.8: The Input Topology of the Case Study

Table A.1: Periodic Traffic Description

Period (ms)	Number of flows	Data payload (bytes)
20	698	92
40	60	92
80	56	92
160	630	1492

Consider the Switched Ethernet network architecture shown in Figure A.8 consisting of about eighty end-systems and seven switches. The different categories of the real-time traffic circulating between the equipments are described in Tables A.1 and A.2. So, one can

Table A.2: Aperiodic Traffic Description

Response time (ms)	Number of flows	Data payload (bytes)
3	106	14
20	420	92
160	215	92
infinity	360	1492

see that for periodic messages, the largest period is about 160 ms and the most common value is 20 ms; and for aperiodic messages, there are different response time bounds and the most urgent one is about 3 ms. We assume that all the switches implement a simple First Come First Serve (FCFS) scheduling.

### A.2.4 Obtained Results

For the considered network, the objective of the designer is to have zero loss, i.e., all the messages meet their respective deadlines. The obtained distribution of the maximal end-to-end delay bounds is described in figure A.9 and as it can be noticed 93% of messages have delay bounds less than 1ms. The obtained loss rate is equal to zero which means that the network architecture is schedulable. Hence, this architecture could be considered as a satisfying solution given the required temporal constraints.

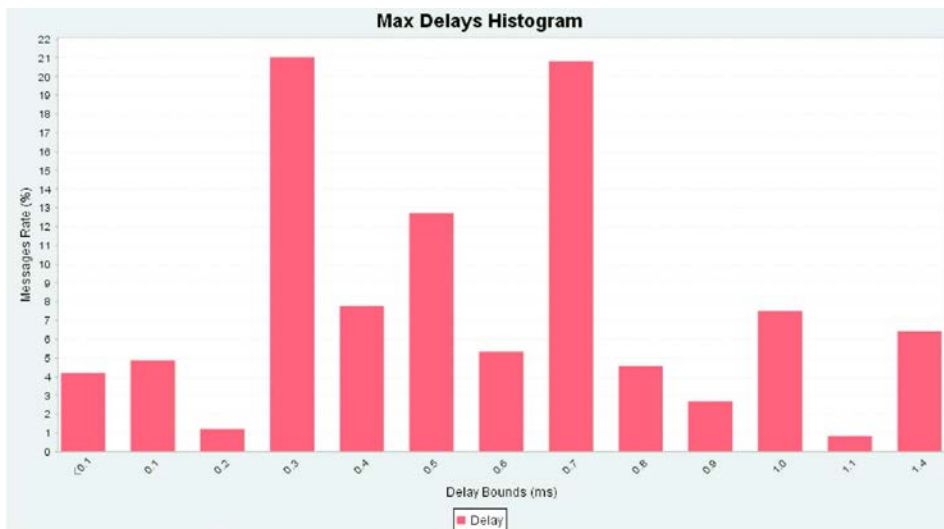


Figure A.9: Maximal Delay Bounds Histogram (1Gbps)

The tool run time for this case study was about 3 seconds and as shown in Figure A.10, the tool run time is less than 15 seconds for different network configurations with a number of hops that varies from 1 to 5 and a number of flows that varies from 200 to 6000.

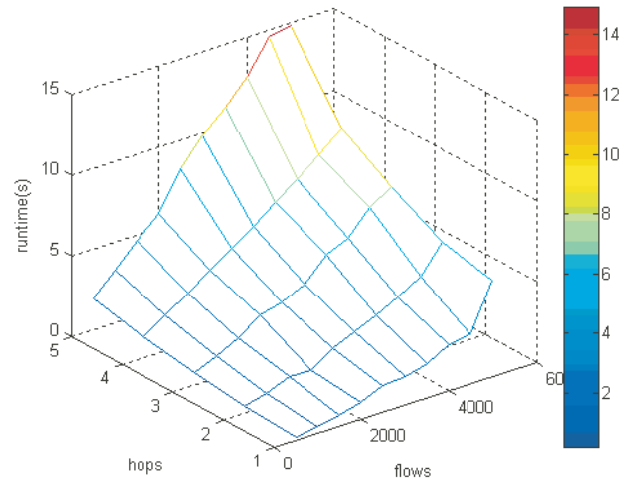


Figure A.10: Tool run time as a function of the number of hops and flows

Hence, we have shown through this case study the ability of WOPANets tool to help the designer to prove the schedulability of an embedded network in a very short time.





# Appendix B

## Generalization for TTCAN bus

In this appendix, we propose a preliminary study of the extended RDC device when using TTCAN [43] instead of native CAN to connect sensors and actuators to the avionics AFDX backbone. This network technology is based on CAN specifications for the physical and data link layers, and specific application layer which presents some differences with the native CAN behavior. The design of our proposed RDC device to interconnect TTCAN with the AFDX is discussed in this appendix and some RDC's functions extensions are proposed. First, the main relevant features of TTCAN for our interconnection problem are presented. Afterwards, some extensions of our proposed RDC device for TTCAN are proposed. Finally, the corresponding timing analysis is detailed.

### B.1 TTCAN Description

TTCAN [43] is a Time-triggered variant of CAN protocol. It adds a session layer to the native CAN protocol [3] and introduces the idea of a predefined schedule known as the TTCAN matrix cycle to control the exchange of messages.

As shown in Figure B.1, TTCAN matrix cycle consists of several basic cycles. Each Basic Cycle (BC) starts with the transmission of a reference message which is transmitted by the master node and consists of several time windows of different sizes and properties. The different types of windows defined by TTCAN protocol are as following:

- **Exclusive time windows:** supporting a predefined periodic message. The network designer has to decide off-line which message must be sent at which exclusive time window in the TTCAN matrix;

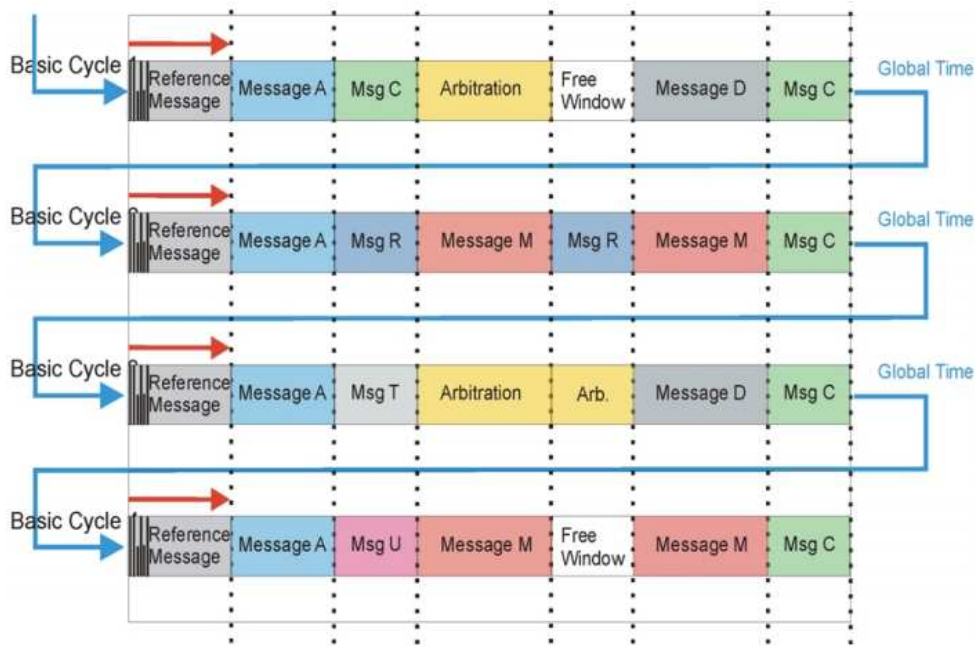


Figure B.1: *TTCAN matrix cycle*

- **Arbitrating time windows:** the native CAN access mechanism decides which message in the TTCAN network will succeed to transmit on the bus. At design time it is allowed to schedule more than one message for an arbitrating time window;
- **Free time windows:** reserved for further extensions of the network. They can be changed to arbitrating or exclusive time windows if new nodes need further bandwidth for communication.

The timing analysis of TTCAN is directly affected by the choice of TTCAN matrix, since the assignment of a time window to a given TTCAN message determines the respect or not of its time constraint. In [44], the authors addressed the problem of building the optimal TTCAN matrix, i.e., which meets temporal constraints and minimizes the TTCAN capacity utilization. Another approach for constructing the TTCAN matrix for a given messages set consists in using a scheduling algorithm to define slots and their number and order in each BC cycle. This latter approach based on scheduling algorithms offers the advantages of simplicity and scalability compared to the approach in [44]. In [45], two scheduling algorithms were proposed for TTCAN matrix construction:

- **Time Division Multiple Access (TDMA):** With this algorithm, the TTCAN

matrix consists of time slots of equal sizes. The TDMA algorithm assigns each free time slot according to the priority order of the messages. Following this rule, the highest priority message is assigned to the first time slot, then the second highest priority message and so on. A message has a pre-allocated window that can remain free when no message instance occurs. An illustrative example is given in Figure B.2 where a dedicated slot of time is affected to each message in the basic cycle. The order and the size of slots are kept even if no message is ready to be sent in a time slot window. The TDMA scheduling induces a higher TTCAN bus utilization rate and leads to an over-dimensioning of communication resources.

<b>Ref</b>	<b>1</b>	<b>2</b>	<b>3</b>	<b>4</b>	<b>5</b>	<b>6</b>	<b>7</b>
<b>Ref</b>	<b>1</b>	<b>2</b>	<b>3</b>	<b>4</b>	<b>5</b>	<b>6</b>	<b>7</b>
<b>Ref</b>	<b>1</b>	<b>2</b>	<b>3</b>	<b>4</b>	<b>5</b>	<b>6</b>	<b>7</b>
<b>Ref</b>	<b>1</b>	<b>2</b>	<b>3</b>	<b>4</b>	<b>5</b>	<b>6</b>	<b>7</b>

Figure B.2: *Example of TTCAN matrix obtained using TDMA scheduling*

- **Pre-Scheduling based on Preemptive Queue (PSPQ):** Based on a preemptive SP queue, this algorithm presents the same messages order pattern as with native CAN protocol when considering a synchronous production of data by all CAN source nodes. An illustrative example is given in Figure B.3 where 7 periodic messages are scheduled using PSPQ. Message 1 is the most prior and thus it is assigned to the first slot of the first BC cycle. Message 7 is the least prior, therefore, it will wait for messages 2, 3, 4, 5 and 6 to be assigned to their slots before being scheduled. For instance, it is assigned to a slot in the second BC cycle since one BC cycle cannot support all the messages. Compared to the TDMA scheduling, the PSPQ approach allows a better network resource utilization since the periods of allocated slots corresponds to the production periods of their associated messages.

It is worth noticing that these two algorithms are used to assign exclusive windows in the TTCAN matrix. However, arbitrating and free windows can be taken into account by considering additional messages with appropriate sizes and priorities and assigning exclusive windows for them. In our case, we focus on the assignment of TTCAN messages to exclusive windows. The free remaining windows can then be used as arbitration windows or simply as free windows for future evolution of the TTCAN network. We make the

<b>Ref</b>	<b>1</b>	<b>2</b>	<b>3</b>	<b>4</b>	<b>5</b>
<b>Ref</b>	<b>1</b>	<b>6</b>	<b>7</b>	-	-
<b>Ref</b>	<b>1</b>	<b>2</b>	<b>3</b>	-	-
<b>Ref</b>	<b>1</b>	-	-	-	-

Figure B.3: Example of TTCAN matrix obtained using PSPQ scheduling

choice of TDMA algorithm to build the TTCAN matrix.

In the rest of this Appendix, we revise our proposed RDC device to support TTCAN interconnection with AFDX. In particular, the frame packing parameters are revised to fit TTCAN time-triggered communication scheme. Then, the timing analysis is adjusted to take into account the frame packing strategies adaptations.

## B.2 TTCAN-AFDX RDC design

To interconnect an I/O TTCAN bus to AFDX, we make the following changes to our proposed CAN-AFDX RDC in Chapter 3:

- since the TTCAN defines the order of slots and their durations for transmitting each upstream or downstream message, which ensures an isolation between upstream and downstream flows, then we deactivate the HTS mechanism.
- we propose to extend both frame packing strategies, namely FWT and MSP, to take into account the time-triggered behavior of TTCAN bus. Compared to CAN protocol, TTCAN offers more precision on data transmission instants since it implements a TDMA mechanism. This fact will impact the parameters of our proposed frame packing strategies, and probably enhances their performance.

### B.2.1 FWT strategy

Consider the example shown in Figure B.4 where a set of upstream flows (7 periodic flows) needs to be sent to the AFDX backbone via the RDC device, and this set is sup-

ported by a TTCAN bus. For an arbitrary value of  $\Delta$ , i.e., waiting time parameter of FWT packing strategy, we need a set of 2 AFDX VLs to support the incoming TTCAN traffic. As can be noticed, the allocated VLs have a common BAG value equal to the basic cycle. However, each VL may have a different MFS, unlike the FWT strategy defined in Chapter 3 for the native CAN.

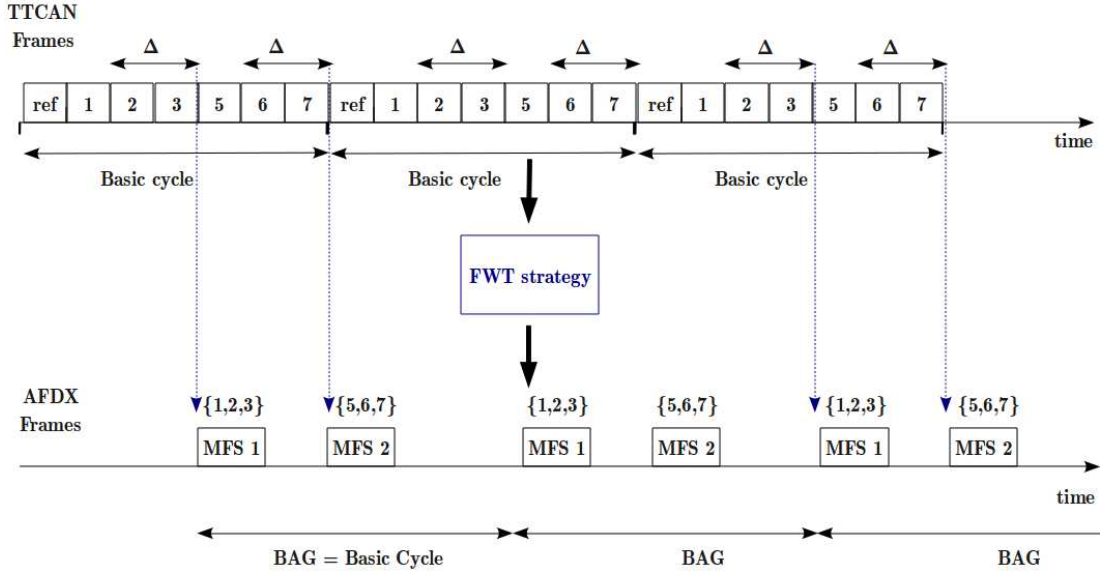


Figure B.4: *FWT strategy for TTCAN I/O network*

Hence, to define a sufficient set of AFDX VLs to support packed AFDX frames for a TTCAN-AFDX RDC device implementing a FWT strategy with a waiting time  $\Delta$ , we follow the allocation methodology illustrated in Figure B.4. After the end of reception of the first message, a waiting time  $\Delta$  is started. Then, when it expires the TTCAN frames that are totally received into the RDC device are packed into the same AFDX frame. The next TTCAN frame will start another instance of  $\Delta$  to activate the packing of another group of frames, and so on. By repeating this packing process to cover the basic cycle duration, we define the AFDX VLs including upstream messages as following:

- Each VL has a BAG equal to the TTCAN basic cycle;
- Each VL has a MFS equal to the size of an AFDX frame built with an explicit structure and including the group of TTCAN data to pack, as described in Section 3.4.2 from Chapter 3. The MFS depends on the number of grouped TTCAN data and their sizes. However, to keep the implementation of FWT strategy simple, we consider a common MFS for the different VLs equal to the maximum AFDX frame

size resulting from the FWT packing process.

### B.2.2 MSP strategy

The MSP strategy consists in partitioning the set of upstream flows incoming to the RDC device from the TTCAN bus to form the set of VLs on the AFDX. Each sub-set of TTCAN frames resulting from the partitioning process of upstream flows will be supported by the same VL on the AFDX side. Then, there are two options to set up the MSP packing process in the RDC device:

- **Option 1:** The transmission of a packed AFDX frame is triggered by the end of reception of the most urgent message among the corresponding sub-set of upstream flows;
- **Option 2:** The transmission of a packed AFDX frame is triggered by the expiration of a timer activated at the reception of the most urgent message among the corresponding sub-set of upstream flows. The duration of this timer has to be selected such to meet timing constraints of upstream flows.

Option 1 was used in Chapter 3 for native CAN bus, and it presents the advantage of favouring urgent flows. However, non-urgent flows may suffer from high waiting delays if they miss the current transmission of the urgent message. Option 2 does not favour urgent messages, however, it keeps relatively low waiting delays for all flows.

Under TTCAN, the order and transmission instants of frames are predefined, and the waiting delays when considering option 2 can be computed with a high precision. Hence, unlike CAN-AFDX RDC, the option 2 will be considered to trigger the frame packing process under MSP strategy for TTCAN-AFDX RDC device.

In Figure B.5, MSP packing strategy is applied for 7 upstream flows which are partitioned into two sub-sets: the first sub-set is composed of flows 1,2 and 3 and the second sub-set is composed of flows 5, 6 and 7. A waiting timer is used to collect messages for each sub-set of flows to form the payload of the packed AFDX frame to send in the corresponding VL. In the example of Figure B.5, two VLs are allocated to upstream flows: VL 1 with a BAG 1 equal to the basic cycle of the TTCAN matrix and an MFS equal to the size of an AFDX frame including messages 1 and 2; and VL 2 with a BAG 2 equal to the basic cycle and an MFS equal to the size of an AFDX frame including messages

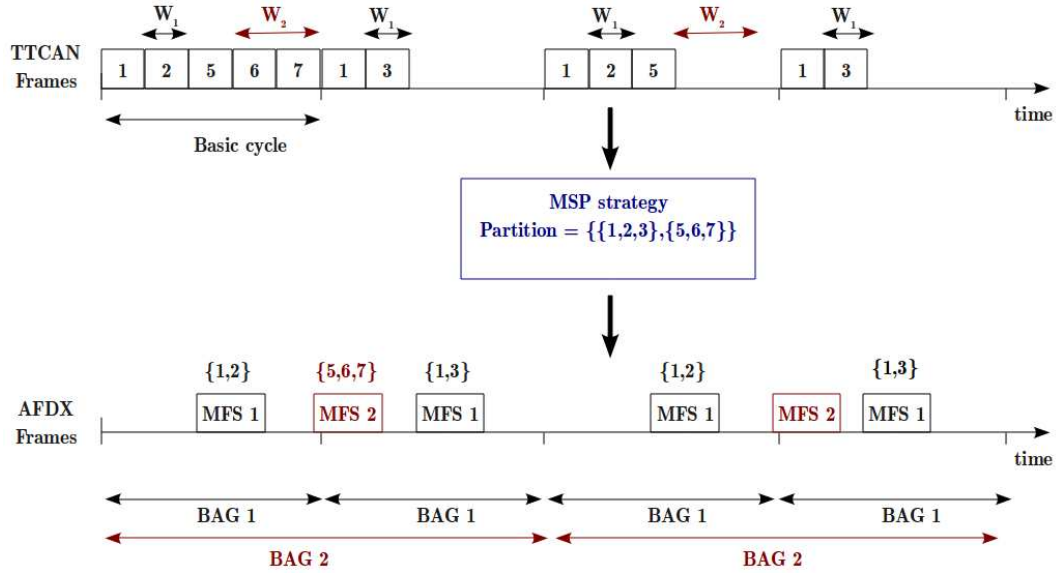


Figure B.5: MSP strategy for TTCAN bus

3, 5, 6 and 7. To set up this MSP strategy in the RDC device, we use a packing queue and a waiting timer  $W_i$  per sub-set of flows packed in VL  $v_i$ . The waiting time  $W_i$  for a given sub-set of flows is chosen as follows: (i) for each basic cycle we find the minimum waiting time to collect data belonging to this sub-set of flows during the considered basic cycle and we form a list of waiting times  $L_{W_i}$ . The waiting time is started at the end of reception of the first received data belonging to the sub-set of flows; (ii) we select the maximum value in  $L_{W_i}$  as the waiting time  $W_i$ . For example, as shown in Figure B.5, waiting time  $W_1$  is used for the sub-set of flows  $\{1, 2\}$ . This timer is started at the end of reception of the message 1, and when it expires an AFDX frame is built and supports the collected messages within the sub-set  $\{1, 2\}$ .

## B.3 Timing Analysis

We consider the same notation of Section 4.2 in Chapter 4. For an upstream or a downstream message  $m$ , we write the schedulability condition using the end-to-end delay metric as following:

$$\forall m \in S_{up} \cup S_{down}:$$

$$\begin{aligned}
 d_{eed}(m) &\leq Dl_m \\
 d_{TTCAN}(m) + d_{RDC}(m) + d_{AFDX}(m) &\leq Dl_m
 \end{aligned}
 \tag{B.1}$$

With reference to timing analysis provided in Section 4.2,  $d_{RDC}(m)$  and  $d_{TTCAN}(m)$  have to be revised to take into account the specificities of TTCAN protocol and the adapted FWT and MSP frame packing strategies for TTCAN.

### B.3.1 Timing Analysis for RDC

#### For Upstream Flows:

For an upstream TTCAN message  $m_j$  crossing the RDC device, the upper bound of RDC delay  $d_{RDC}(m_j)$  is the sum of: (i) a technological latency  $\epsilon$  due to payload extraction and relaying process, called  $\epsilon$ ; (ii) waiting time in the RDC due to the frame packing process between the reception instant of the CAN message and the transmission instant of its associated AFDX frame  $WT(m_j)$ ,

$$d_{RDC}(m_j) = \epsilon + WT(m_j) \tag{B.2}$$

For FWT strategy, there is no difference in terms of the maximum waiting time compared to results of Section 4.2. The maximum waiting time  $WT(m_j)$  in the RDC device is equal to  $\Delta$  for all upstream messages  $m_j$ .

For MSP strategy, a message  $m_j$  has to wait for the expiration of the waiting timer  $W_j$  used to collect data belonging to its corresponding sub-set of flows, as illustrated in Figure B.4. Therefore, an upper bound on  $WT(m_j)$  under MSP strategy is:

$$d_{RDC}(m_j) = \epsilon + W_j \tag{B.3}$$

#### For Downstream Flows:

Since the HTS mechanism is deactivated within TTCAN-AFDX RDC, the delay  $d_{RDC}$  for downstream flows is simply the technological latency  $\epsilon$ . This latency is due to the payload extraction, unpacking and data encapsulation applied for downstream flows.



### B.3.2 Timing Analysis on TTCAN

For an upstream or a downstream message  $m_j$  to be transmitted on the TTCAN bus given a predefined schedule, we compute a worst case response time. The TTCAN matrix is obtained using TDMA algorithm and an example is described in Figure B.6 for 7 periodic flows.

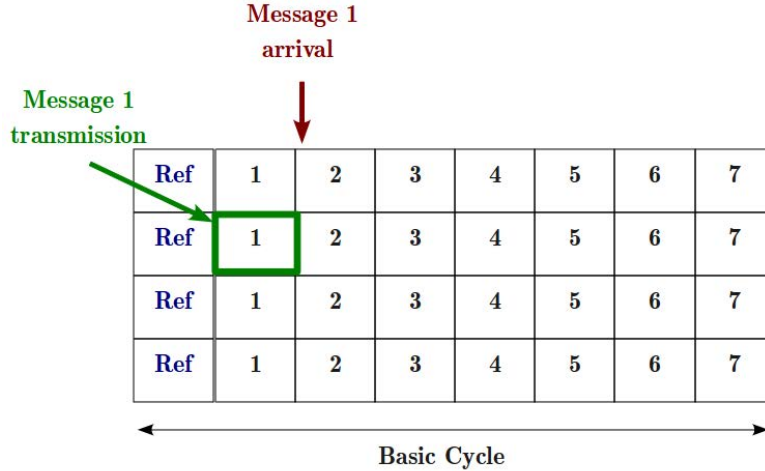


Figure B.6: *Worst Case Response Time on TTCAN*

Following the transmission schedule of Figure B.6, the worst case for the transmission of a message corresponds to its arrival immediately after the end of its allocated slot in the currently basic cycle. The message must wait for its slot in the next basic cycle to be transmitted on TTCAN bus. Hence, the worst case response time on TTCAN for message  $m_j$  is simply:

$$d_{TTCAN}(m_j) = BC \quad (\text{B.4})$$

where  $BC$  is the basic cycle duration.

### B.3.3 Illustrative Example

To illustrate the extension of our proposed RDC device to TTCAN bus, we consider the test case shown in Figure B.7. In this test case, one sensors TTCAN bus is connected to the AFDX backbone using our enhanced RDC device implementing the adapted FWT

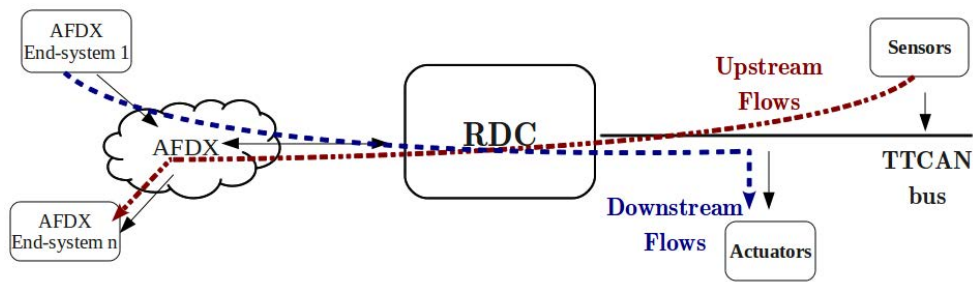


Figure B.7: TTCAN bus interconnected to the AFDX

and MSP strategies. The TTCAN supports upstream flows reported in Table B.1. Especially, we focus on the impact of frame packing on the AFDX bandwidth consumption.

Table B.1: Upstream flows description

Messages	Number	Payload(bytes)	Period(ms)
$m_1$	3	8	4
$m_2$	2	8	8
$m_3$	16	2	16
$m_4$	4	2	32

The considered TTCAN schedule to transmit these upstream flows is shown in Figure B.8. The basic cycle is considered equal to  $T_1/2 = 2ms$ . For space limitation reasons, we reported the consecutive slots assigned for messages from the same type as one slot denoted by  $n_j \times m_j$ , where  $n_j$  is the number of messages from type  $m_j$ . For example, cell  $3 \times m_1$  in the schedule of Figure B.8 corresponds to three consecutive slots supporting messages of type  $m_1$ .

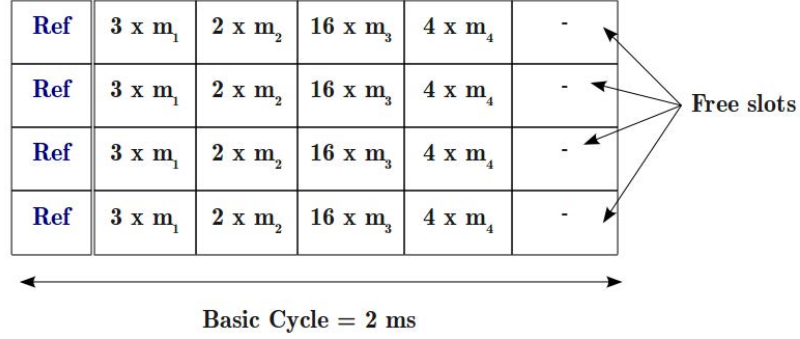


Figure B.8: TTCAN schedule example for TTCAN upstream flows

Table B.2: VLS characteristics under FWT for TTCAN

FWT configuration	BAG (ms)	MFS (bytes)	VLS number	rate (Mbps)
$\Delta_1 = 0.5ms$	2	99	5	1.98
$\Delta_1 = 1ms$	2	117	3	1.4

Table B.3: End-to-end delay bounds under FWT strategy with  $\Delta = 1ms$ 

Message type	$T(ms)$	$d_{eed}(ms)$
$m_1$	4	3.95
$m_2$	8	4.1
$m_3$	16	4.3
$m_4$	32	4.7

The allocated VLS for upstream flows under FWT strategies with  $\Delta$  equal to  $0.5ms$  and  $1ms$  are reported in Table B.2. For instance, implementing FWT strategy with  $\Delta = 1ms$  requires 3 VLS with a BAG of 2 ms and a MFS of 117 bytes. The end-to-end delay bound is computed for each message under each of the considered FWT configurations and is then compared to its respective deadline. For instance, in Table B.3, the end-to-end delay bounds for upstream flows of Table B.1 under FWT strategy in the RDC device with waiting time  $\Delta = 1ms$  are reported. As we can see, the RDC device configuration is schedulable, when considering the deadline of each message equal to its period. The technological latency of the RDC device is assumed  $\epsilon = 0.05ms$ .

Table B.4: MSP configurations

	VL allocation	Waiting Timers ( $W_j$ )
$conf_1$	$v_1 : \{3 * m_1\}, v_2 : \{2 * m_2\}, v_3 : \{16 * m_3\}, v_4 : \{4 * m_4\}$	$W_1 = 0.42ms, W_2 = 0.14ms, W_3 = 1.2ms, W_4 = 0.24ms$
$conf_2$	$v_1 : \{3 * m_1, 2 * m_2\}, v_2 : \{16 * m_3, 4 * m_4\}$	$W_1 = 0.7ms, W_2 = 1.55ms$

Then, we consider two MSP packing configurations in the RDC device as shown in Table B.4. Configuration  $conf_1$  corresponds to packing all the messages of type  $m_i$  within the same AFDX frame supported by the virtual link  $v_i$ . Whereas, configuration  $conf_2$  consists in packing messages from types  $m_1$  and  $m_2$  in virtual link  $v_1$ , and packing messages from types  $m_3$  and  $m_4$  in virtual link  $v_2$ . The waiting timers used to perform the frame packing process for each configuration are also provided. For instance, to set up  $conf_2$  in the RDC device, we have  $W_1 = 0.7ms$  for  $v_1$  and  $W_2 = 1.55$  for  $v_2$ .

Table B.5: TTCAN-AFDX RDC: schedulability test and AFDX bandwidth consumption

Configuration	Number of VLs	AFDX Bandwidth (in Mbps)	Schedulability
(1:1)	25	1.42	OK
FWT ( $\Delta = 1ms$ )	3	1.4	OK
MSP ( $conf_1$ )	4	1.39	OK
MSP ( $conf_2$ )	2	0.85	OK

As we can notice from Table B.5, although the FWT strategy with  $\Delta = 1ms$  reduces the number of allocated VLs for the RDC device on AFDX, the induced bandwidth consumption is similar to (1:1) strategy. The MSP strategy offers the best resource utilization performance, with reference to (1:1) and FWT strategies. For instance, using the adapted MSP strategy for TTCAN under  $conf_2$  reduces the AFDX bandwidth consumption where a reduction of 40% is noticed with reference to the (1:1) and FWT strategies. Hence, the FWT does not offer AFDX bandwidth enhancements when used in the RDC device with TTCAN, whereas, MSP offers an improvement compared to the (1:1) strategy. This is mainly due to the fact that TTCAN is based on a static schedule for data transmission and it is more convenient to use MSP which is a static packing strategy. The MSP performs a more accurate VLs allocation and overcomes the over-dimensioning problem of the FWT strategy.

# Bibliography

- [1] Airlines Electronic Engineering Committee. Aircraft Data Network Part 7, AFDX network, Arinc Specification 664. Annapolis, Maryland, 2002. Aeronautical Radio.
- [2] Avionic Systems Standardisation Committee. Guide to avionics data buses, ARINC 429. 1995.
- [3] Robert Bosch GmbH. CAN specification Version 2.0. 1991.
- [4] Airlines Electronic Engineering Committee. ARINC Report 655: Remote Data Concentrator(RDC) generic description. Annapolis, Maryland, 1999. Aeronautical Radio.
- [5] Avionic Systems Standardisation Committee. Avionics Application Software Standard Interface Part 1-2, ARINC Specification 653P1-2. 2005.
- [6] A. Mifdaoui and H. Ayed. WOPANets: a tool for Worst case Performance Analysis of embedded Networks. *CAMAD 2010*.
- [7] C. Watkins and R. Walter. Transitioning From Federated Avionics Architectures To integrated Modular Avionics. *Digital Avionics Systems Conference (DASC), 2007*.
- [8] Condor Engineering Incorporated. MIL-STD-1553 Designer guide. <http://www.condoreng.com/support/downloads/tutorials/MIL-STD-1553Tutorial>, 1982.
- [9] Avionic Systems Standardisation Committee. ARINC 629 P1-4 Multi-Transmitter Data Bus, Part1, Technical Description. 1995.
- [10] P. Bieber, F. Boniol, M. Boyer, E. Noulard, and C. Pagetti. New Challenges for Future Avionic Architectures. *Aerospacelab*, Issue 4, May 2012.
- [11] R.I. Davis, A. Burns, R.J. Bril, and J.J. Lukkien. CAN schedulability analysis: Refuted, revisited and revised. *Real-Time Systems*, 35(3):239–272, 2007.
- [12] A. Al Sheikh, O. Brun, M. Cheramy, and P.E. Hladik. Optimal Design of Virtual Links in AFDX Networks. *Real-Time Systems*, May 2013.
- [13] A. Al Sheikh, O. Brun, and P.E. Hladik. Partition Scheduling on an IMA Platform with Strict Periodicity and Communication Delays. In *18th International Conference on Real-Time and Network Systems*, November 2010.

- [14] R. Saket and N. Navet. Frame packing algorithms for automotive applications. *Journal of Embedded Computing*, 2:93–102, 2006.
- [15] S.M. Ricardo, N. Navet, and F. Simonot-Lion. Frame Packing under real-time constraints. *5th IFAC*, 2003.
- [16] P. Pop, P. Eles, and Z. Peng. Schedulability-driven frame packing for multicluster distributed embedded systems. *ACM Transactions on Embedded Computing Systems (TECS)*, February 2005.
- [17] J. Grieu. *Analyse et valuation de techniques de commutation Ethernet pour l'interconnexion de systemes avioniques*. PhD thesis, INP, Toulouse, 2004.
- [18] Henri Bauer, Jean-Luc Scharbarg, and Christian Fraboul. Improving the worst-case delay analysis of an AFDX network using an optimized trajectory approach. *IEEE Transactions on Industrial Informatics*, 2010.
- [19] E. Clarke, O. G. Jr., and D. A. Peled. *Model Checking*. MIT Press, Cambridge, MA, USA, 2000.
- [20] J.Y. Leboudec and P. Thiran. *Network Calculus*. Springer Verlag LNCS volume 2050, 2001.
- [21] F. Frances, C. Fraboul, and J. Grieu. Using Network Calculus to optimize the AFDX Network. Proceedings of the 3rd European Congress Embedded Real Time Software, 2006.
- [22] S. Martin. *Maîtrise de la dimension temporelle de la qualité de service dans les réseaux*. PhD thesis, Université Paris XII, 2004.
- [23] J. Migge. *L'ordonnancement sous contraintes temps-réel : un modèle à base de trajectoires*. PhD thesis, INRIA, Sophia Antipolis, 1999.
- [24] H. Charara, J.L Scharbarg, J. Ermont, and C. Fraboul. Methods for bounding end-to-end delays on an AFDX network. Proceedings of the 18th Euromicro Conference on Real-Time Systems, 2006.
- [25] K.W. Tindell, A. Burns, and A. J. Wellings. Calculating Controller Area Network (CAN) message response times. *Control Engineering Practice*, 3, August 1995.
- [26] R.I. Davis, S. Kollmann, V. Pollex, and F. Slomka. Controller Area Network (CAN) Schedulability Analysis with FIFO Queues. *23rd Euromicro Conference on Real-Time Systems*, 2011.
- [27] R.I. Davis, N. Navet, D. Bertrand, and P.M. Yomsi. Controller Area Network (CAN): Response Time Analysis with Offsets. *Real-Time Systems*, 35(3):239–272, 2007.
- [28] J.L. Scharbarg, M. Boyer, and C. Fraboul. CAN-Ethernet architectures for real-time applications. *IEEE ETFA*, 2005.

- 
- [29] B. Somers. *Investigation of a Flexray - CAN Gateway in the Implementation of Vehicle Speed Control*. PhD thesis, Waterford Institute of Technology, Ireland, 2009.
- [30] Stock Flight Systems. CANAerospace: Interface specification for airborne CAN applications V 1.7. 2006.
- [31] Airlines Electronic Engineering Committee. ARINC Specification 825-2: General standardization of CAN (Controller Area Network) bus protocol for airborne use. Annapolis, Maryland, 2011. Aeronautical Radio.
- [32] S. Zeng and N. Uzun. A hierarchical traffic shaper for packet switches. *Global Telecommunications Conference, GLOBECOM*, 1999.
- [33] J. S. Turner. New Directions in Communications (or Which Way to the Information Age?). *IEEE Communications Magazine*, 1986.
- [34] J.L. Valenzuela, A. Monleon, I. San Esteban, M. Portoles, and O. Sallent. A hierarchical token bucket algorithm to enhance qos in ieee 802.11: proposal, implementation and evaluation. In *Vehicular Technology Conference, 2004*.
- [35] T. Nolte, M. Sjodin, and H. Hansson. Server-based scheduling of the CAN bus. *Emerging Technologies and Factory Automation (ETFA)*, 2003.
- [36] Z. Iqbal, L. Almeida, R. Marau, M. Behnam, and T. Nolte. Implementing hierarchical scheduling on cots ethernet switches using a master/slave approach. In *7th IEEE International Symposium on Industrial Embedded Systems, 2012*.
- [37] E. Wandeler, A. Maxiaguine, and L. Thiele. On the Use of Greedy Shapers in Real-Time Embedded Systems. *Embedded Computing Systems*, 2012.
- [38] R.I. Davis and N. Navet. Traffic Shaping to Reduce Jitter in Controller Area Network (CAN). *24th Euromicro Conference on Real-Time Systems*, 2012.
- [39] P. Narasimhan, L. Moser, and P. Melliar-Smith. Message packing as a performance enhancement strategy with application to the totem protocols. In *Global Telecommunications Conference (GLOBECOM)*, 1996.
- [40] R. Marau, N. Figueiredo, R. Santos, P. Pedreiras, L. Almeida, and T. Nolte. Towards Server-based Switched Ethernet for real-time communications. *Proceedings of the 1st Workshop on Compositional Theory and Technology for Real-Time Embedded Systems*, 2008.
- [41] E. G. Coffman, M. R. Garey, and D. S. Johnson. *Approximation algorithms for NP-hard problems*. PWS Publishing Company, 1996.
- [42] E. L. Lawler and D. E. Wood. Branch-and-bound methods: A survey. *Operations Research*, 1966.

- [43] A. Albert, R. Strasser, and A. Trachtler. Migration from CAN to TTCAN for a Distributed Control System. *ICC*, 2003.
- [44] Xin Qiao, Kun-Feng Wang, Yuan Sun, Wu-Ling Huang, and Fei-Yue Wang. A Genetic Algorithms based optimization for TTCAN. In *IEEE International Conference on Vehicular Electronics and Safety*, 2007.
- [45] A. Hara, K. Fonseca, and L. Scandelari. CAN/TTCAN Simulator System based on Educational DSP Hardware Kits. *ICC*, 2003.